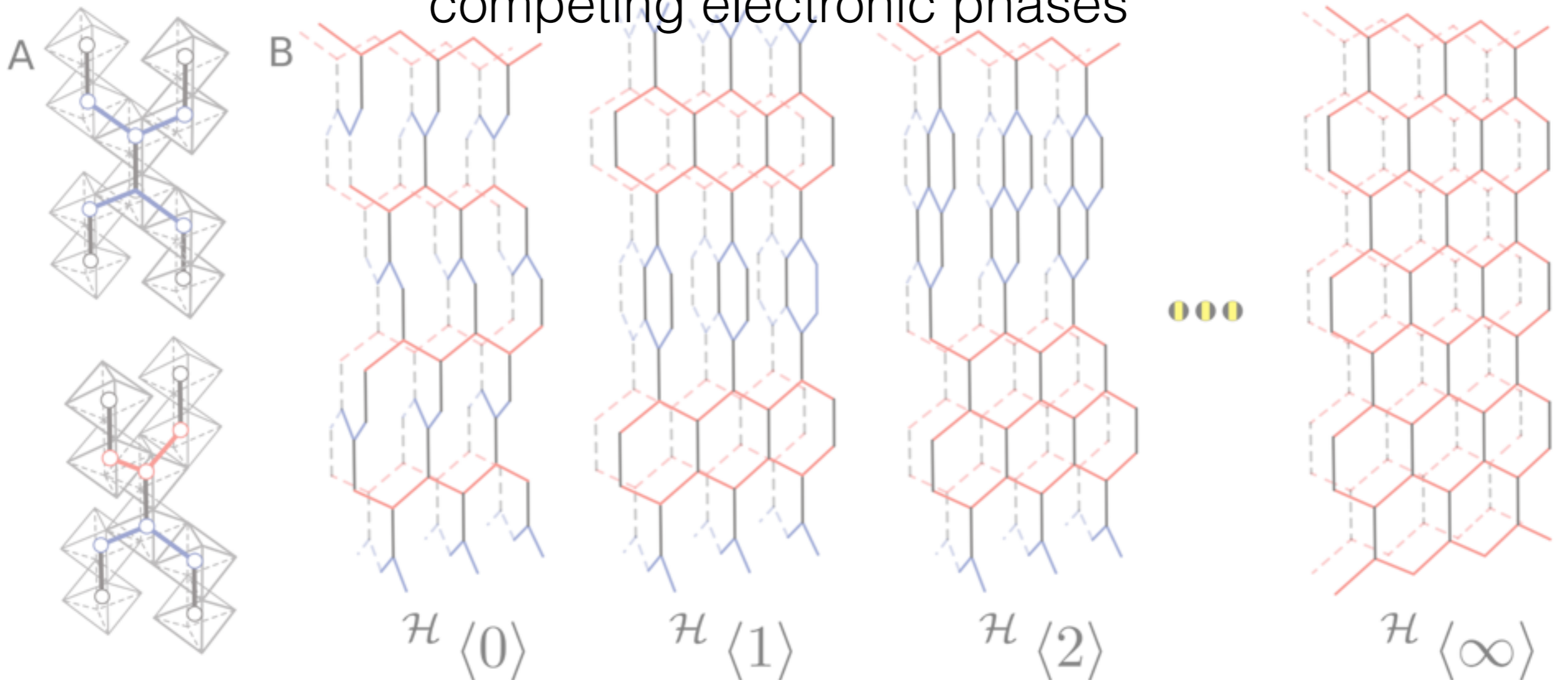




# From synthesis to thermodynamics

The interplay of competing crystalline phases and competing electronic phases



# Quantum oscillations in Weyl semi-metals

Quantum oscillatory phenomena from Fermi Arcs

Philip J. M. W. Moll, Nityan Nair, James G. Analytis  
*University of California, Berkeley*

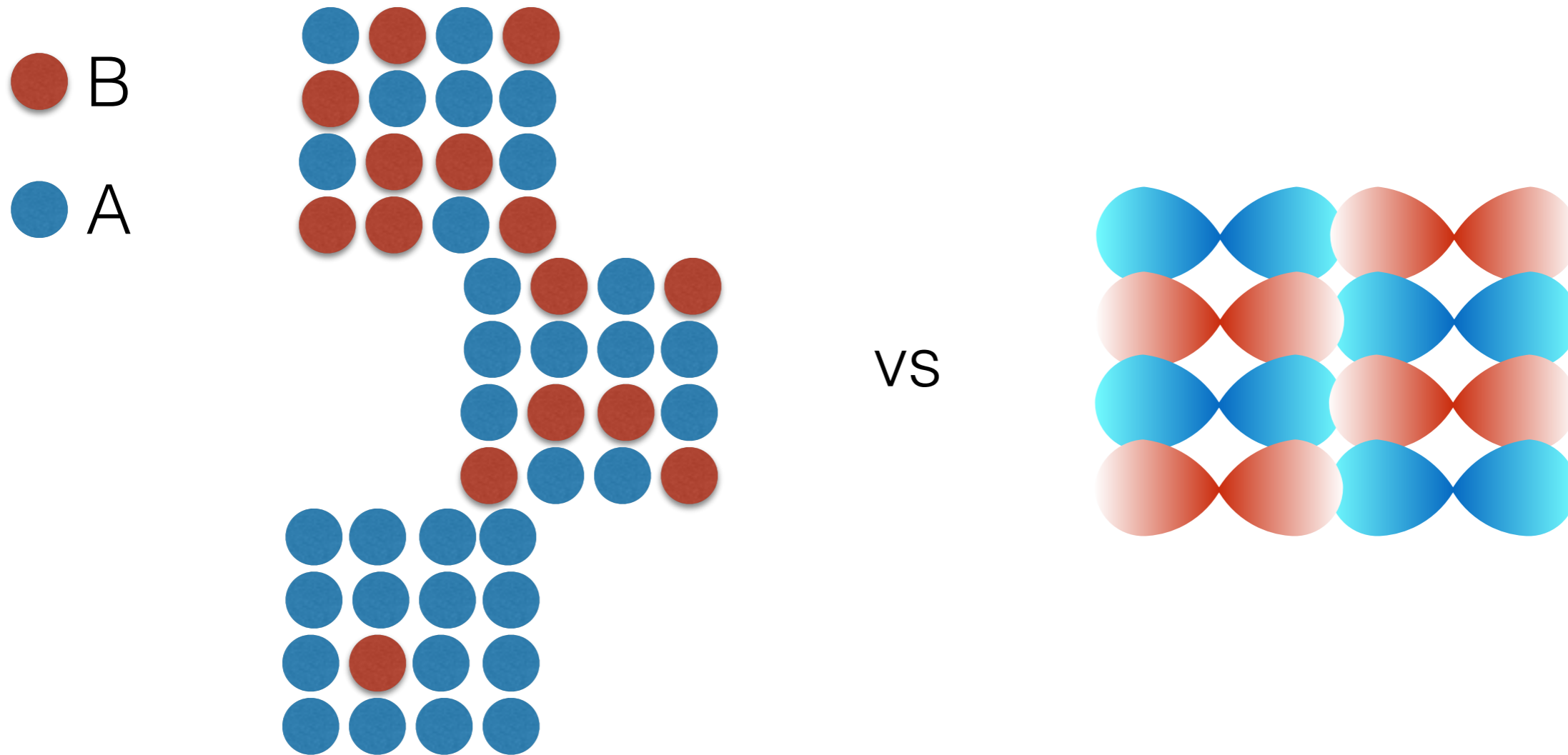
GORDON AND BETTY  
**MOORE**  
FOUNDATION



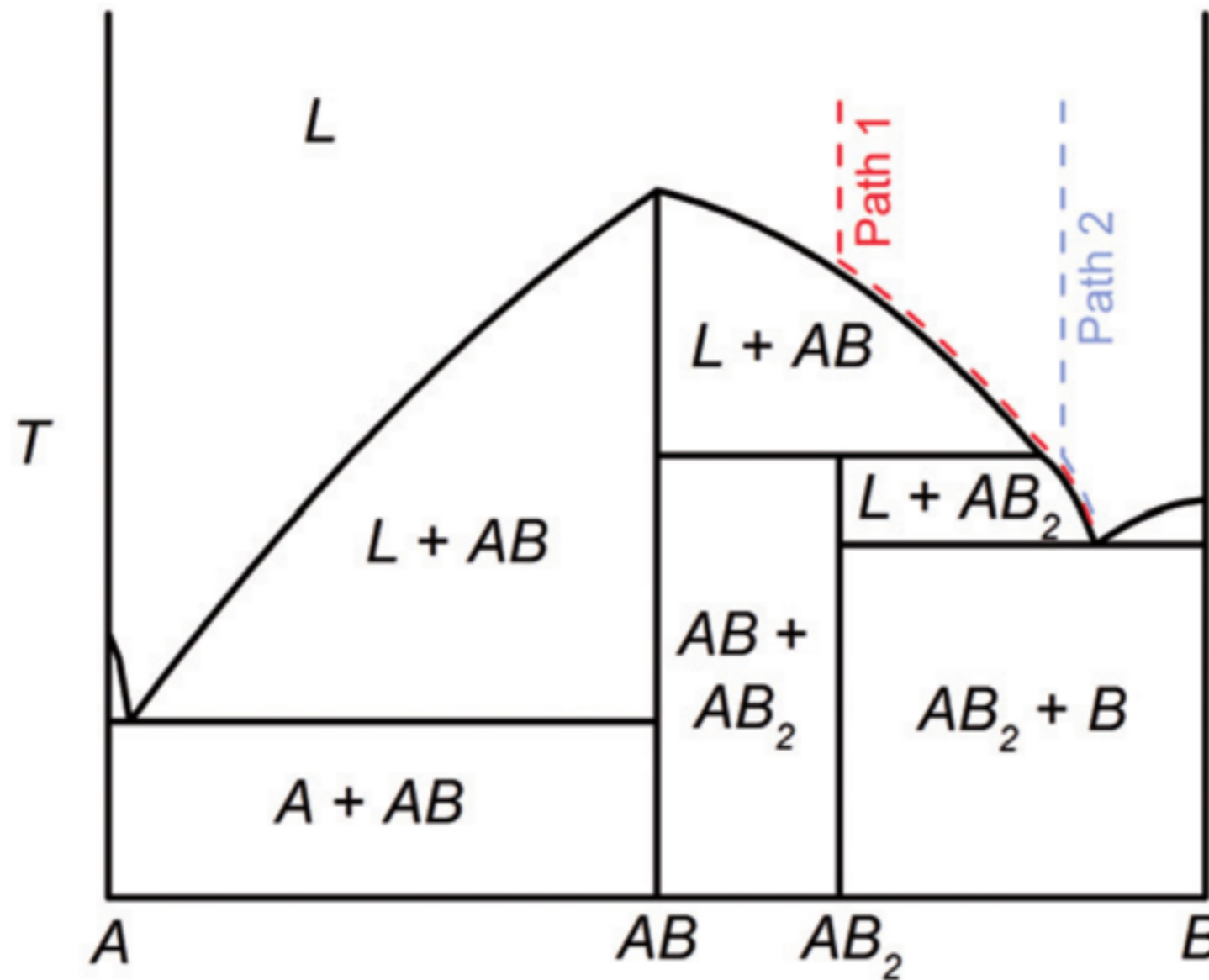
# Synthesis

- What techniques do we use to make these materials?
- Why are some materials difficult to make and other easy?

# Making compounds



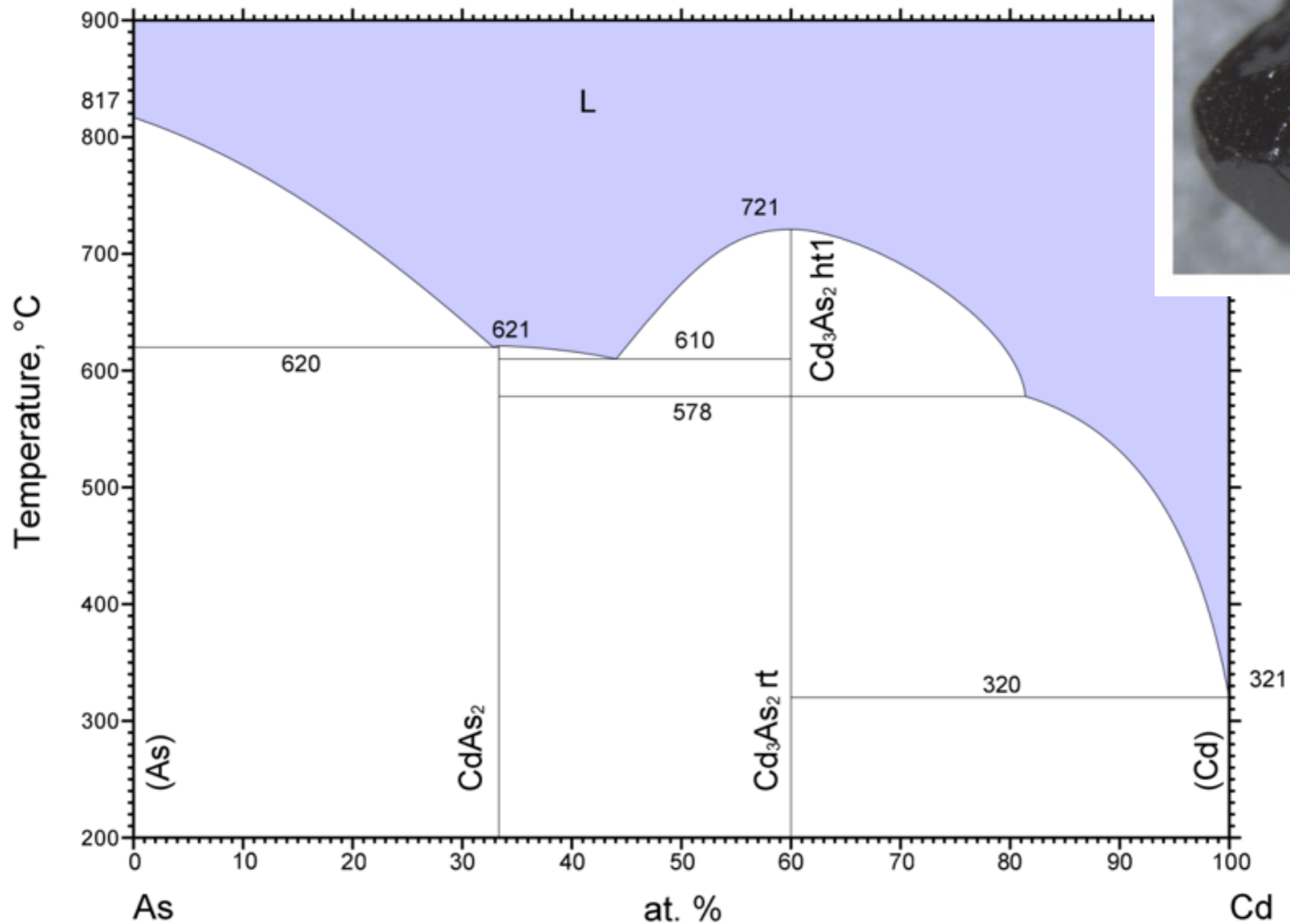
- The compounds that one can make are generally determined by where the minimum in the free energy occurs, which in turn depends on a balance of the entropy (generally the change in configurational entropy) and the enthalpy (mostly the gain in energy in bonding).



# Binary phase diagrams

Fisher/Shapiro/Analytis Philosophical Magazine 2012

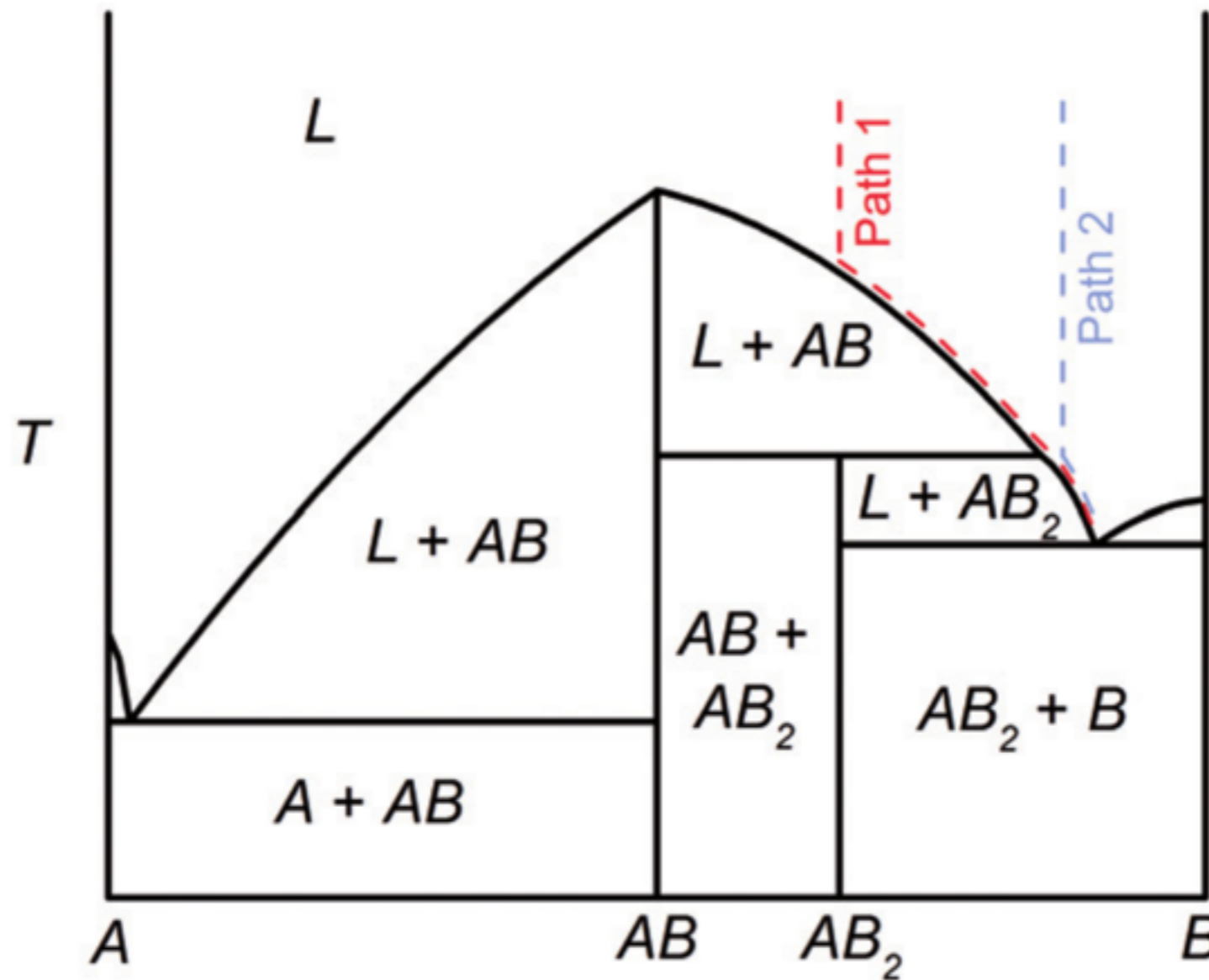
# Phase diagram of $\text{Cd}_3\text{As}_2$



# Congruent and incongruent melts

- In many binary phase diagrams more than one solid phase can be made.
- Intermediate phases can be classed as either
  - *congruently melting* (melt from a homogeneous solid to a homogeneous liquid)
  - *incongruently melting* (the solid decomposes on heating to a two-phase mixture of solid and liquid where multiple solid phases may be in equilibrium)

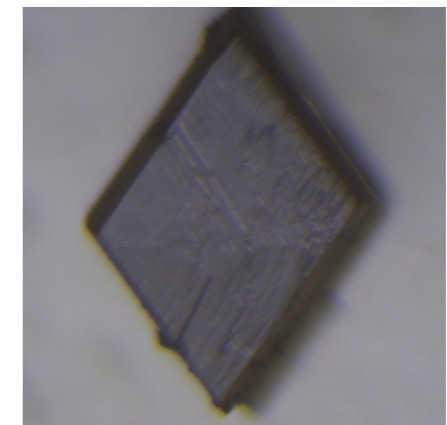
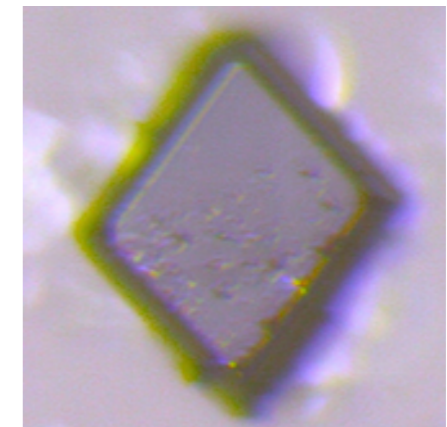
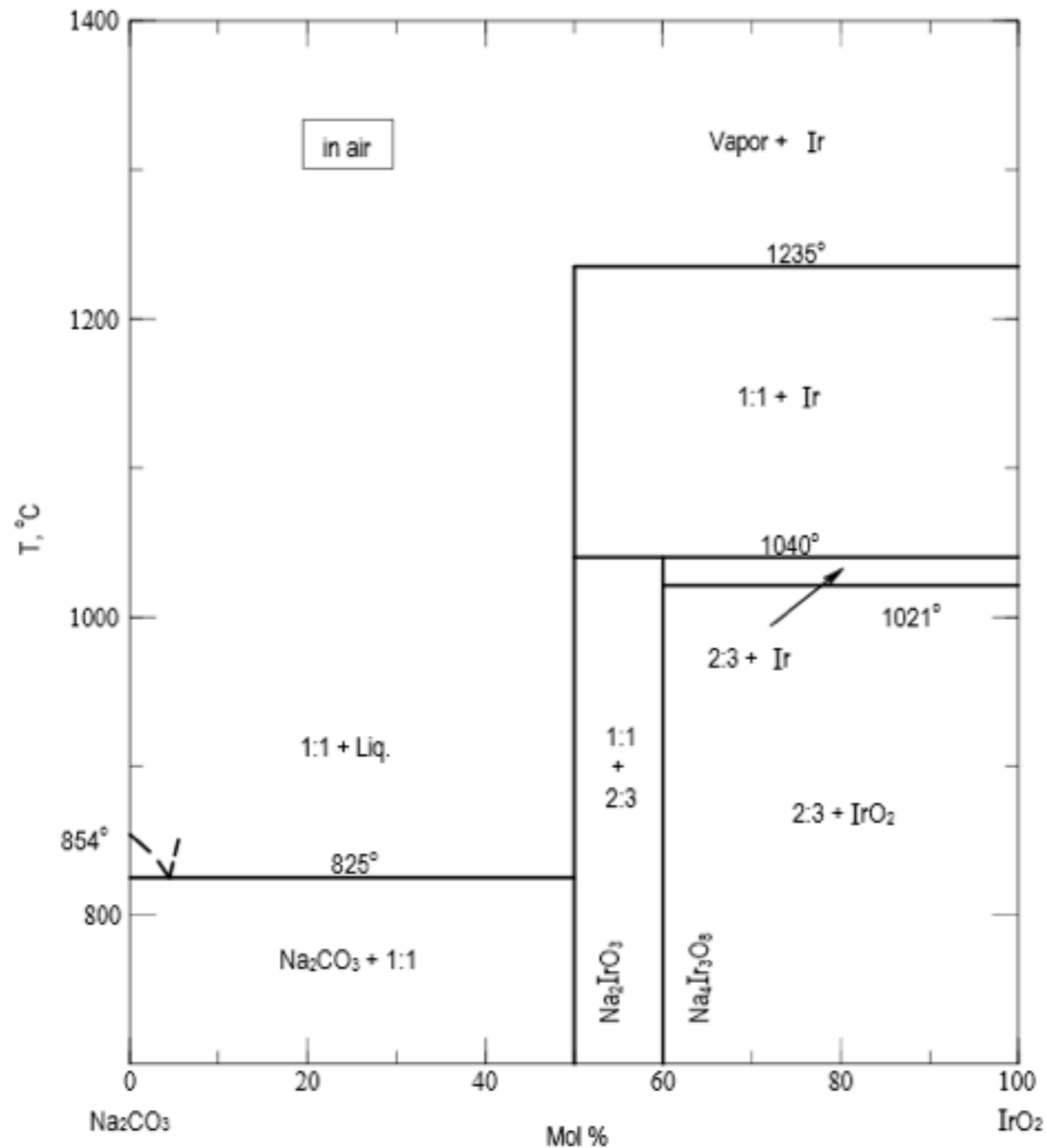




# Binary phase diagrams

Fisher/Shapiro/Analytis Philosophical Magazine 2012

# Phase diagram of $\text{Na}_2\text{CO}_3$ - $\text{IrO}_2$



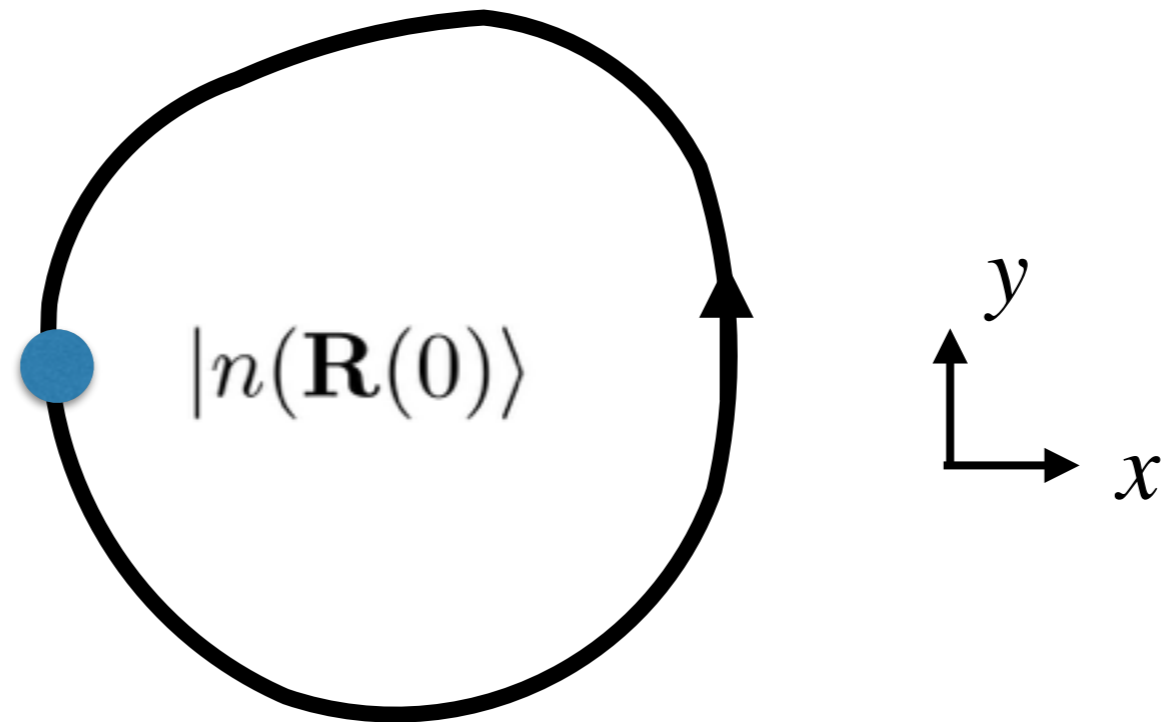
See Ruiz (Sunday afternoon)

# PART II:

Adiabaticity, Quantum Oscillations and the  
Berry's phase.

# Adiabatic theorem

$$|n(\mathbf{R}(0))\rangle \rightarrow e^{i\gamma_B} e^{i\phi} |n(\mathbf{R}(t))\rangle$$

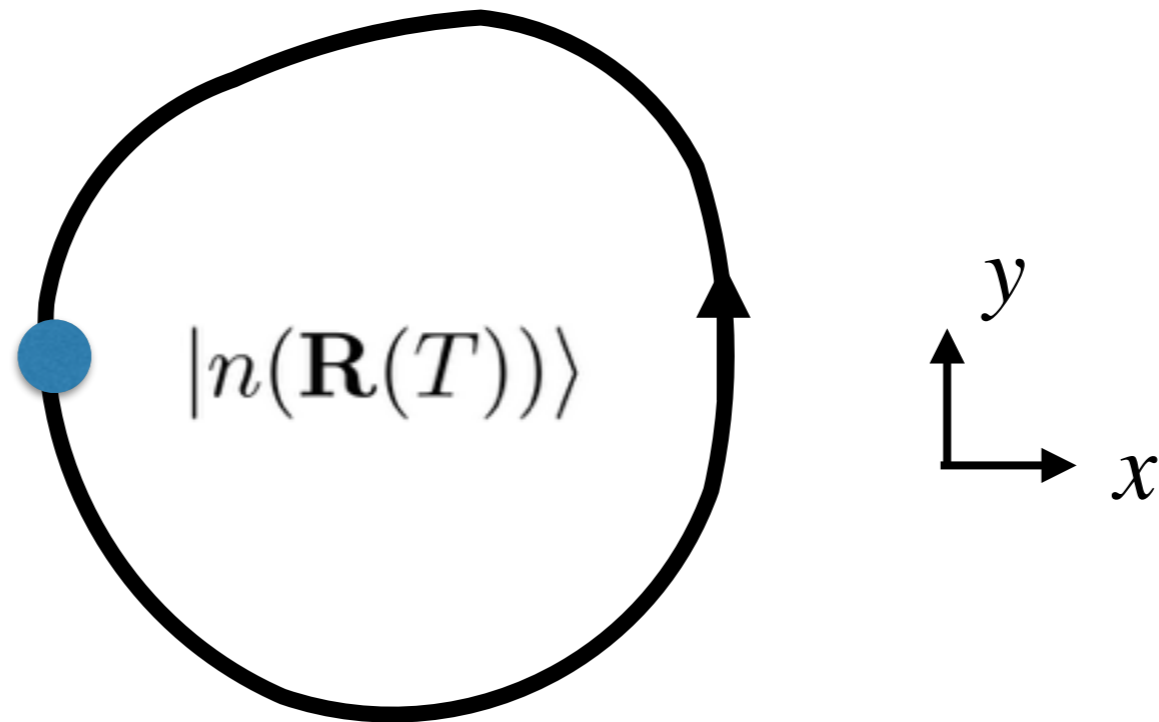


$$\phi = -\frac{1}{\hbar} \int_0^T E_n(\mathbf{R}(t)) dt$$

$$\gamma_B(C) = i \oint_C \langle n(\mathbf{R}) | \nabla_{\mathbf{R}} | n(\mathbf{R}) \rangle$$

# Adiabatic theorem

$$|n(\mathbf{R}(0))\rangle \rightarrow e^{i\gamma_B} e^{i\phi} |n(\mathbf{R}(t))\rangle$$



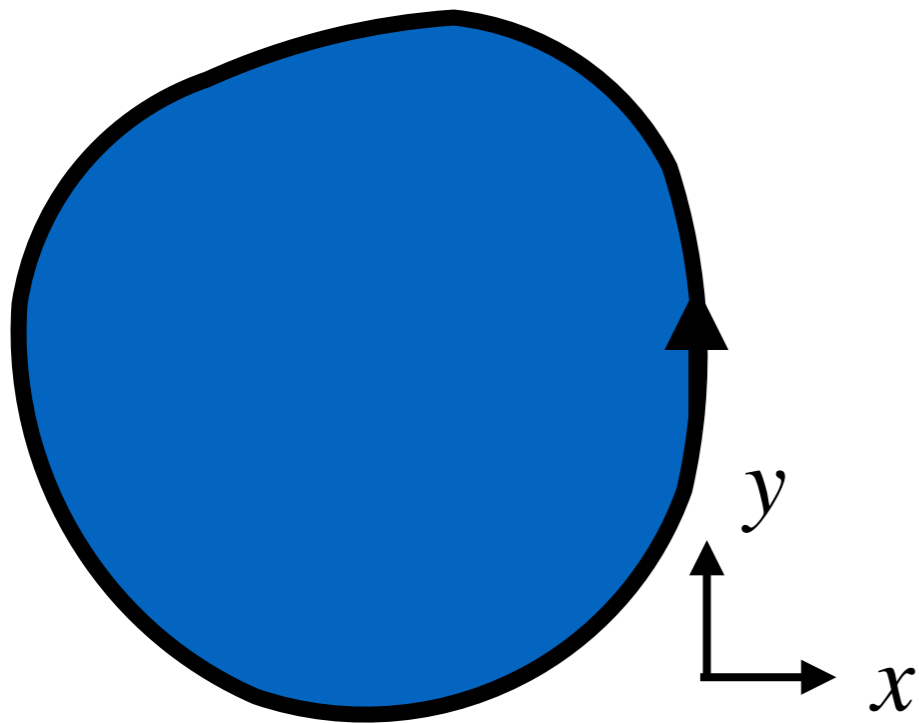
$$\phi = -\frac{1}{\hbar} \int_0^T E_n(\mathbf{R}(t)) dt$$

$$\gamma_B(C) = i \oint_C \langle n(\mathbf{R}) | \nabla_{\mathbf{R}} | n(\mathbf{R}) \rangle$$

# Onsager's argument

$$\oint_C \mathbf{p} \cdot d\mathbf{q} = (n + \gamma) 2\pi \hbar$$

**Adiabatic invariant**

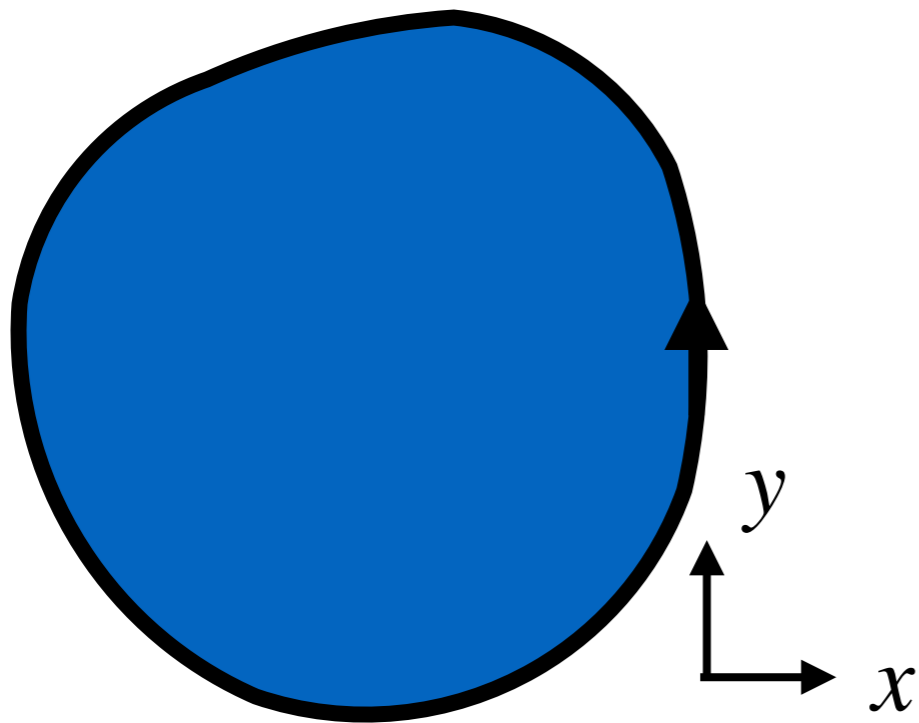


# Onsager's argument

$$\oint_C \mathbf{p} \cdot d\mathbf{q} = (n + \gamma) 2\pi \hbar$$

**Adiabatic invariant**

$$\mathbf{p} = \hbar \mathbf{k} - e\mathbf{A}$$



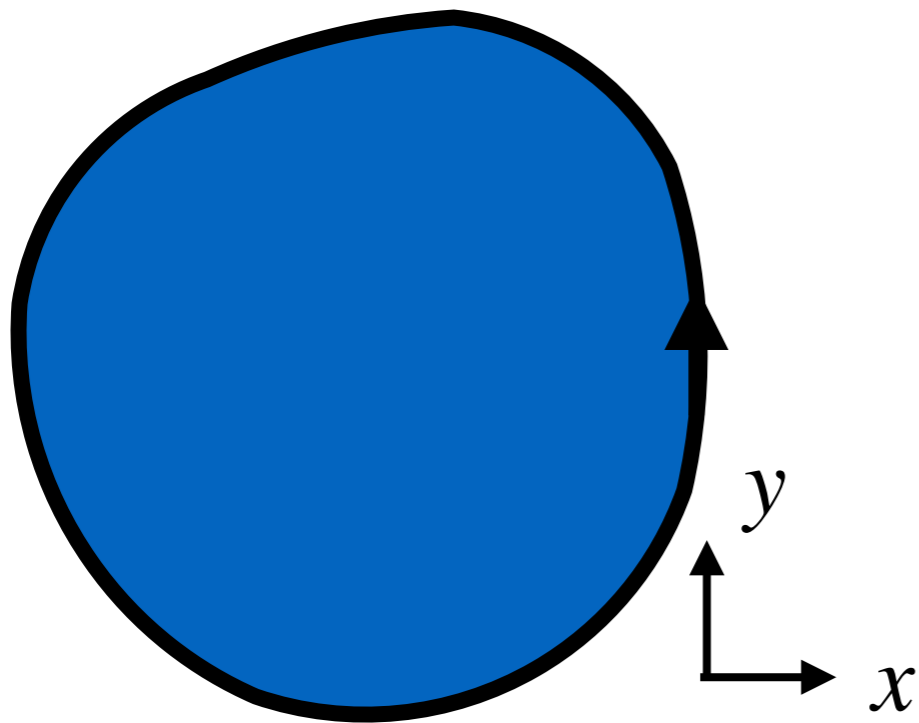
# Onsager's argument

$$\oint_C \mathbf{p} \cdot d\mathbf{q} = (n + \gamma) 2\pi \hbar$$

**Adiabatic invariant**

$$\mathbf{p} = \hbar \mathbf{k} - e\mathbf{A}$$

$$\Phi \equiv BA = (n + \gamma) 2\pi \frac{\hbar}{e}$$





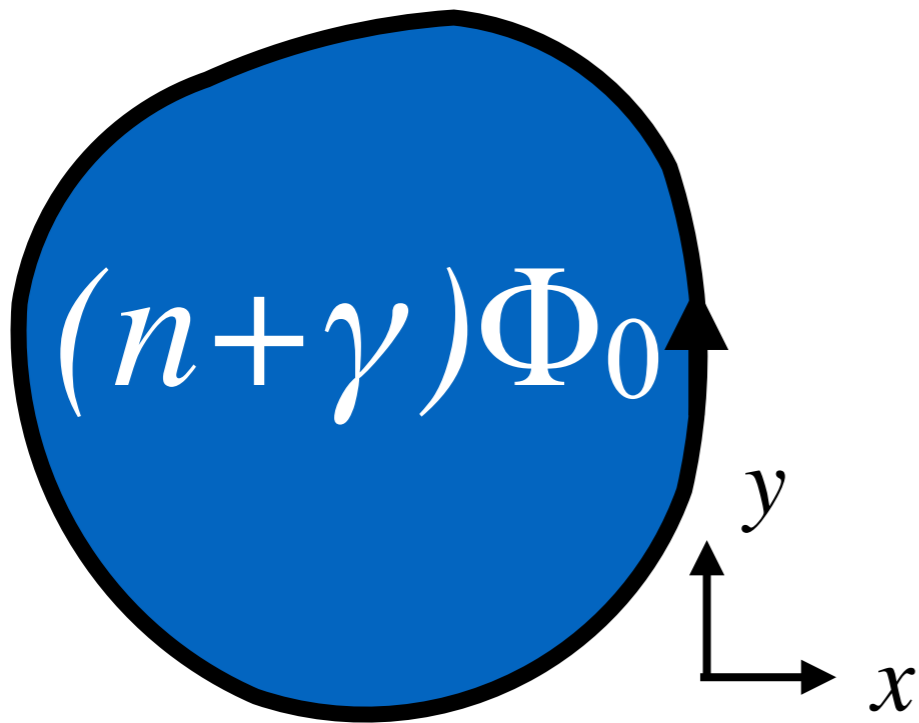
# Onsager's argument

$$\oint_C \mathbf{p} \cdot d\mathbf{q} = (n + \gamma)2\pi\hbar$$

**Adiabatic invariant**

$$\mathbf{p} = \hbar\mathbf{k} - e\mathbf{A}$$

$$\begin{aligned}\Phi &\equiv BA = (n + \gamma)2\pi\frac{\hbar}{e} \\ &= (n + \gamma)\Phi_0\end{aligned}$$

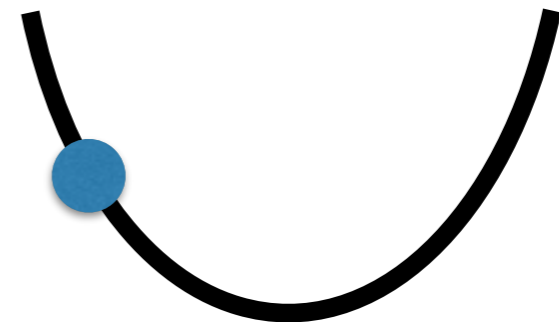
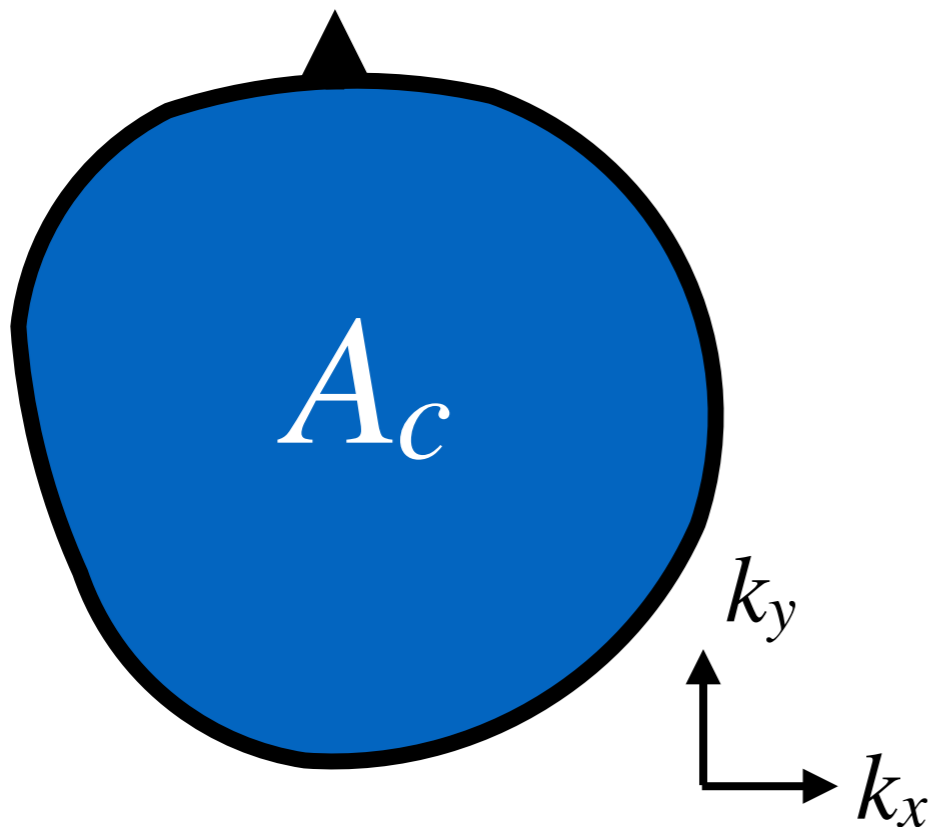


# From flux quantization to energy quantization

$$A_c = (n + \gamma)4\pi^2 B / \Phi_0$$

$$\omega_c = \frac{eB}{m^*}$$

$$\varepsilon_c = (n + \gamma)\hbar\omega_c$$

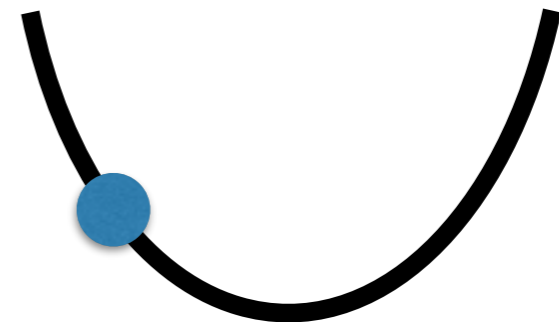
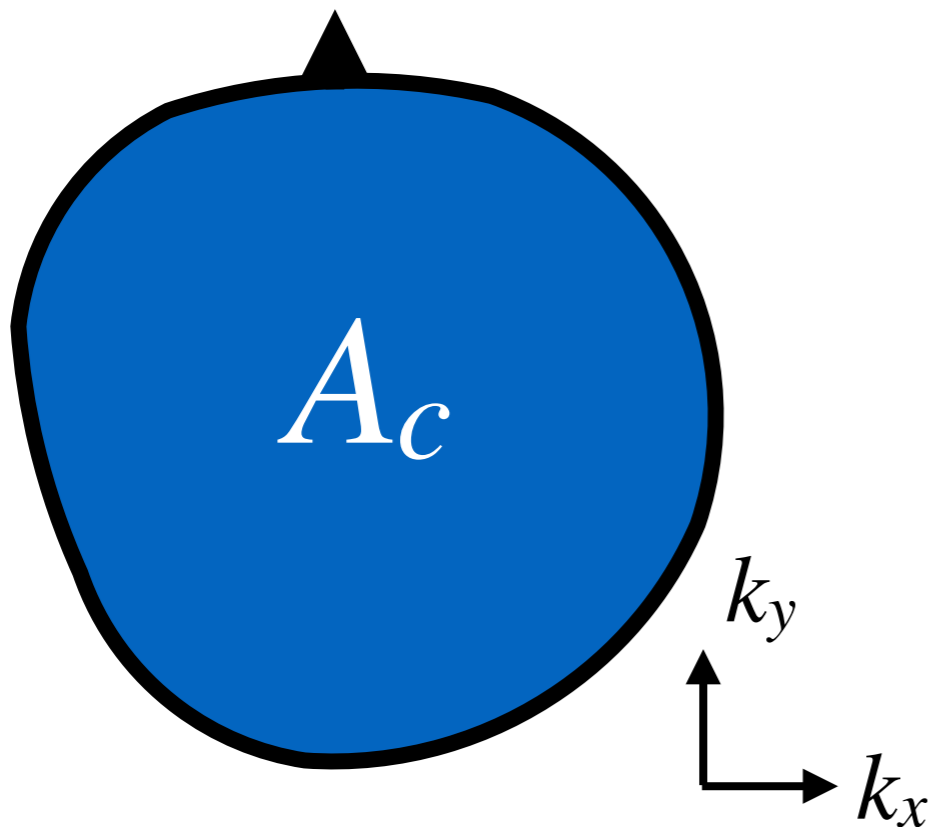


# From flux quantization to energy quantization

$$A_c = (n + \gamma)4\pi^2 B / \Phi_0$$

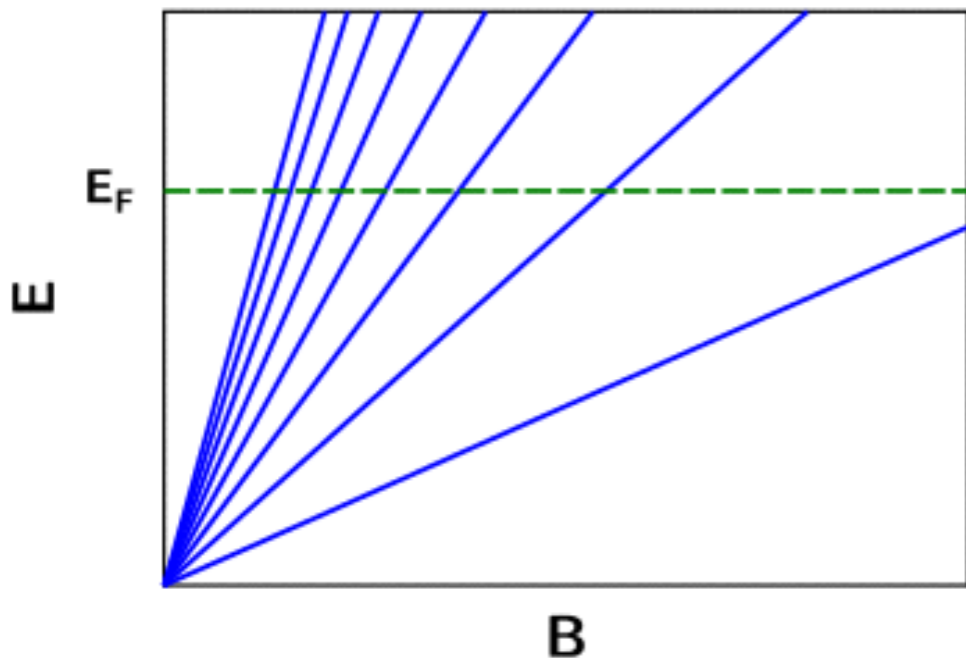
$$\omega_c = \frac{eB}{m^*}$$

$$\varepsilon_c = (n + \gamma)\hbar\omega_c$$



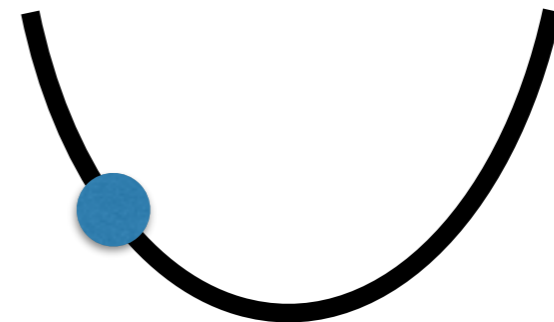
# From flux quantization to energy quantization

$$A_c = (n + \gamma) 4\pi^2 B / \Phi_0$$



$$\omega_c = \frac{eB}{m^*}$$

$$\varepsilon_c = (n + \gamma) \hbar \omega_c$$

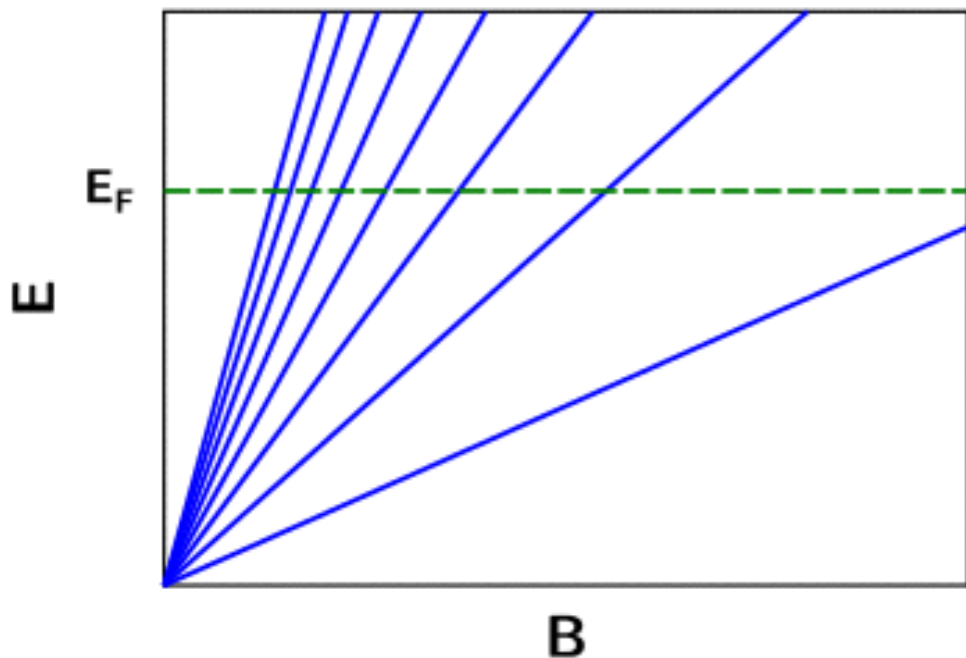


# From flux quantization to energy quantization

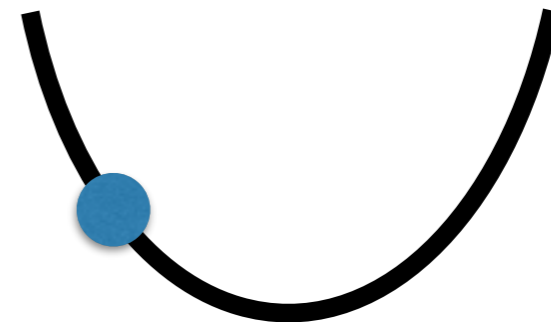
$$A_c = (n + \gamma)4\pi^2 B / \Phi_0$$



$$\omega_c = \frac{eB}{m^*}$$

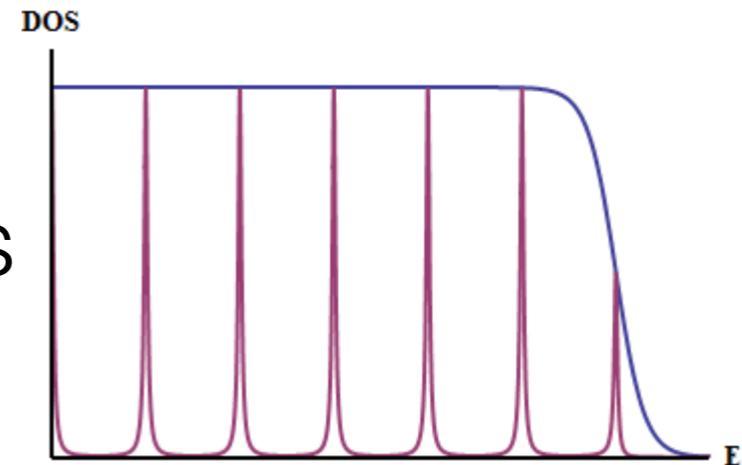
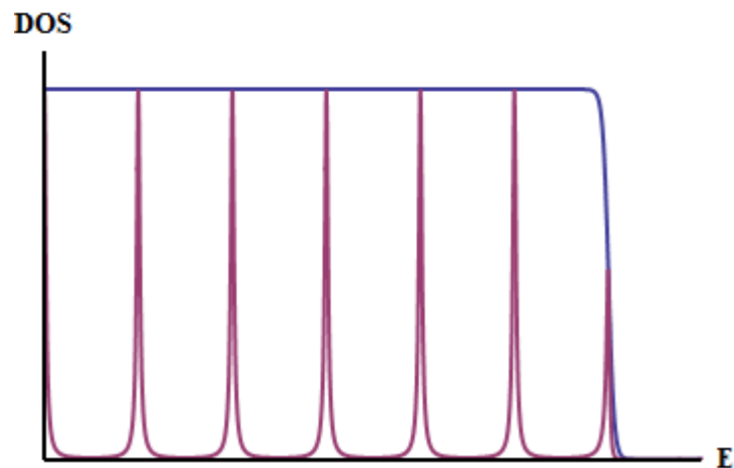


$$\varepsilon_c t_c = (n + \gamma)2\pi\hbar$$

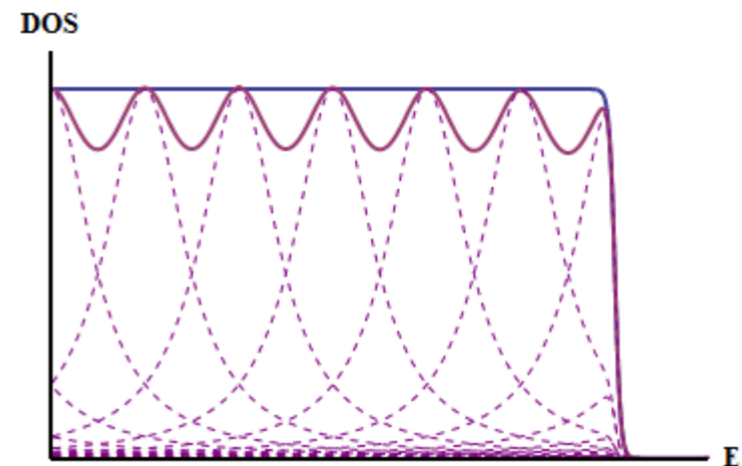


# Disorder and thermal fluctuations

Thermal fluctuations



Disorder



# Quantum oscillations are a litmus test for metal purity

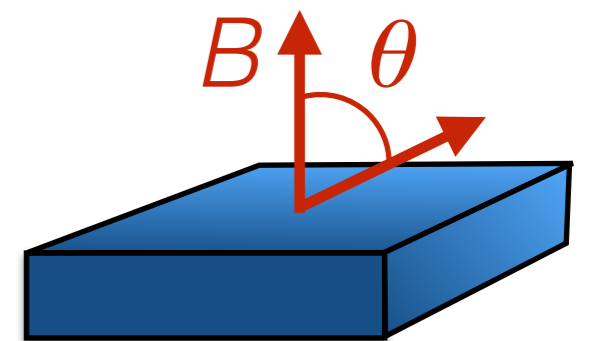
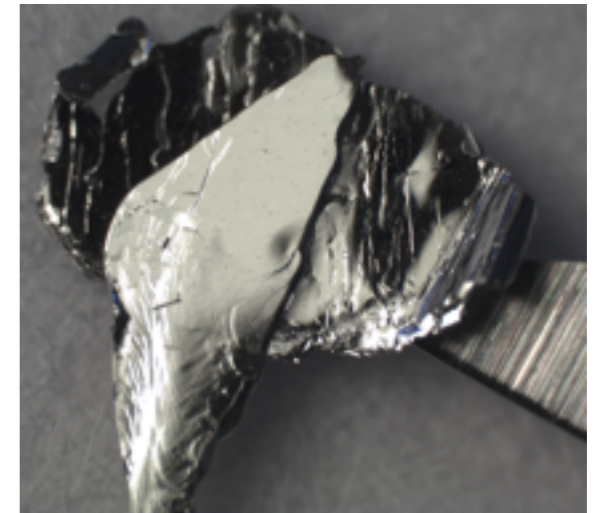
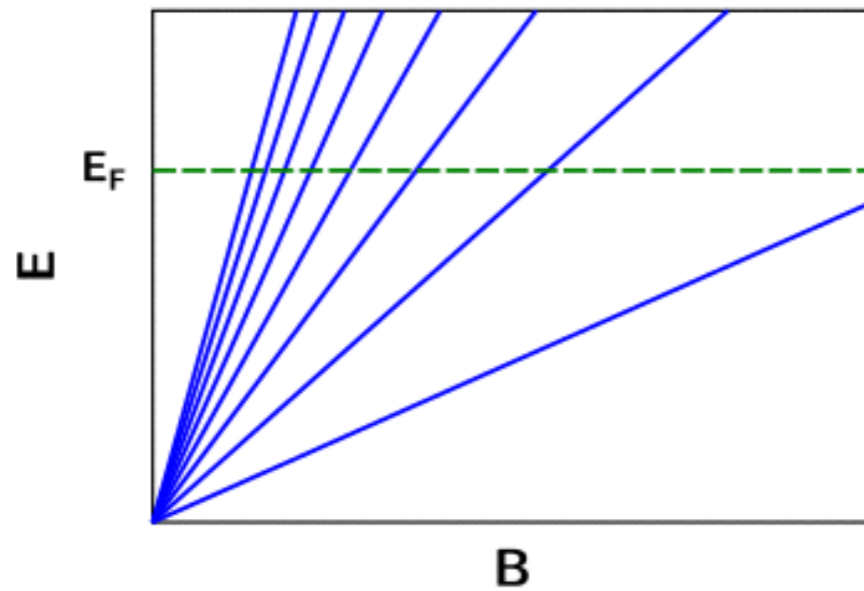
- Consider a really clean metal with a Fermi velocity of  $1 \times 10^6 \text{ m/s}$  and a mean free path 100nm.
- At 10T, the quantum oscillations are suppressed to **1:1000**.

# Quantum oscillations are a litmus test for metal purity

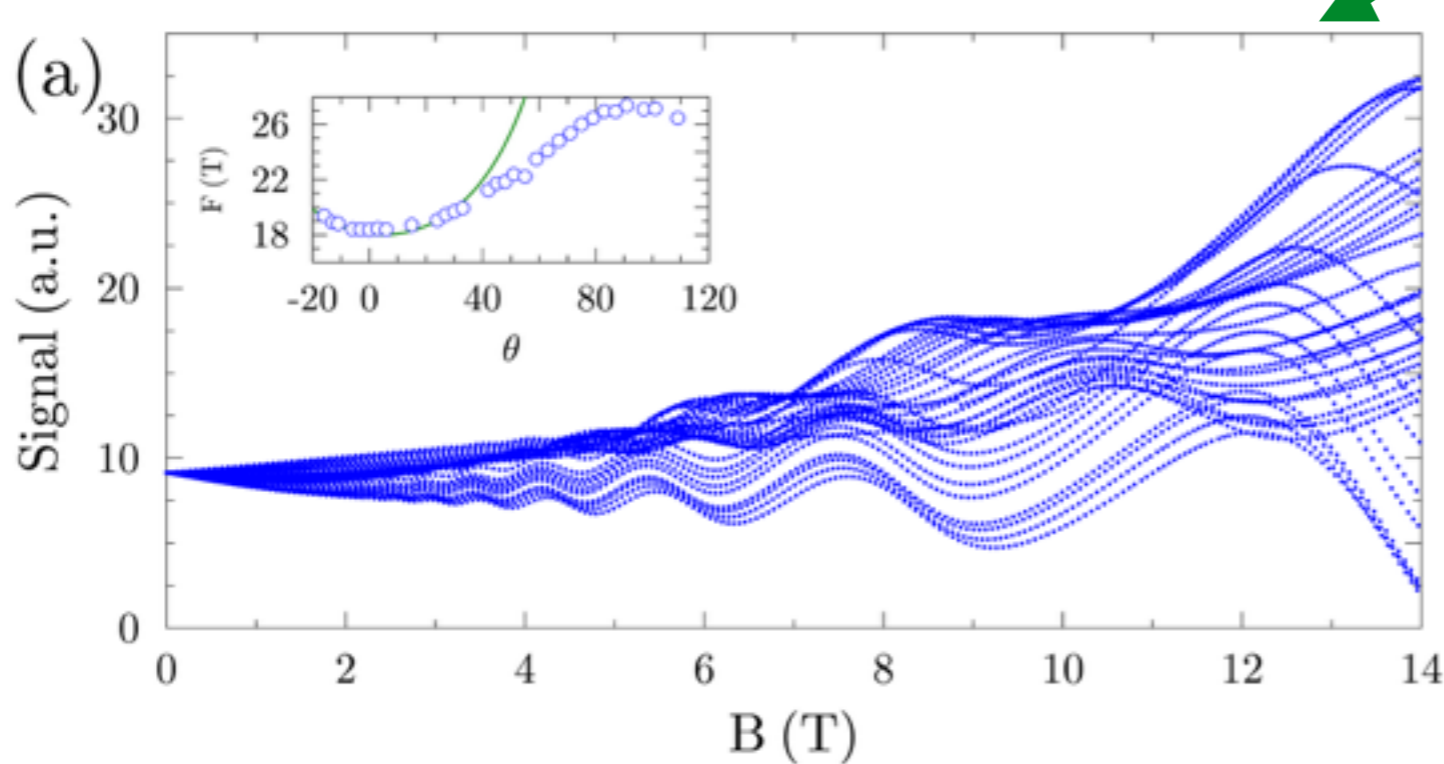
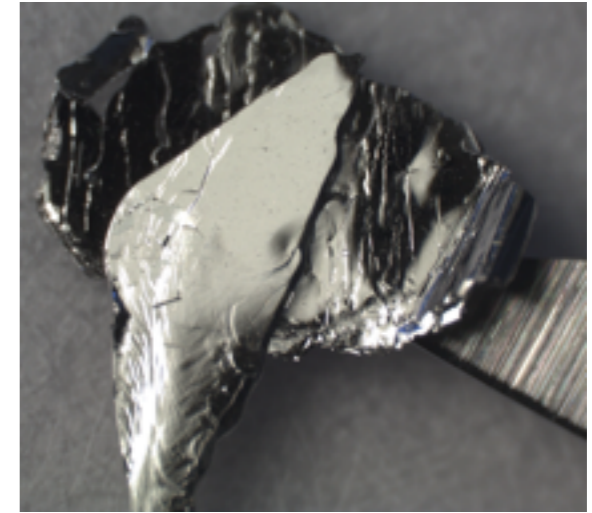
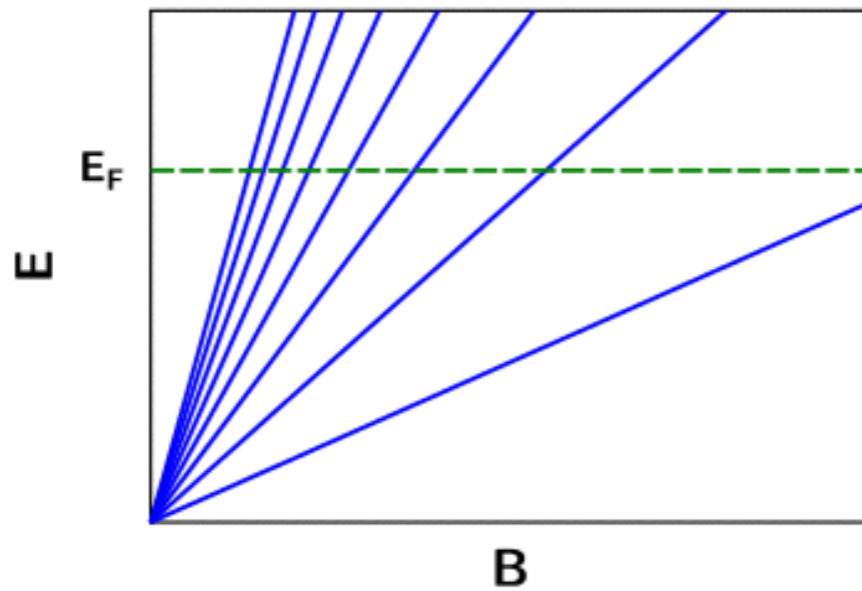
- Consider a really clean metal with a Fermi velocity of  $1 \times 10^6 \text{m/s}$  and a mean free path  $100 \text{nm}$ .
- At  $10 \text{T}$ , the quantum oscillations are suppressed to **1:1000**.
- Now consider a pretty good metal with a Fermi velocity of  $1 \times 10^6 \text{m/s}$  and a mean free path  $10 \text{nm}$ .
- At  $10 \text{T}$ , the quantum oscillations are suppressed to **1:10<sup>27</sup>!**



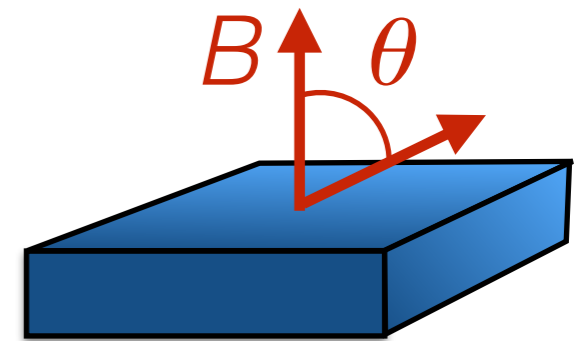
# Bulk Quantum oscillations in $\text{Bi}_2\text{Se}_3$



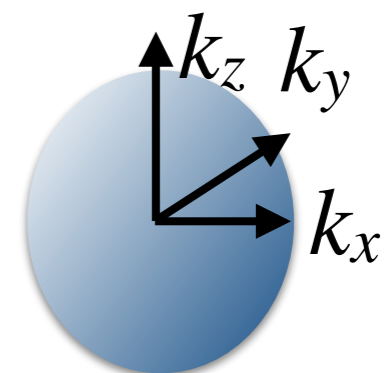
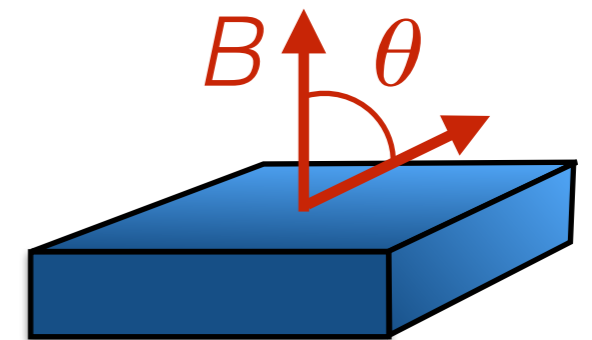
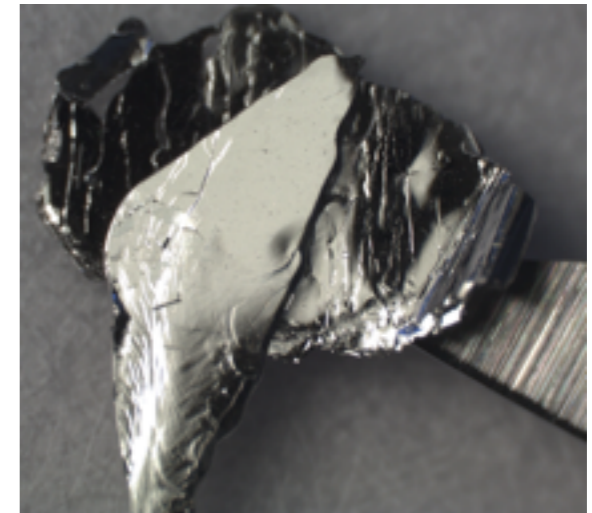
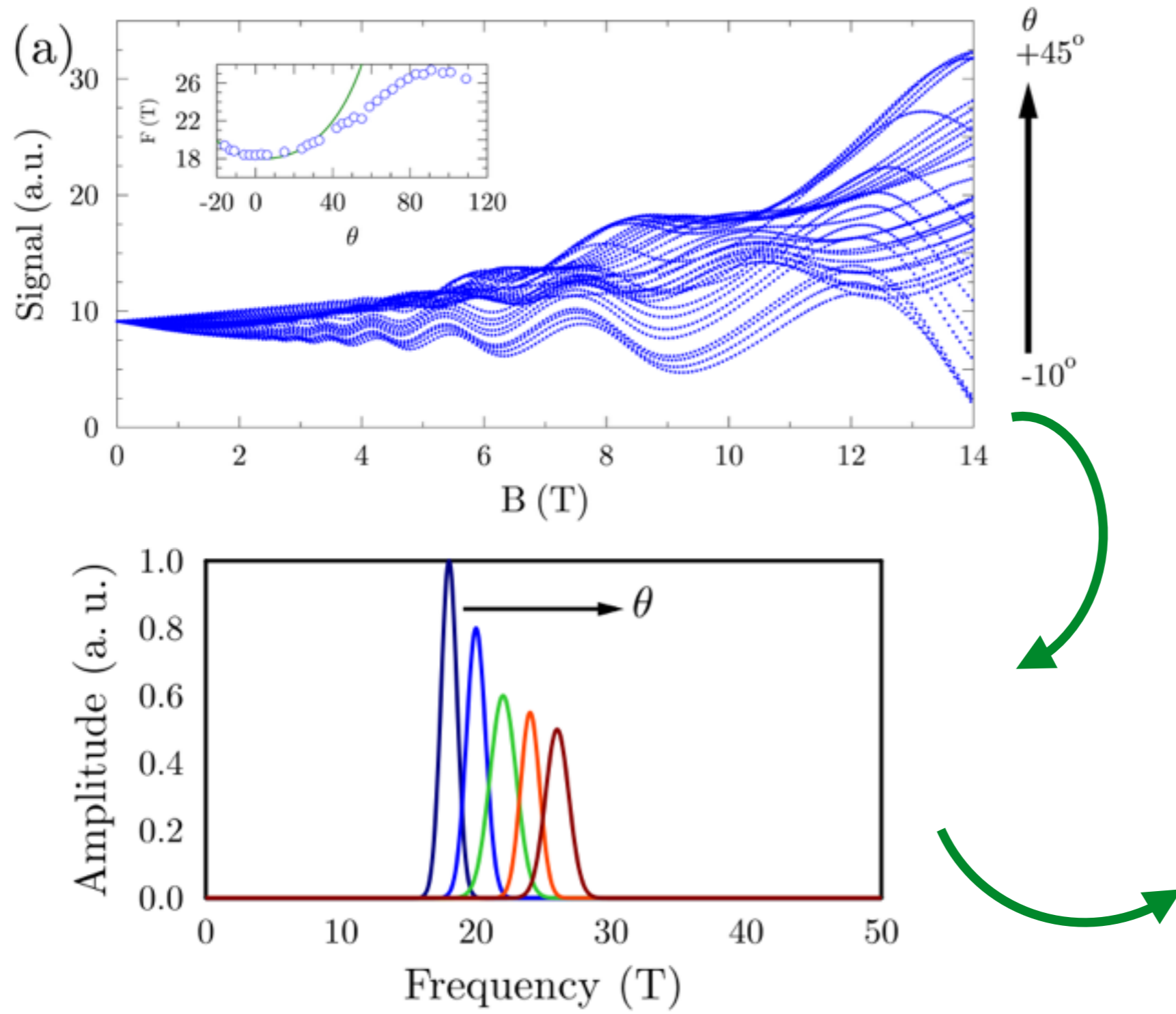
# Bulk Quantum oscillations in $\text{Bi}_2\text{Se}_3$



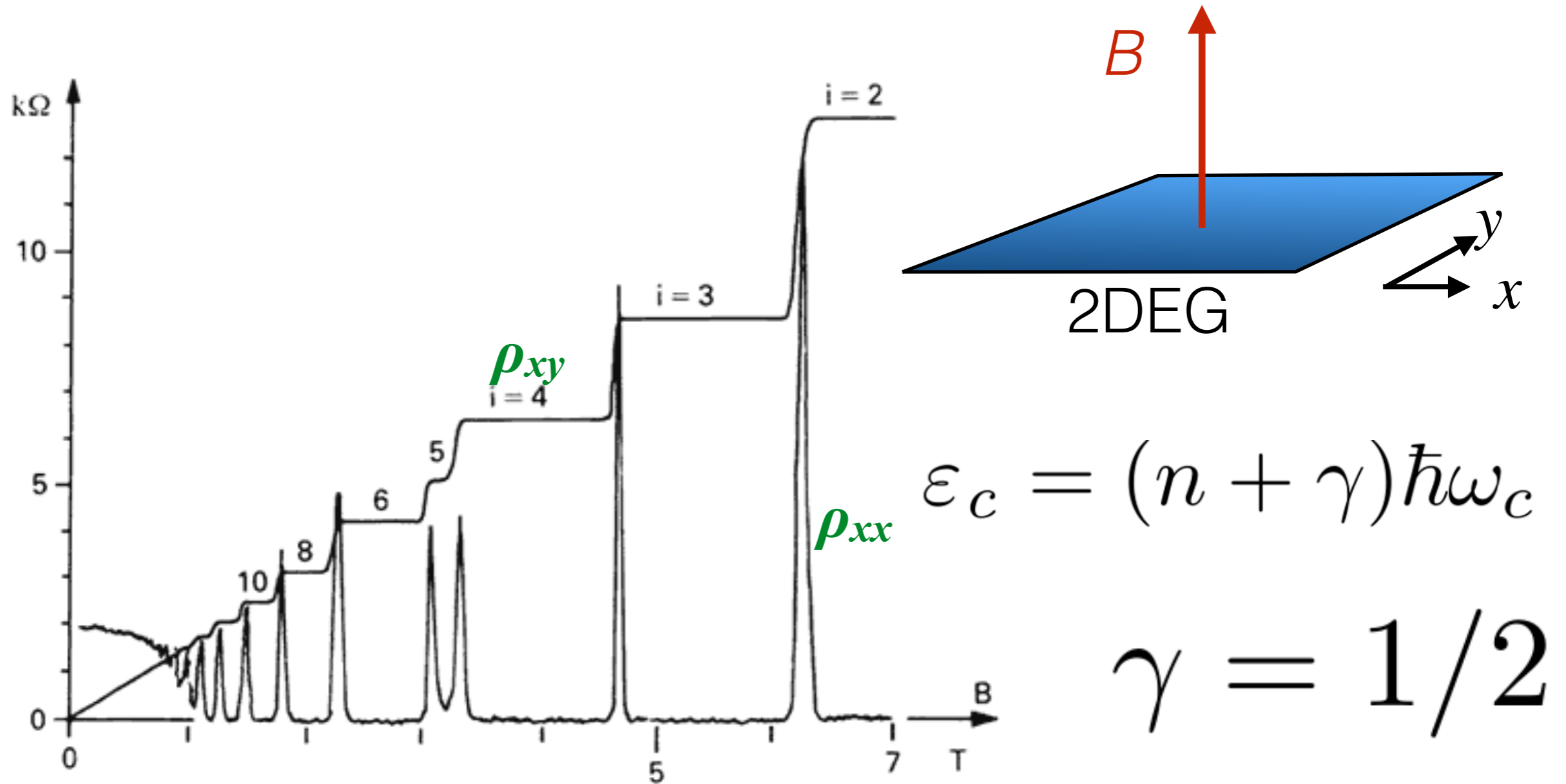
$\theta$   
 $+45^\circ$   
 $-10^\circ$



# Bulk Quantum oscillations in $\text{Bi}_2\text{Se}_3$

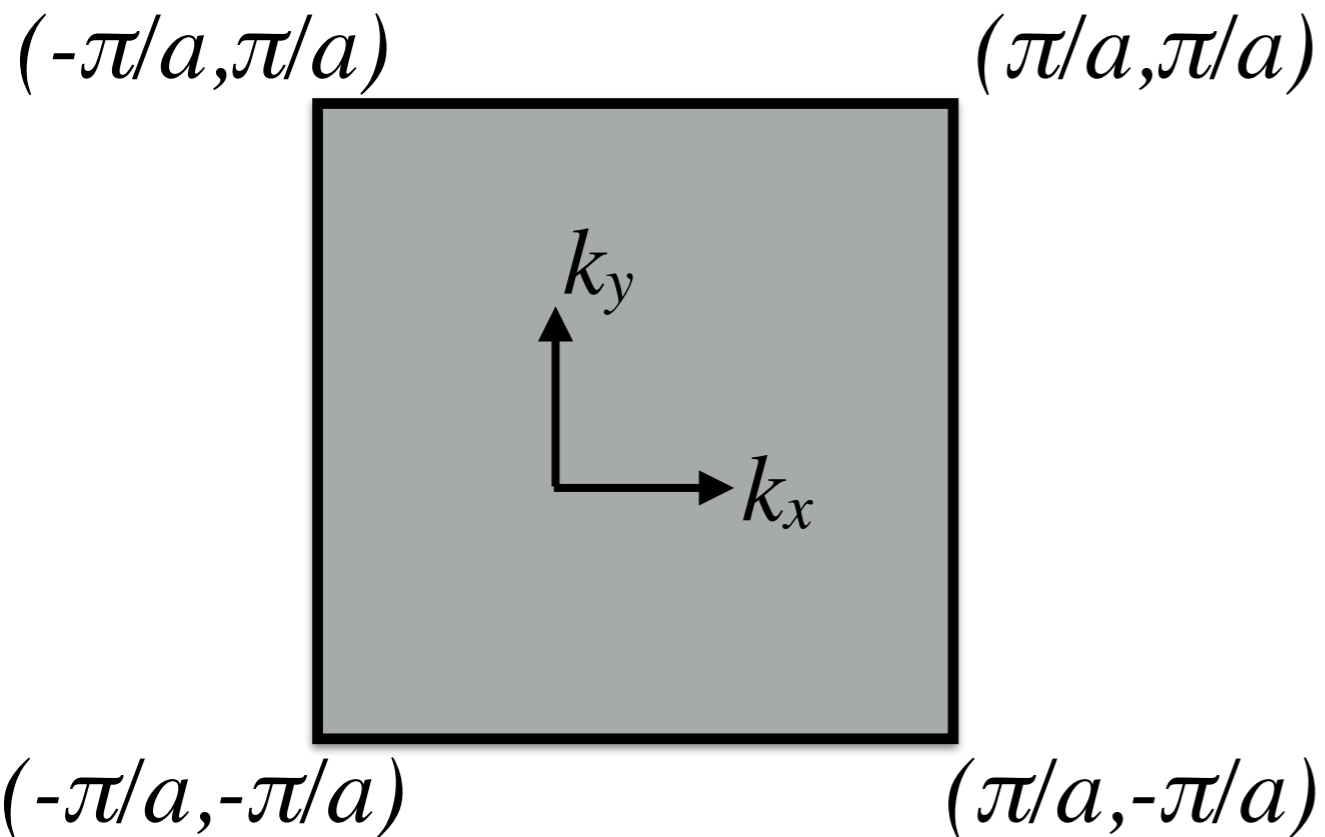


# Integer quantum Hall effect



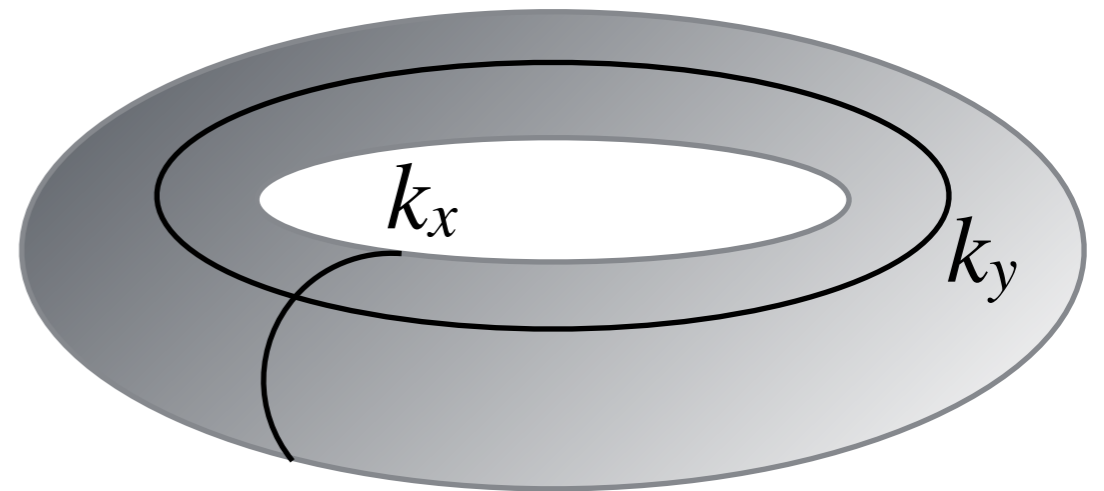
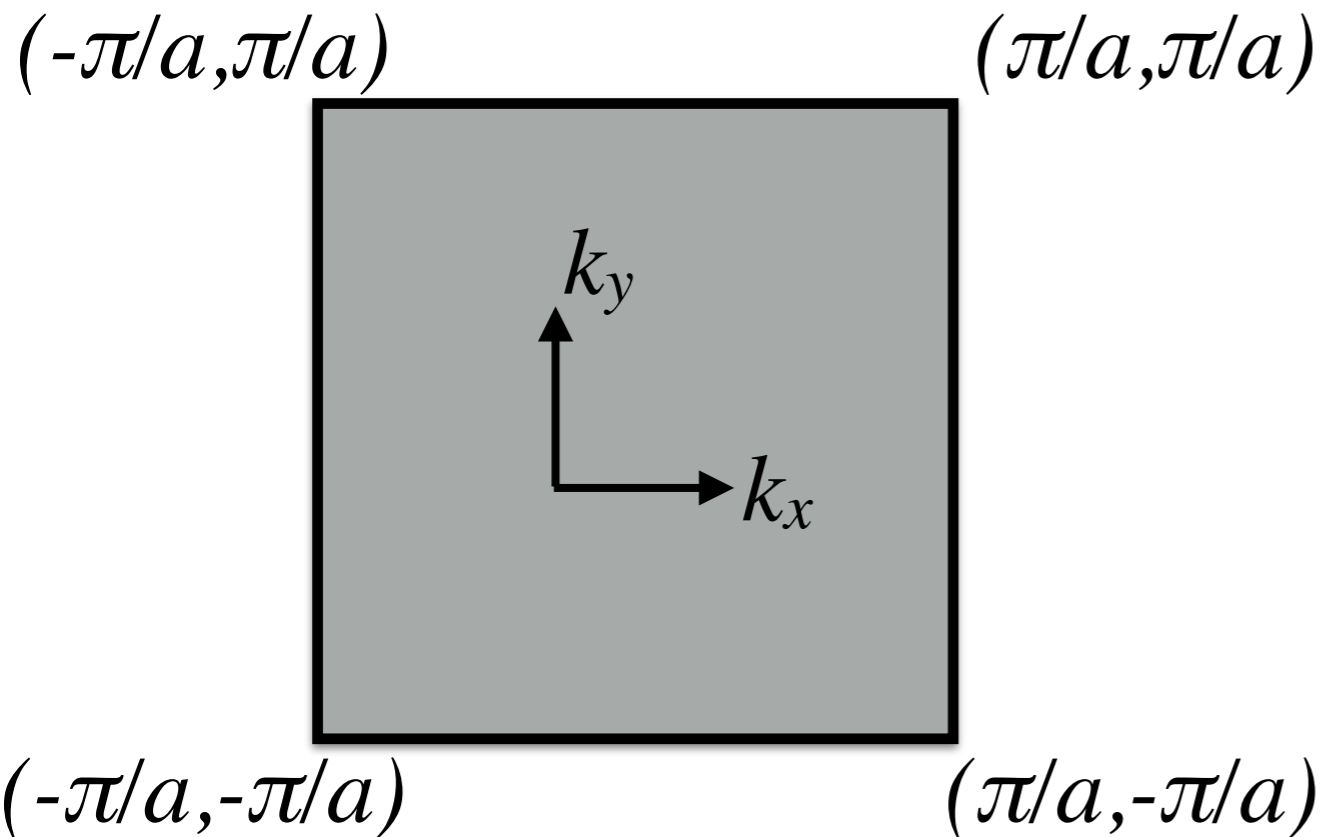
von Klitzing, Dorda and Pepper, PRL 1980

# Berry curvature



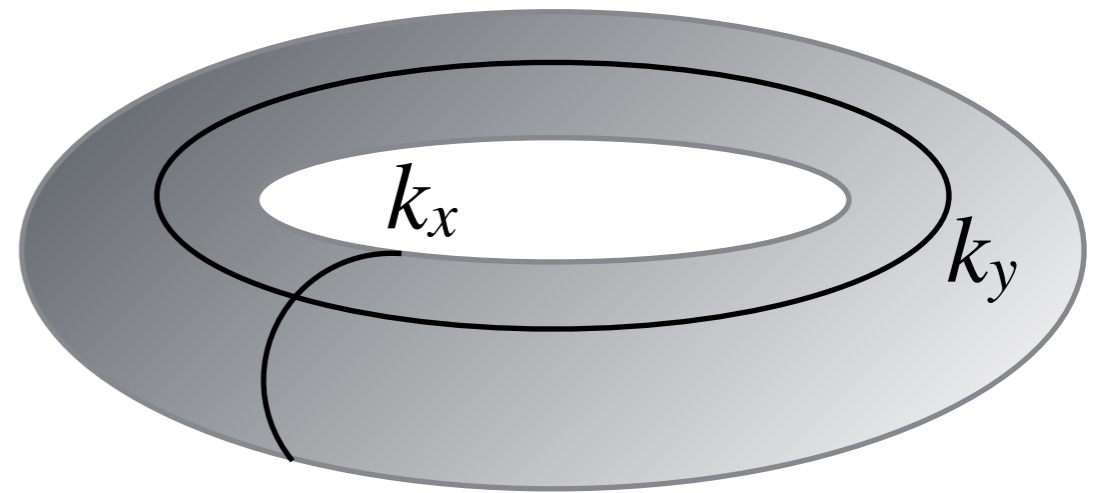
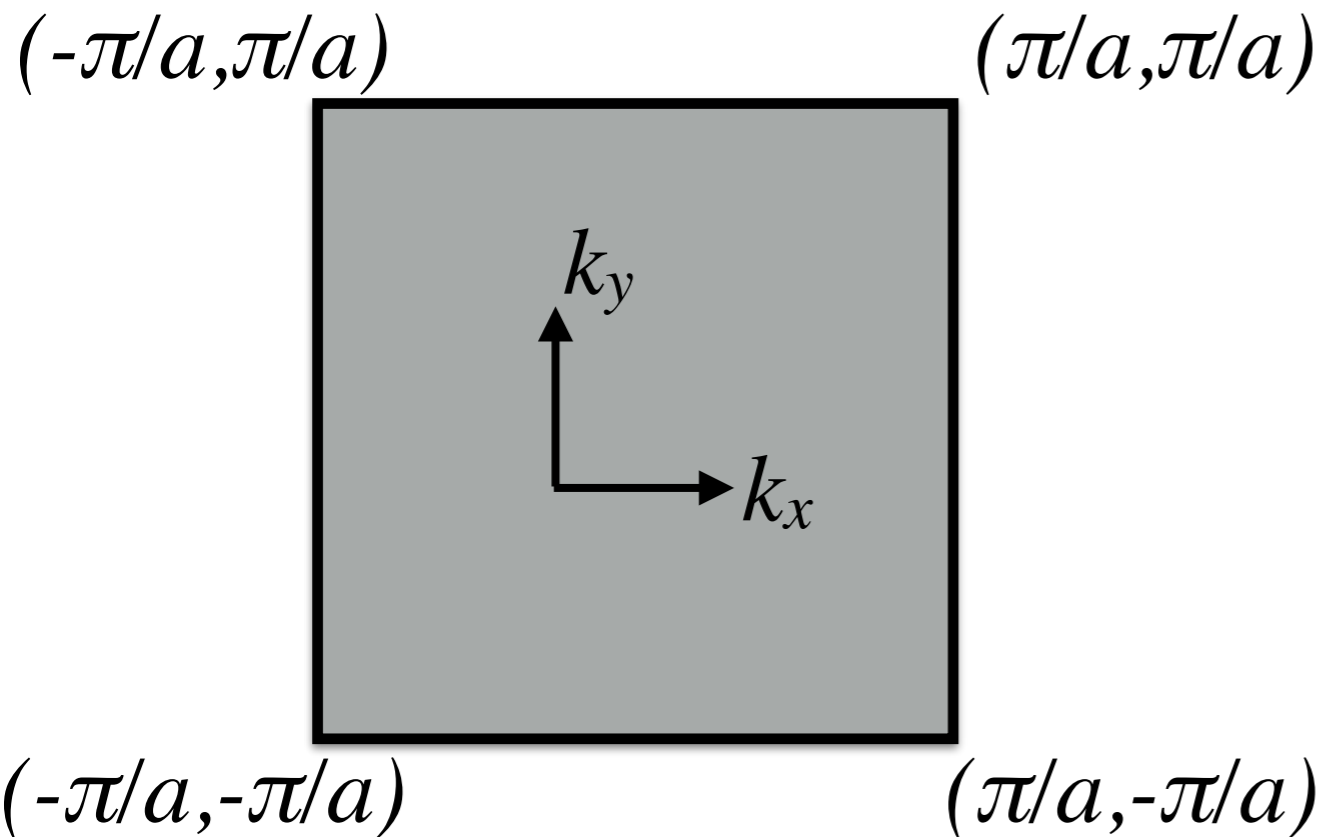
- IQHE can be understood as a topological invariant arising from the topology of wave functions, which in this case exist in a (magnetic) Brillouin zone with the topology of a torus.

# Berry curvature



- IQHE can be understood as a topological invariant arising from the topology of wave functions, which in this case exist in a (magnetic) Brillouin zone with the topology of a torus.

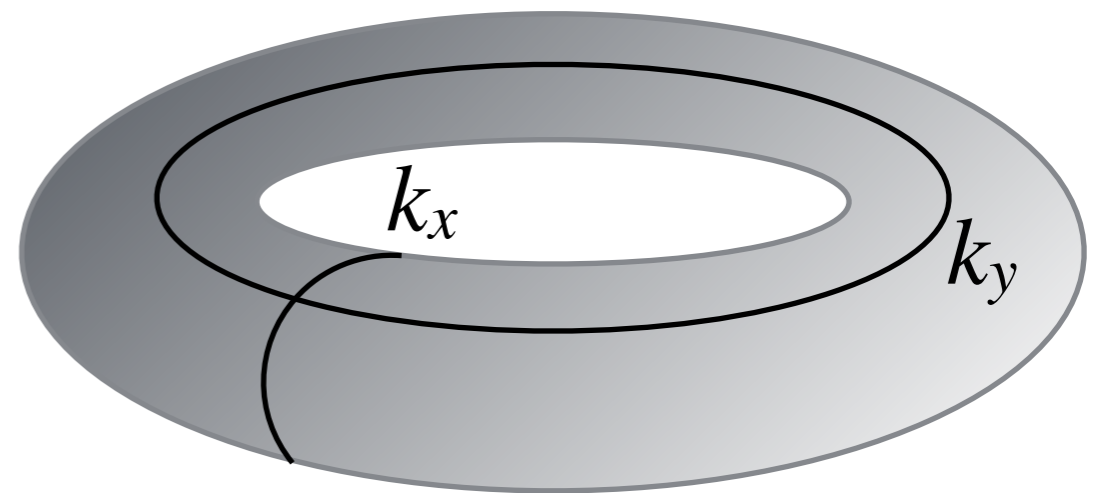
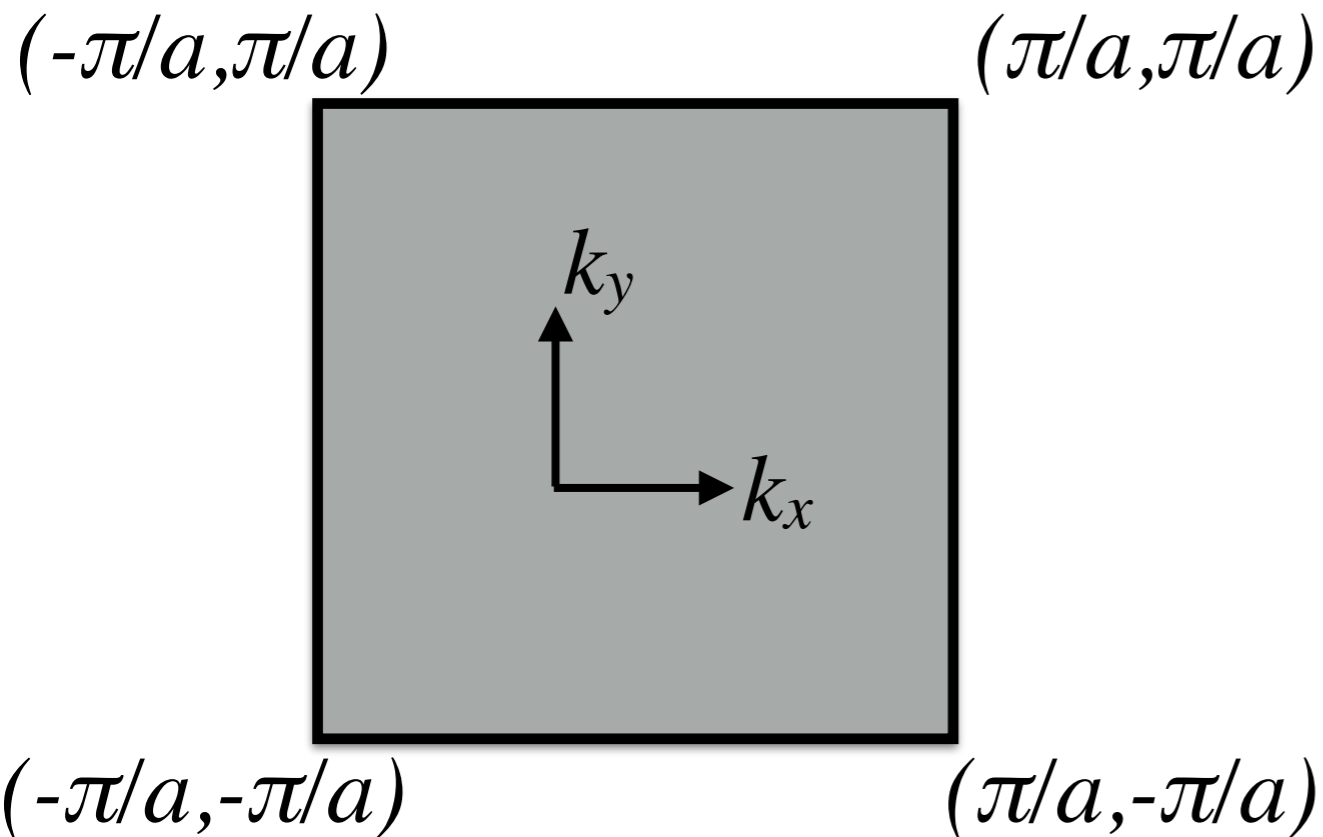
# Berry curvature



$$\gamma_B(C) = i \oint_C \langle n(\mathbf{R}) | \nabla_{\mathbf{R}} | n(\mathbf{R}) \rangle$$

- IQHE can be understood as a topological invariant arising from the topology of wave functions, which in this case exist in a (magnetic) Brillouin zone with the topology of a torus.

# Berry curvature



$$\gamma_B(C) = i \oint_C \langle n(\mathbf{R}) | \nabla_R | n(\mathbf{R}) \rangle$$

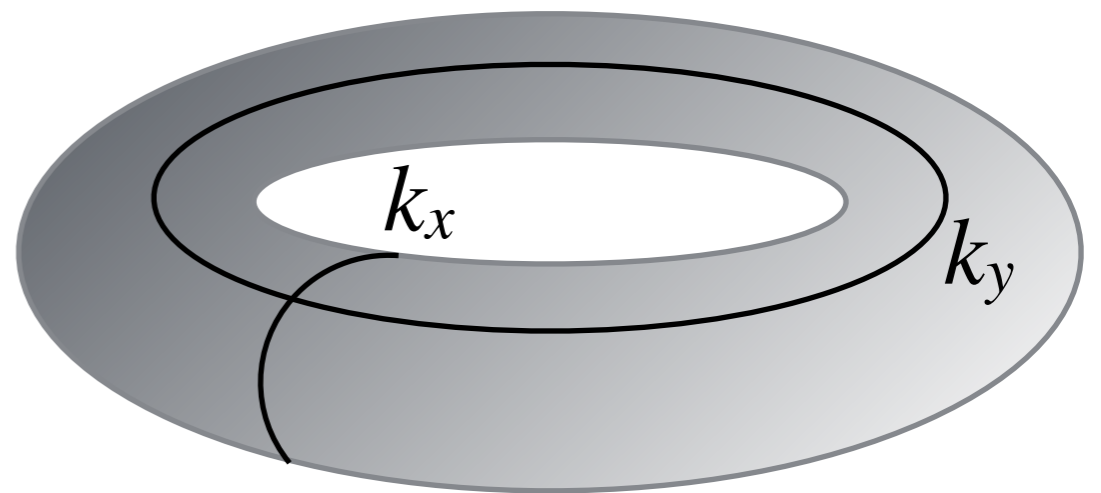
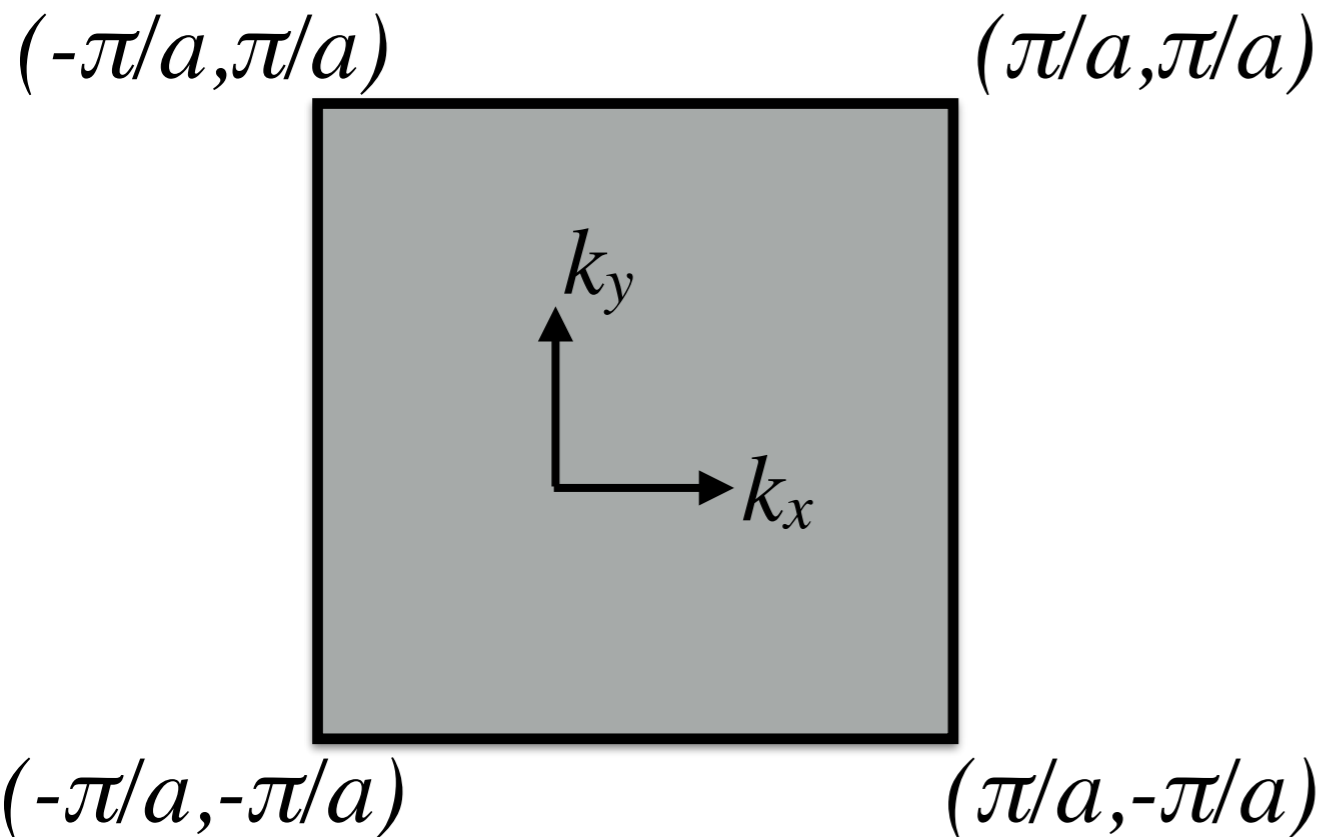
$$\Omega = \nabla \times \langle n(\mathbf{R}) | \nabla_R | n(\mathbf{R}) \rangle$$



- IQHE can be understood as a topological invariant arising from the topology of wave functions, which in this case exist in a (magnetic) Brillouin zone with the topology of a torus.



# Berry curvature



$$\Omega = \nabla \times \langle n(\mathbf{R}) | \nabla_{\mathbf{R}} | n(\mathbf{R}) \rangle$$

$$\gamma_B(C) = i \oint_C \langle n(\mathbf{R}) | \nabla_{\mathbf{R}} | n(\mathbf{R}) \rangle$$

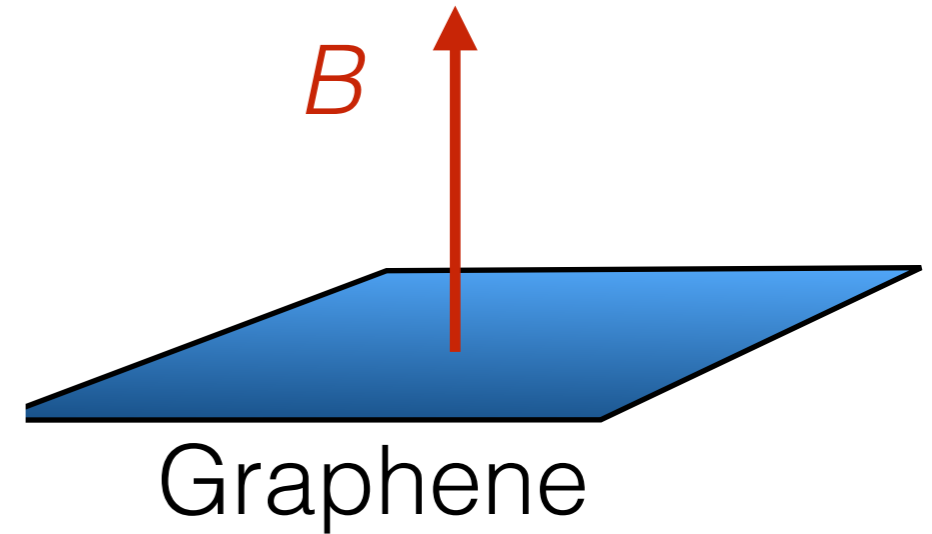
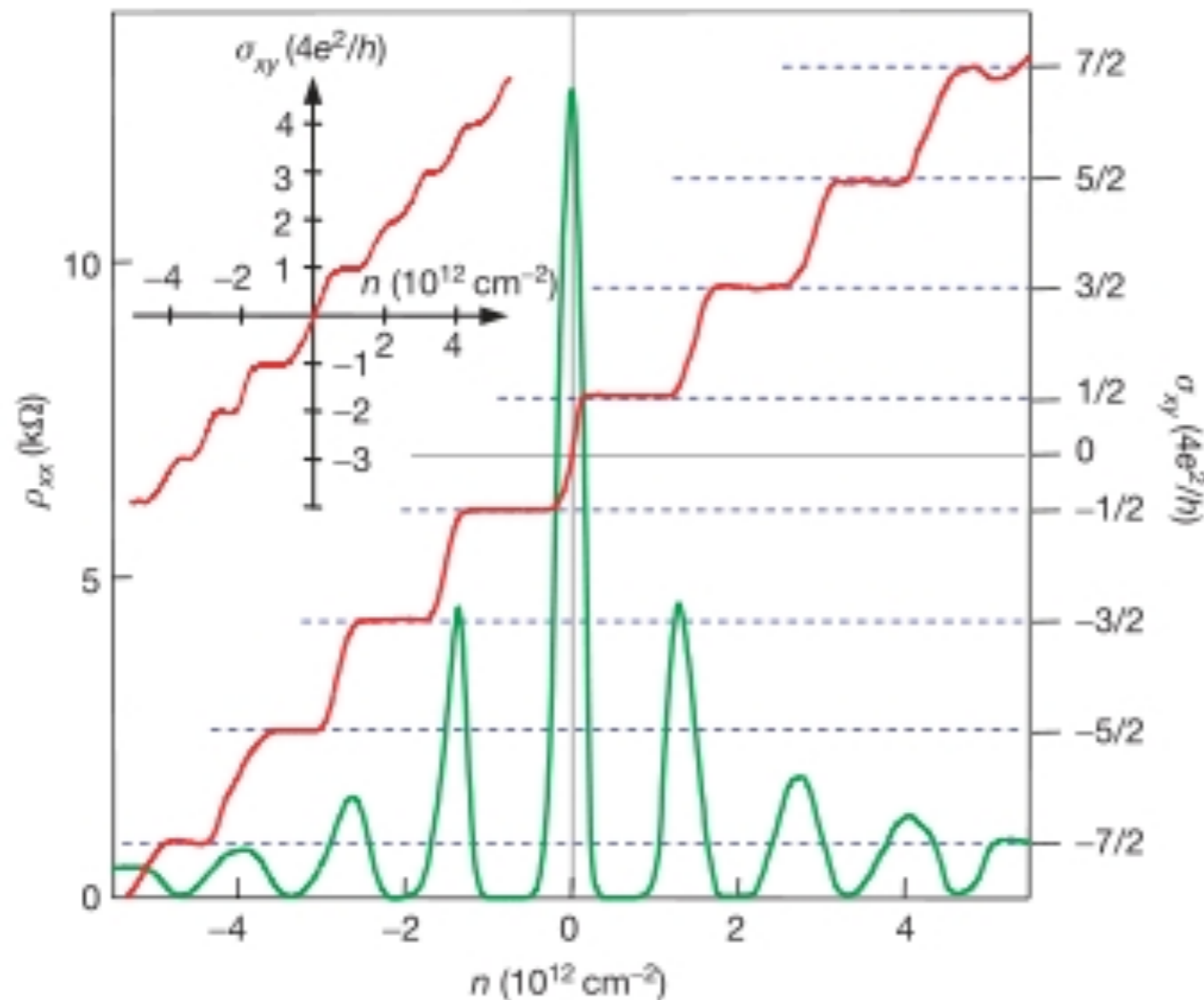
$$\sigma_{xy} = \frac{e^2}{\hbar} \int_{BZ} \frac{d^2 k}{(2\pi)^2} \Omega$$

- IQHE can be understood as a topological invariant arising from the topology of wave functions, which in this case exist in a (magnetic) Brillouin zone with the topology of a torus.

$$\gamma = \gamma(0) - \frac{\gamma_B}{2\pi} \approx 1/2 - \frac{\gamma_B}{2\pi}$$

Mikitik and Sharlai PRL 1999, also Laura Roth PRB 1966

# Integer quantum Hall effect (graphene)

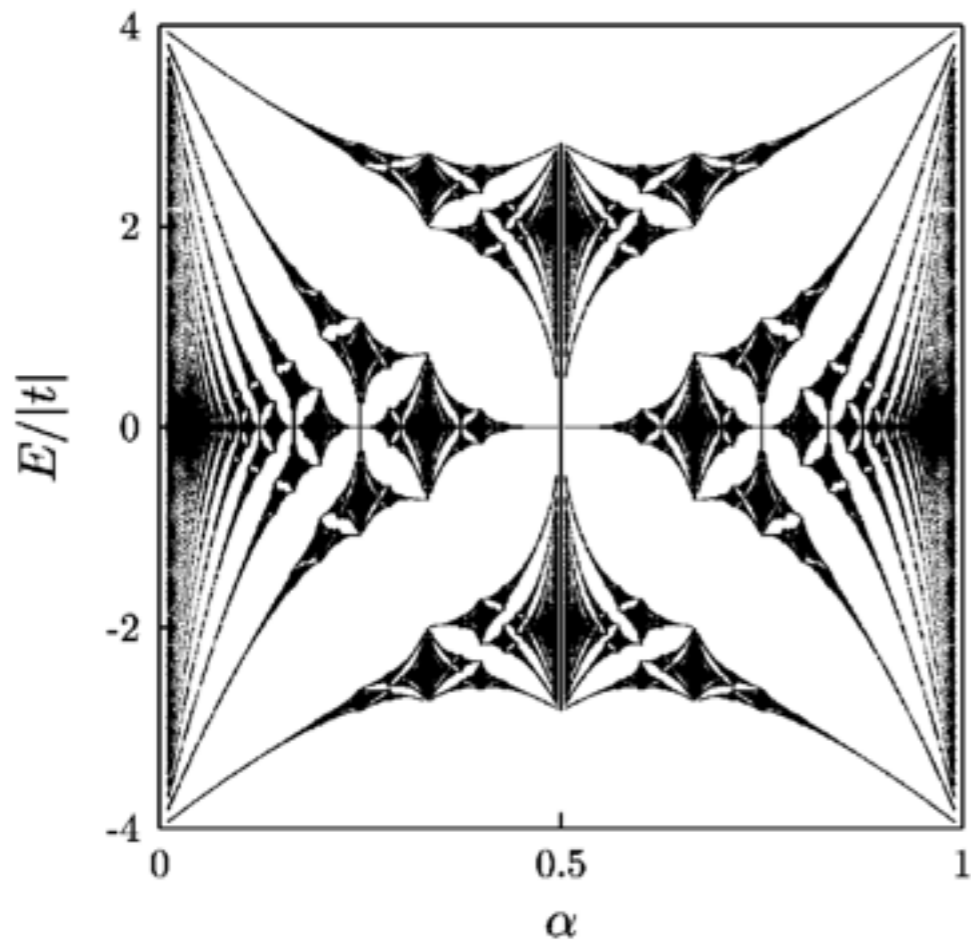


$$\varepsilon_n = \pm v_F \sqrt{2ne\hbar B}$$

$$\gamma = 0$$

P. Kim & Novoselov/Geim *Nature* 2005

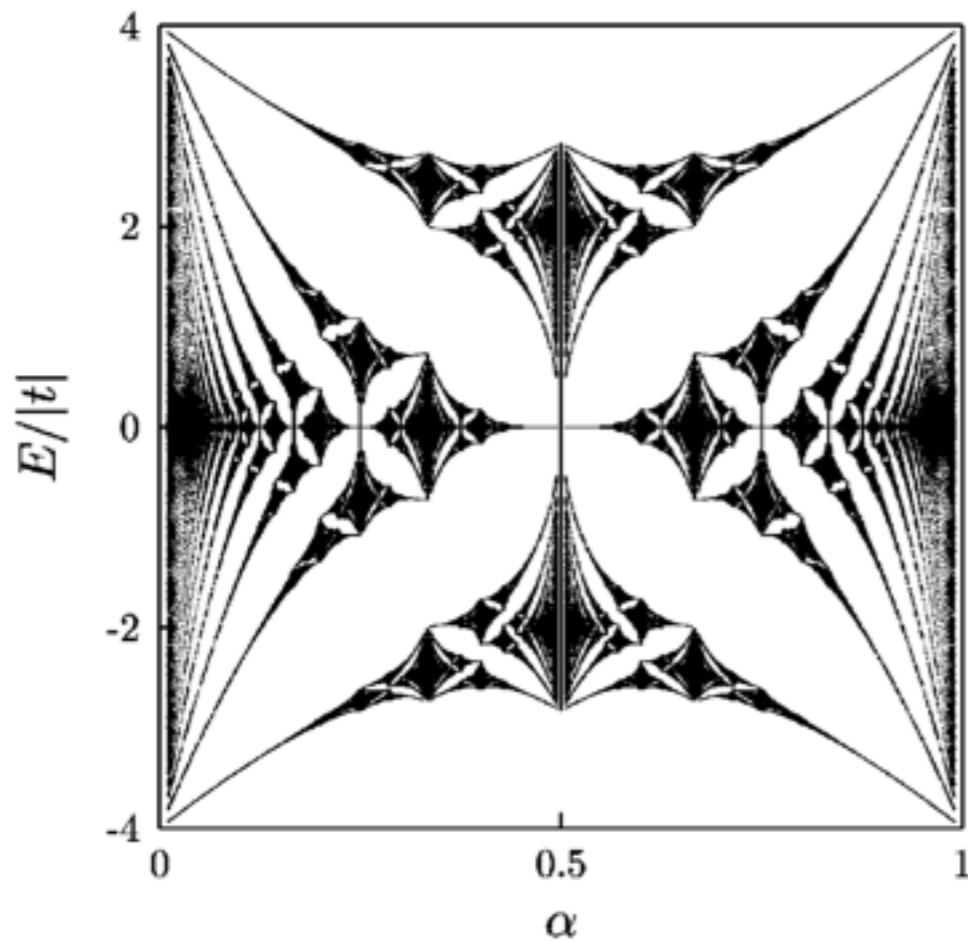
# Landau quantization in a 2D square lattice



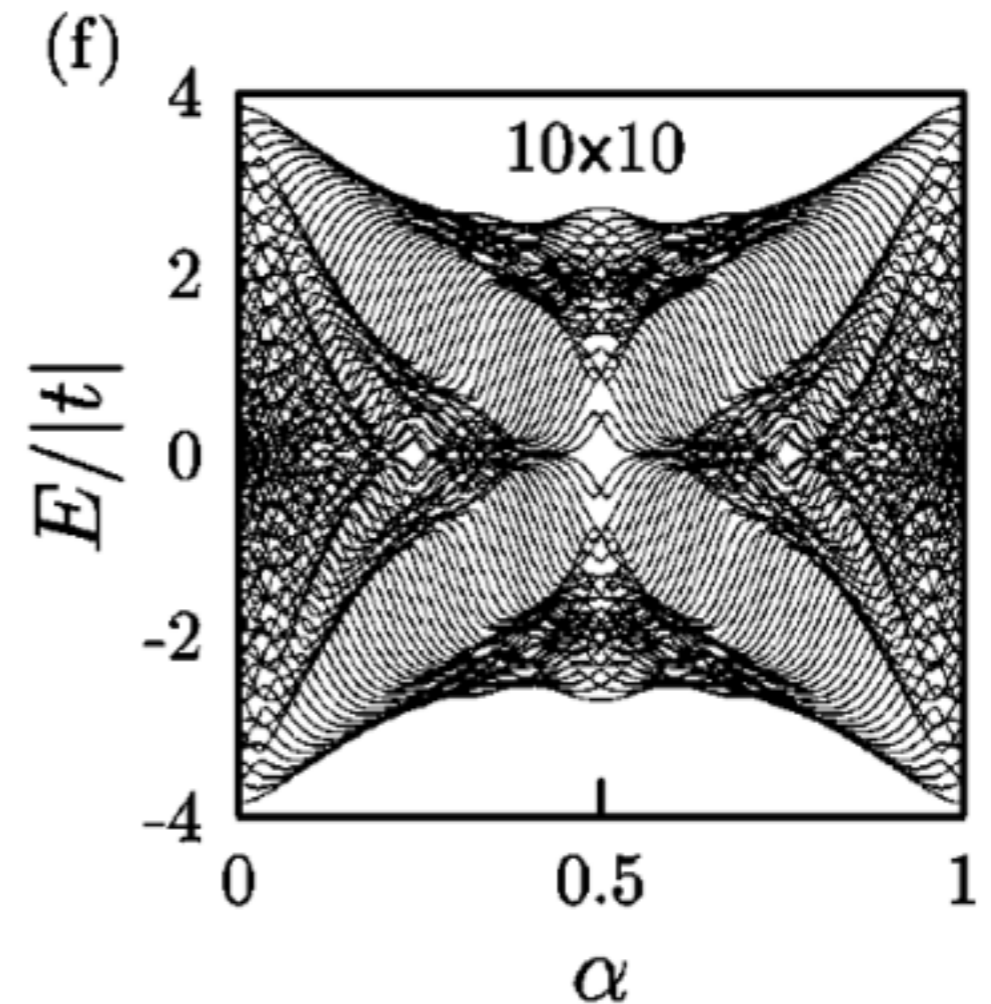
Hofstadter Butterfly (PRB 1976)

Analytis AMJP 2004

# Landau quantization in a 2D square lattice

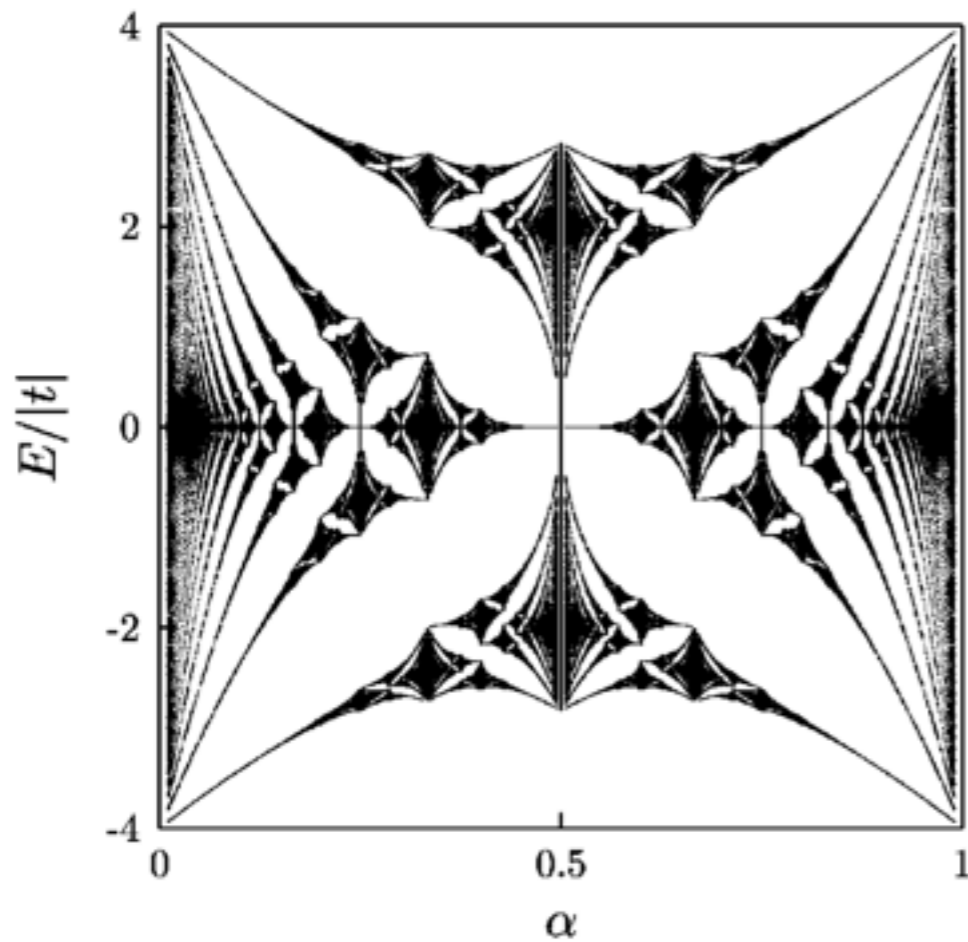


Hofstadter Butterfly (PRB 1976)

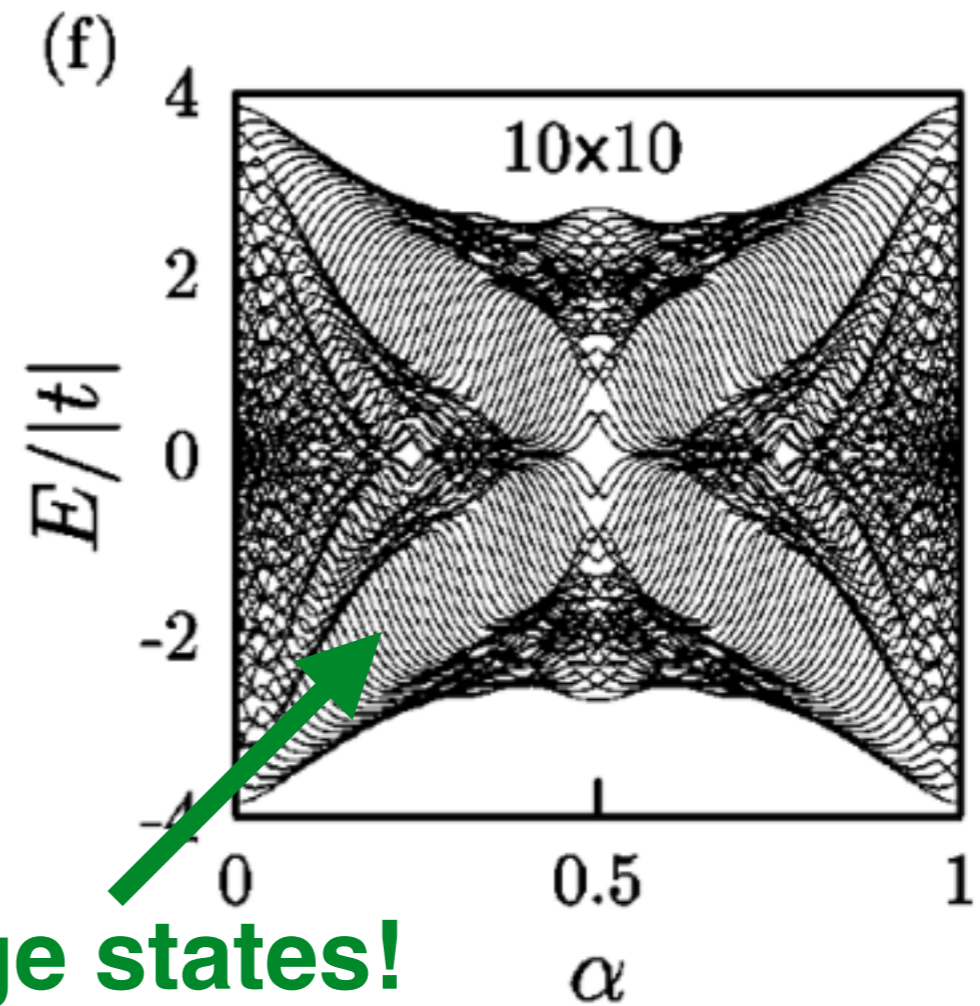


Analytis AMJP 2004

# Landau quantization in a 2D square lattice



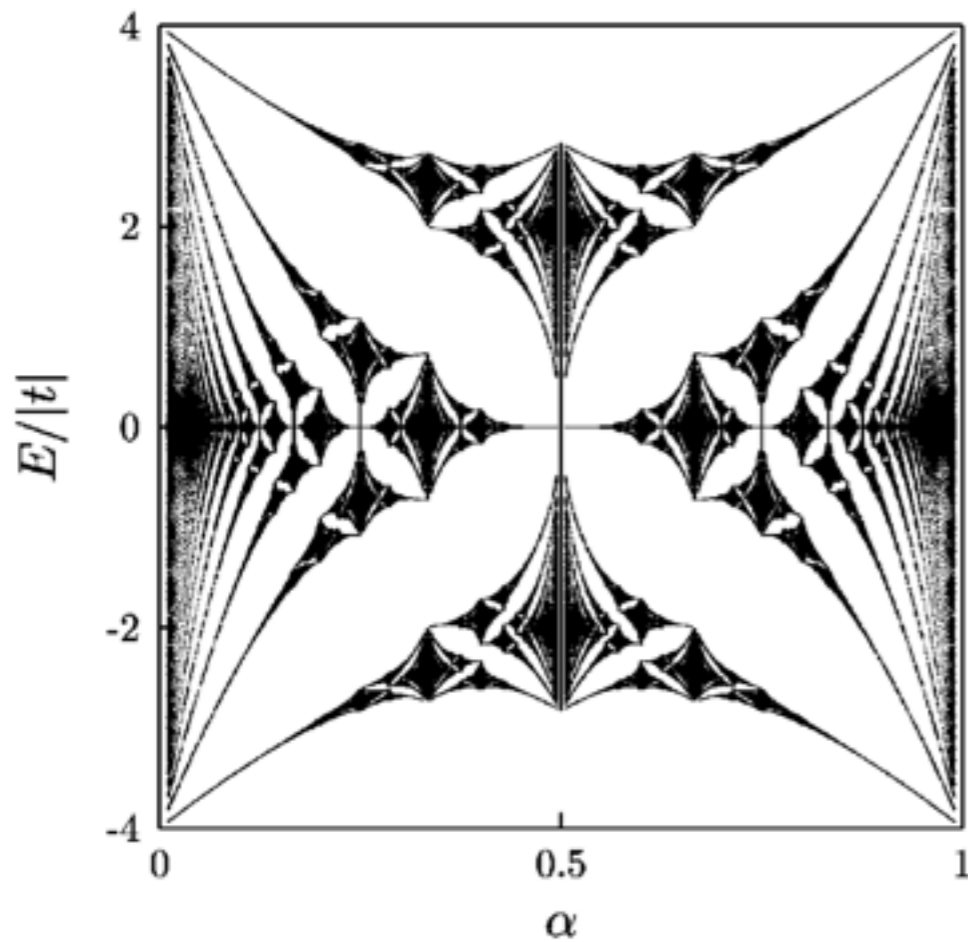
Hofstadter Butterfly (PRB 1976)



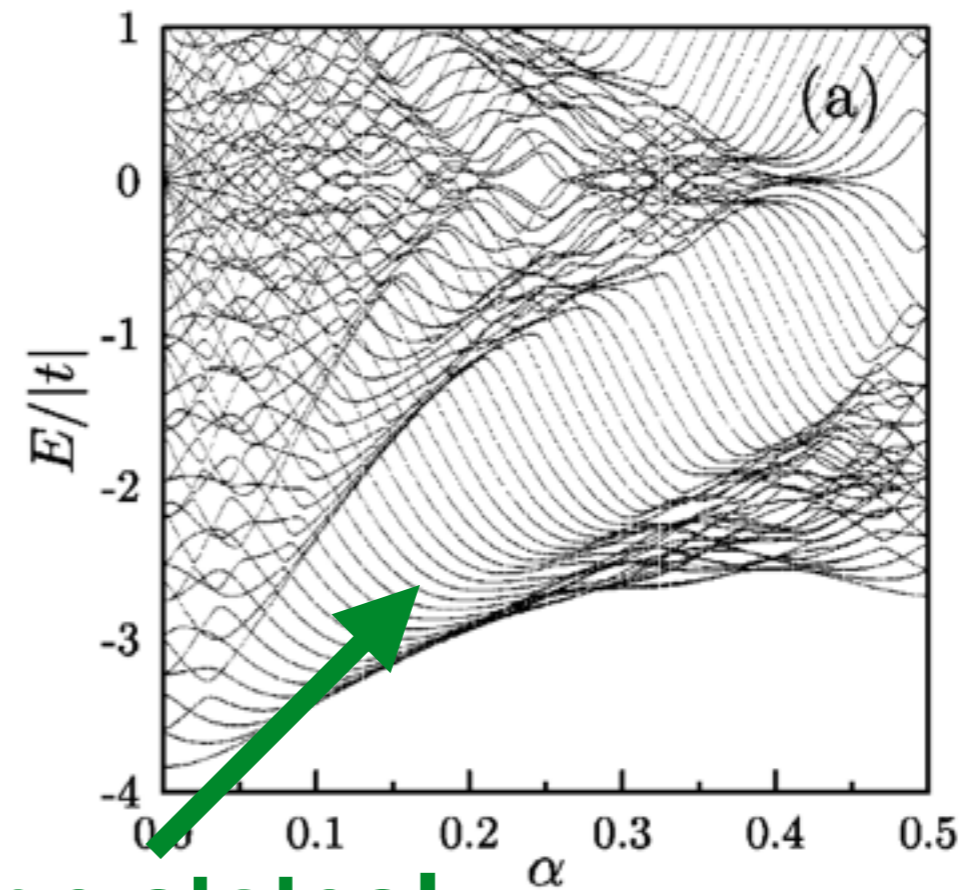
**Edge states!**

Analytis AMJP 2004

# Landau quantization in a 2D square lattice



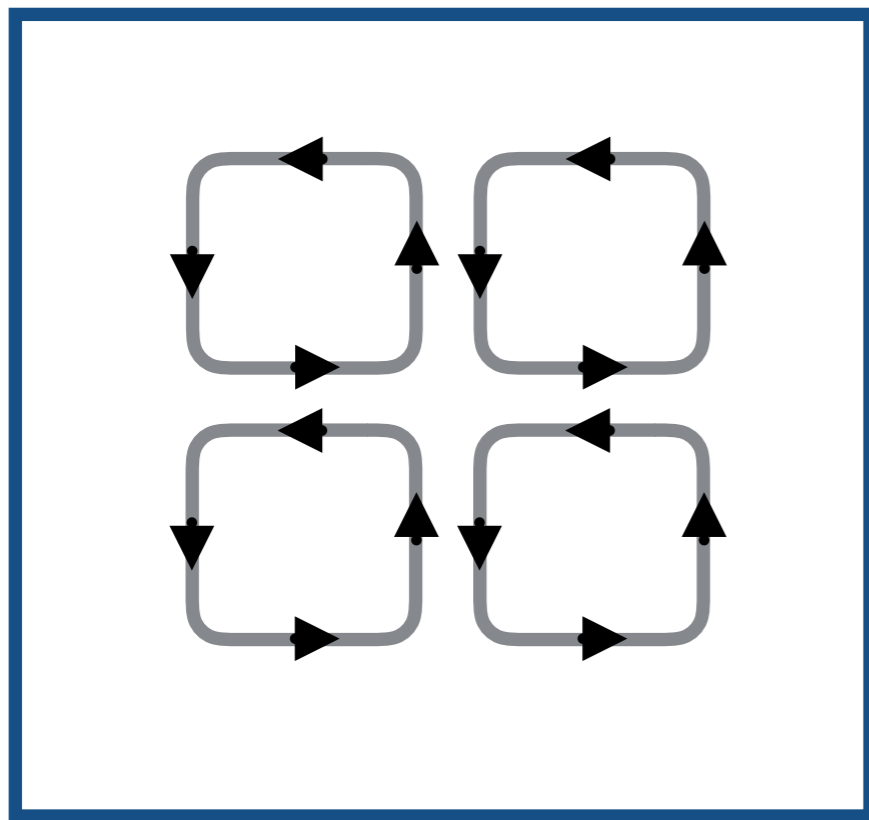
Hofstadter Butterfly (PRB 1976)



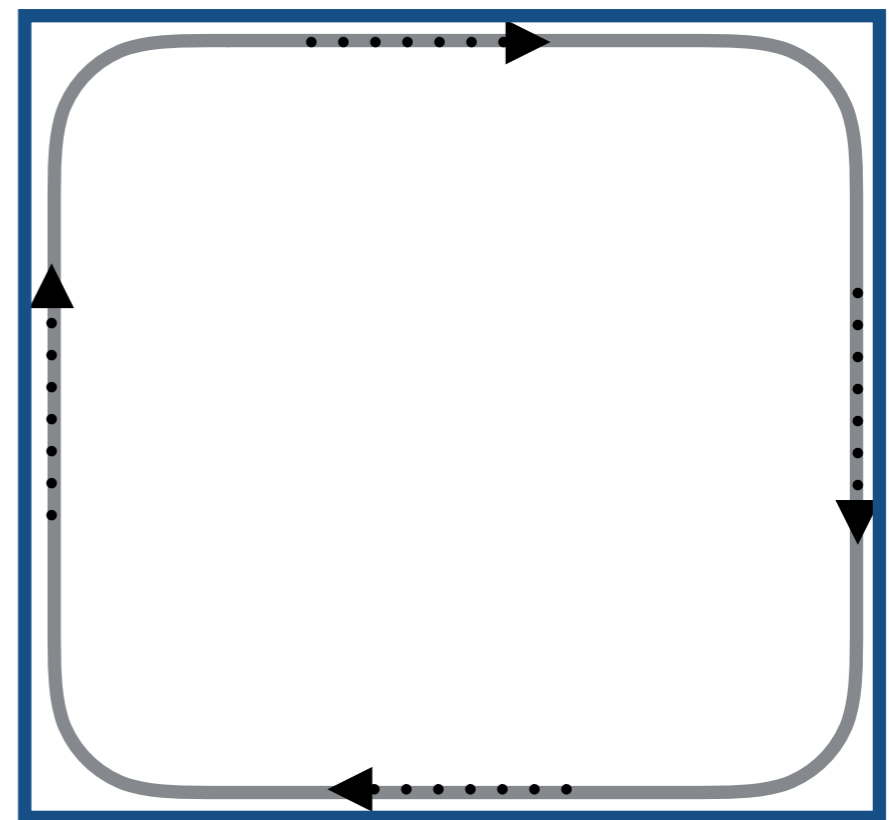
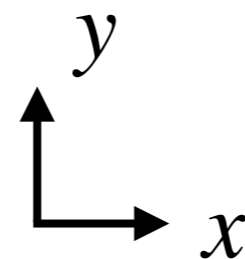
**Edge states!**

Analytis AMJP 2004

# Landau quantization in a 2D square lattice



Bulk states



Edge states

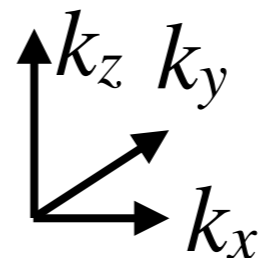
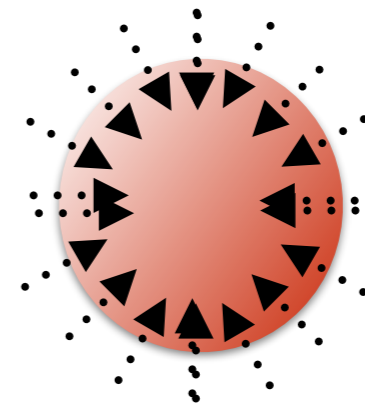
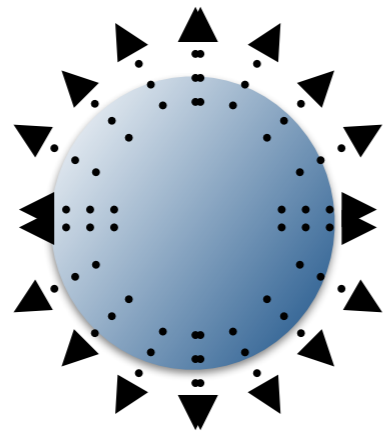
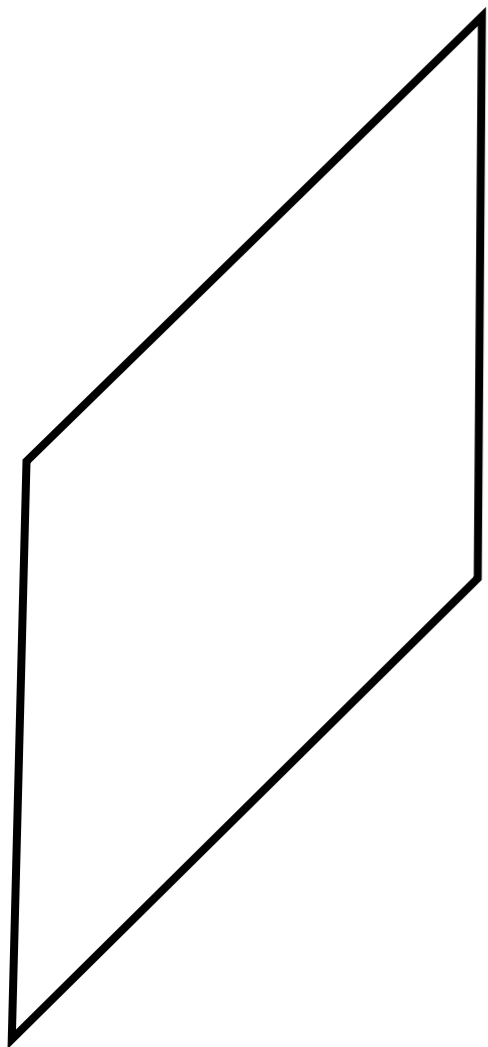
By breaking the translation symmetry at the boundary, we immediately get edge states that connect the bulk states



# Part II: Fermi arcs and Weyl orbits

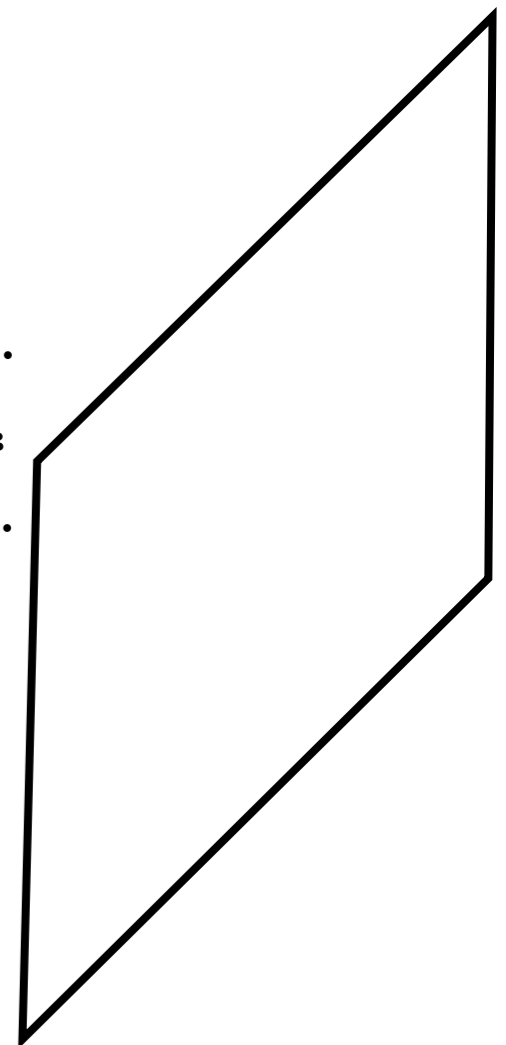
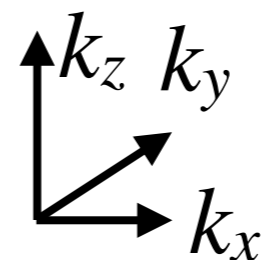
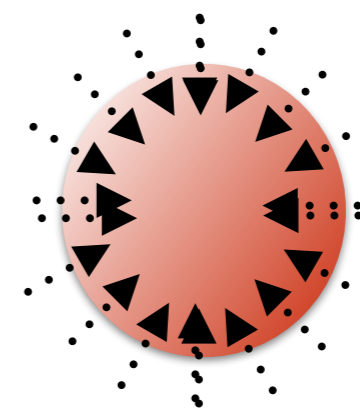
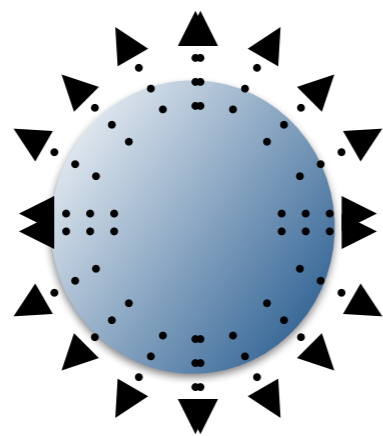
# Weyl nodes - 'magnetic monopoles' in reciprocal space

$$H_{\pm} = \pm v_F (k_x \sigma_x + k_y \sigma_y + k_z \sigma_z)$$



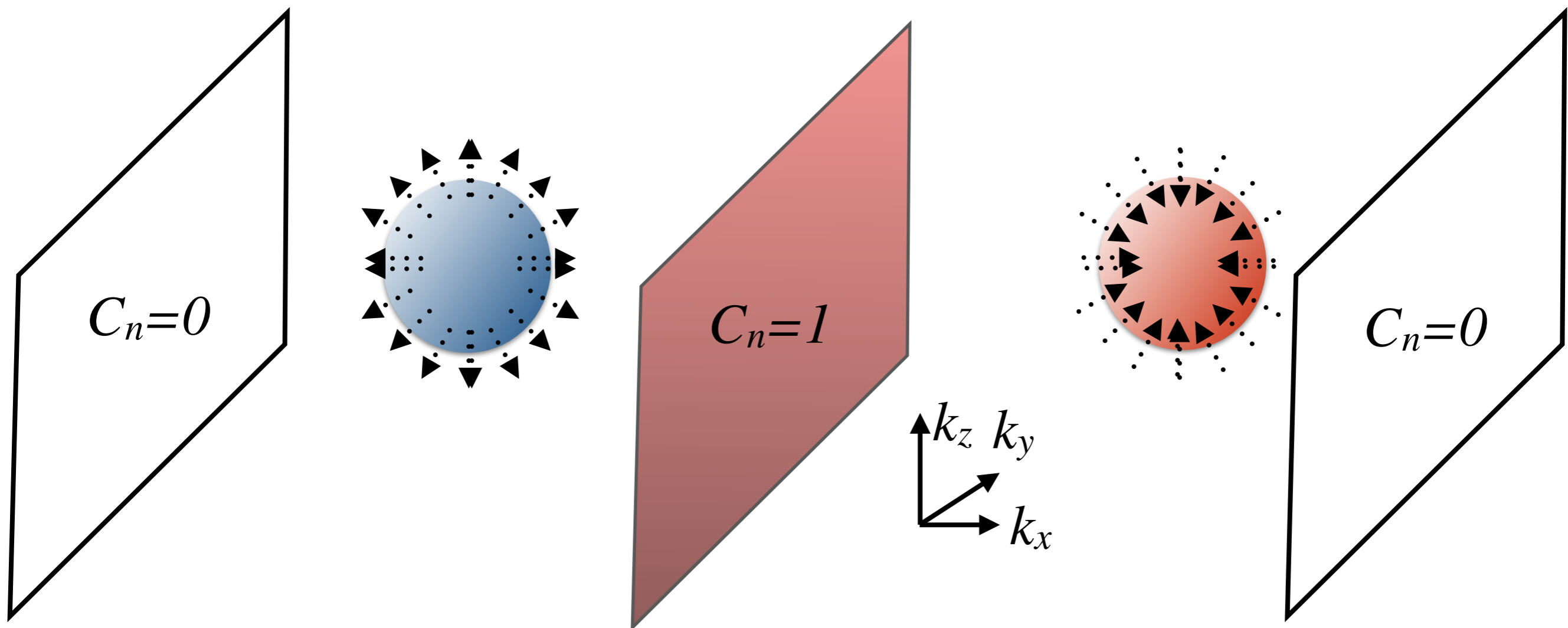
# Weyl nodes - 'magnetic monopoles' in reciprocal space

$$H_{\pm} = \pm v_F (k_x \sigma_x + k_y \sigma_y + k_z \sigma_z)$$

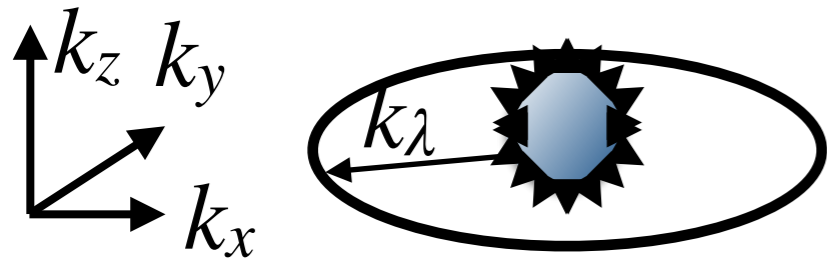


# Weyl nodes - 'magnetic monopoles' in reciprocal space

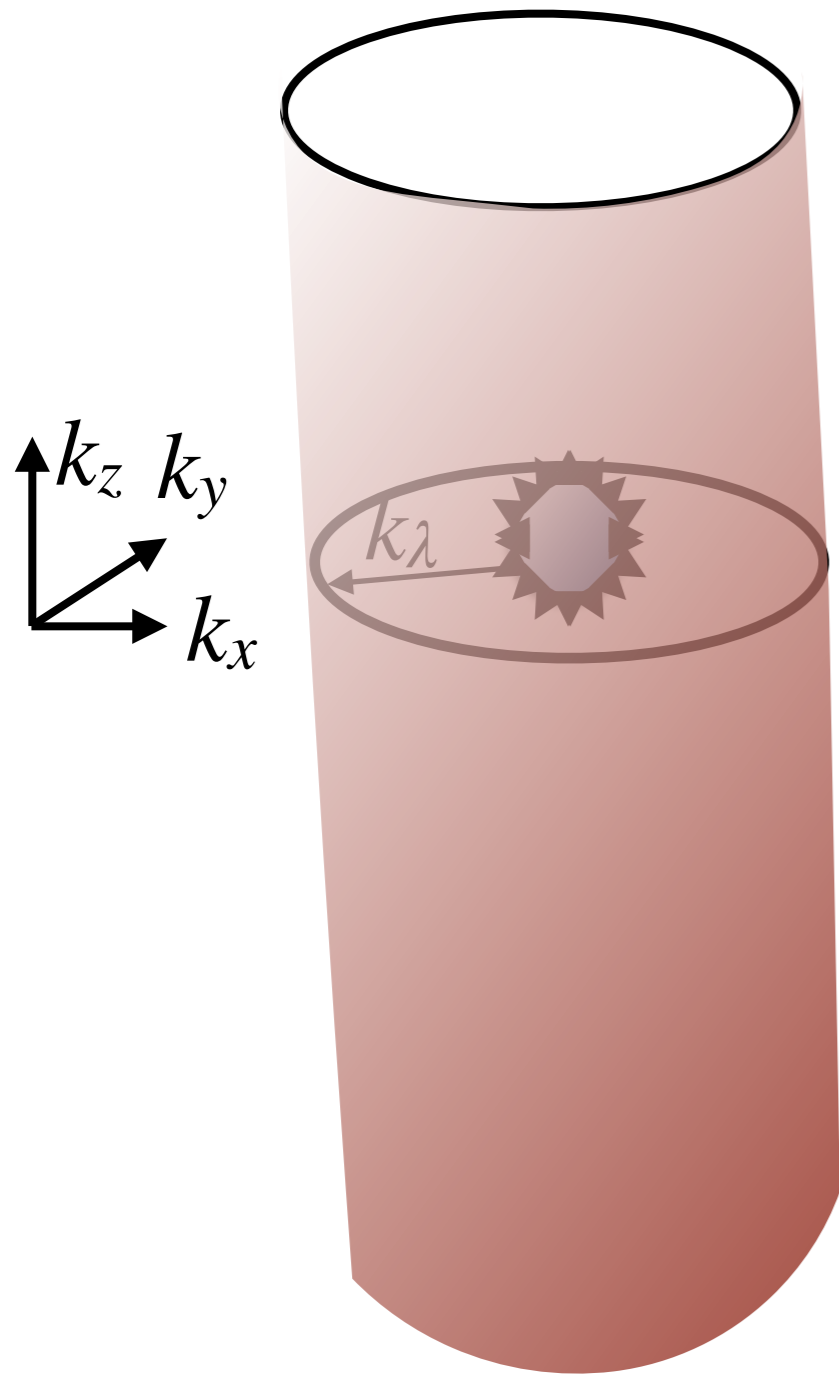
$$H_{\pm} = \pm v_F (k_x \sigma_x + k_y \sigma_y + k_z \sigma_z)$$



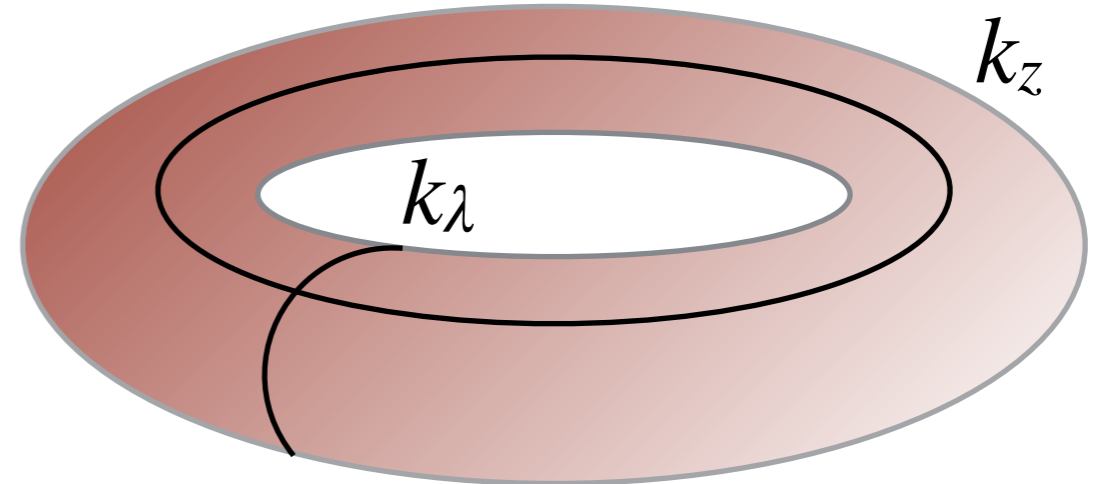
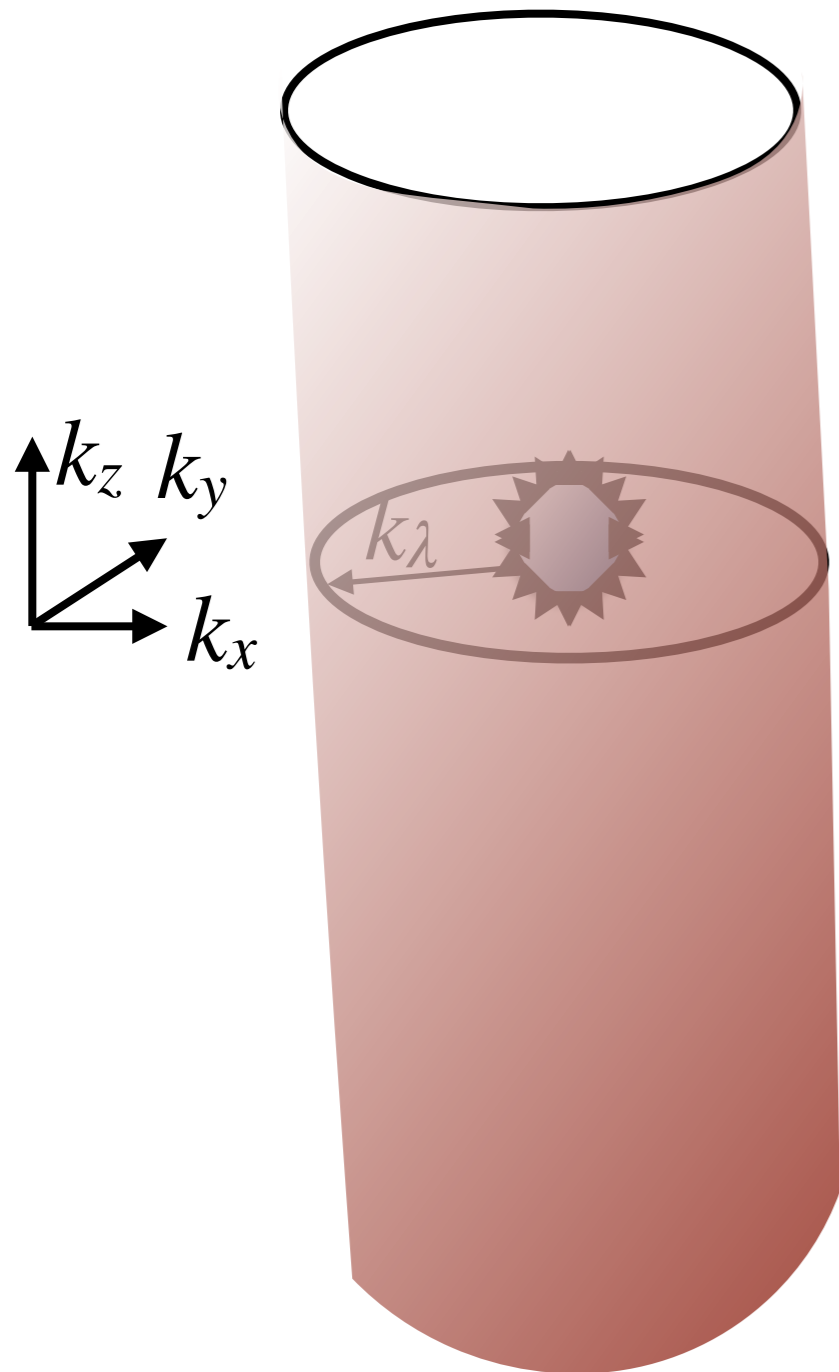
# Weyl nodes - 'magnetic monopoles' in reciprocal space



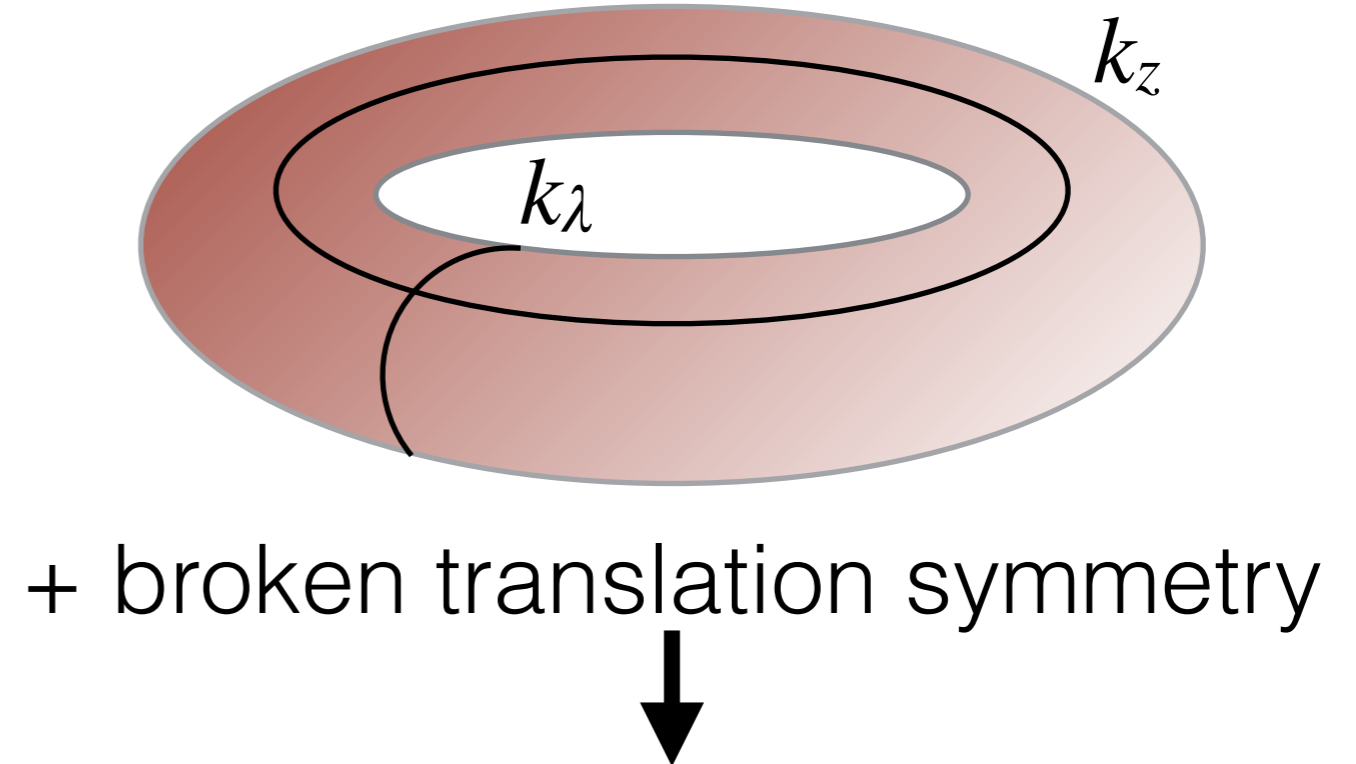
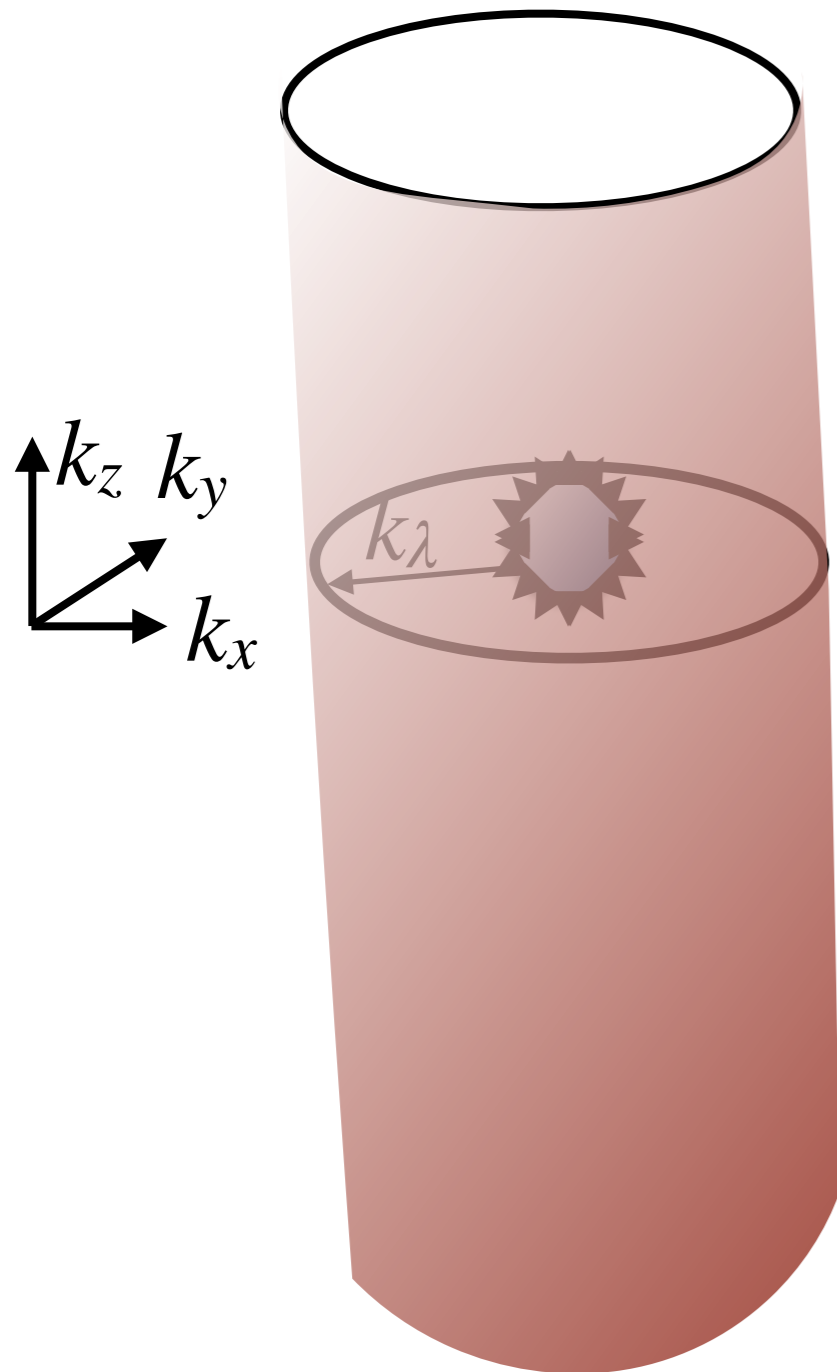
# Weyl nodes - 'magnetic monopoles' in reciprocal space



# Weyl nodes - 'magnetic monopoles' in reciprocal space

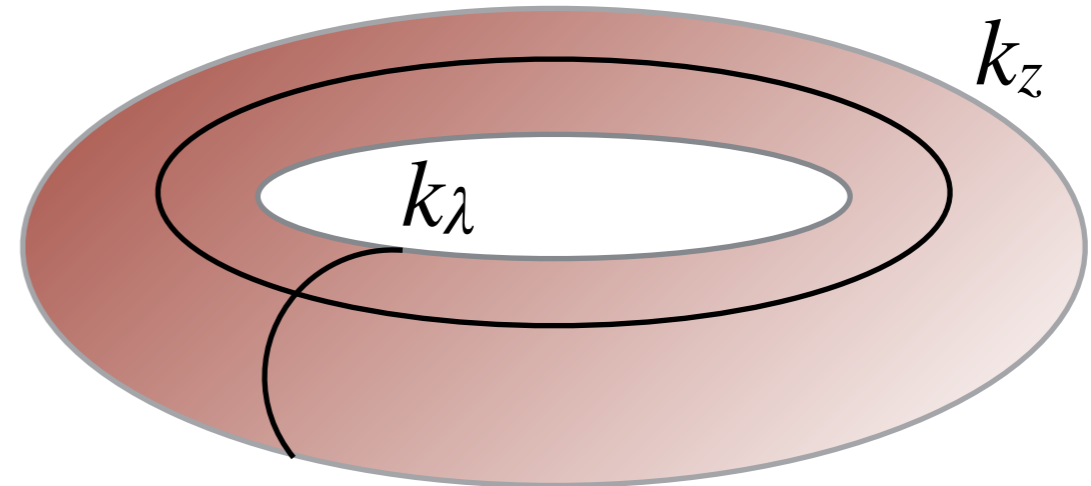
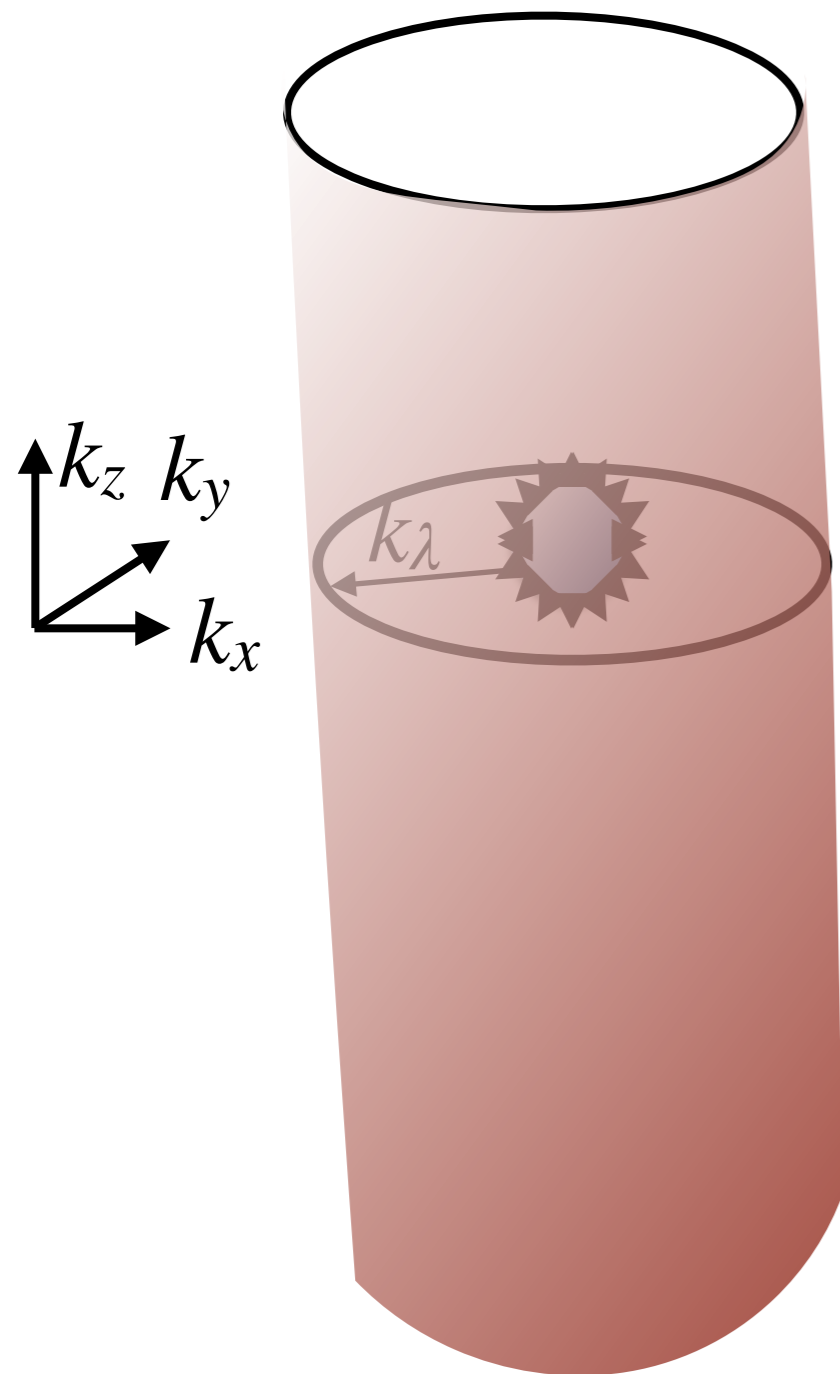


# Weyl nodes - 'magnetic monopoles' in reciprocal space

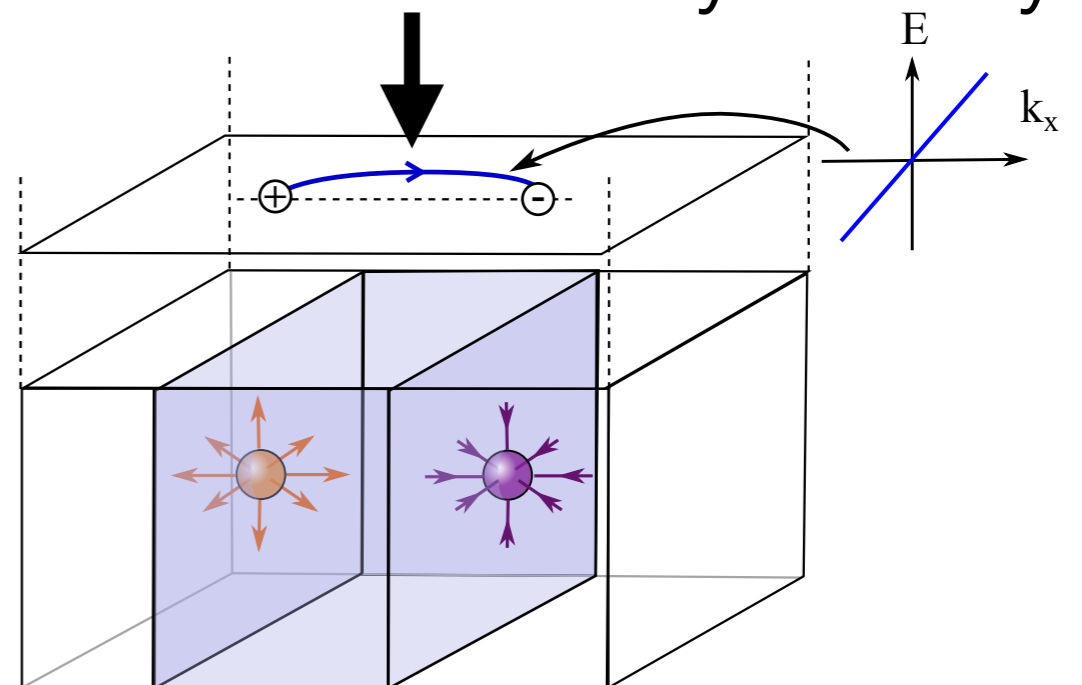




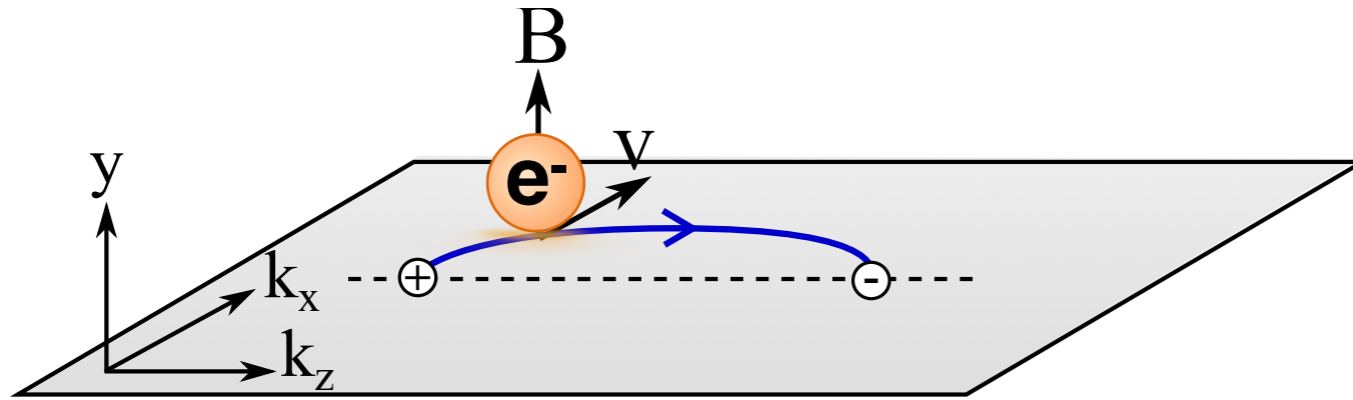
# Weyl nodes - 'magnetic monopoles' in reciprocal space



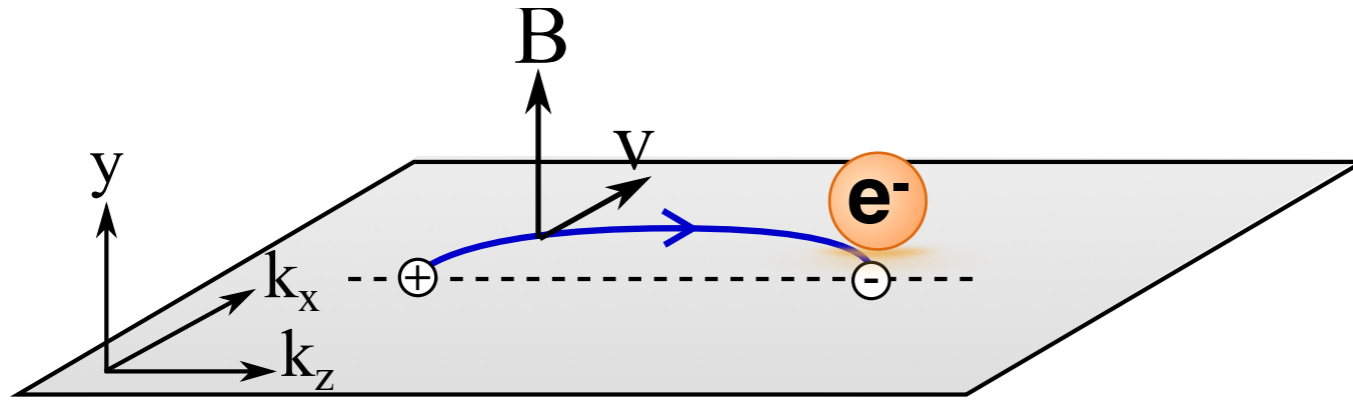
+ broken translation symmetry



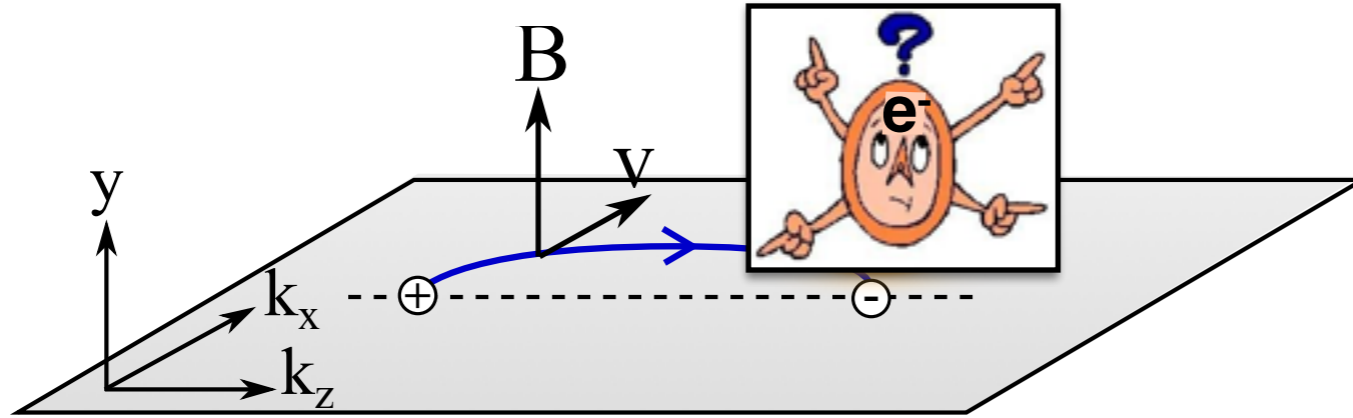
# The chirality conveyor belt



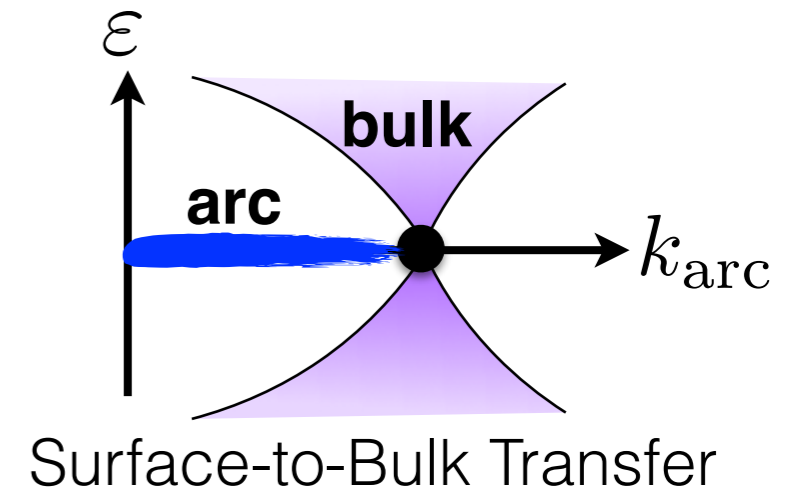
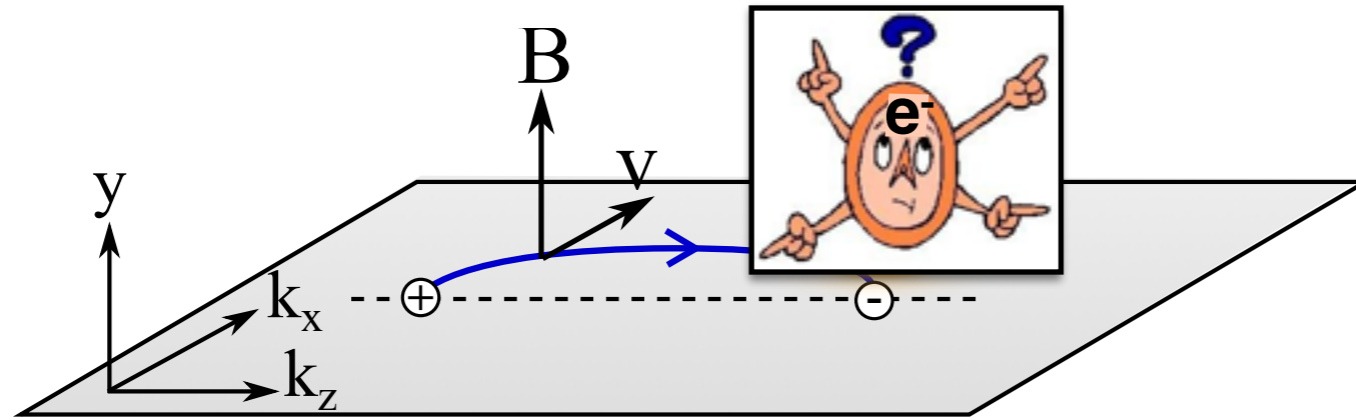
# The chirality conveyor belt



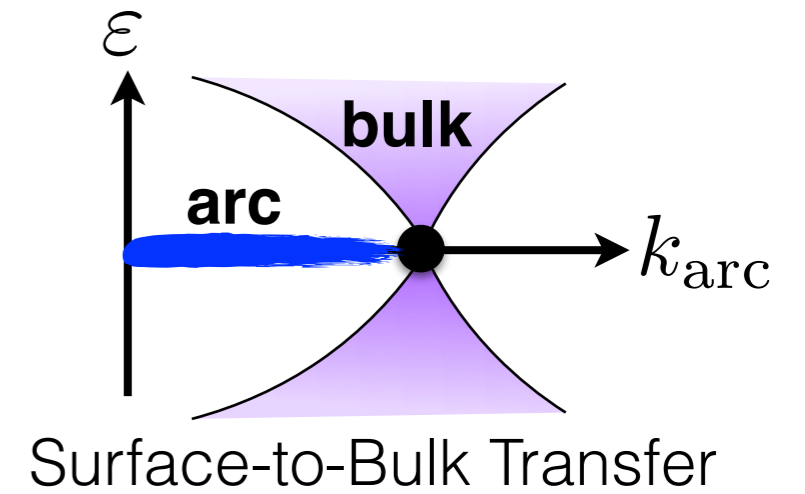
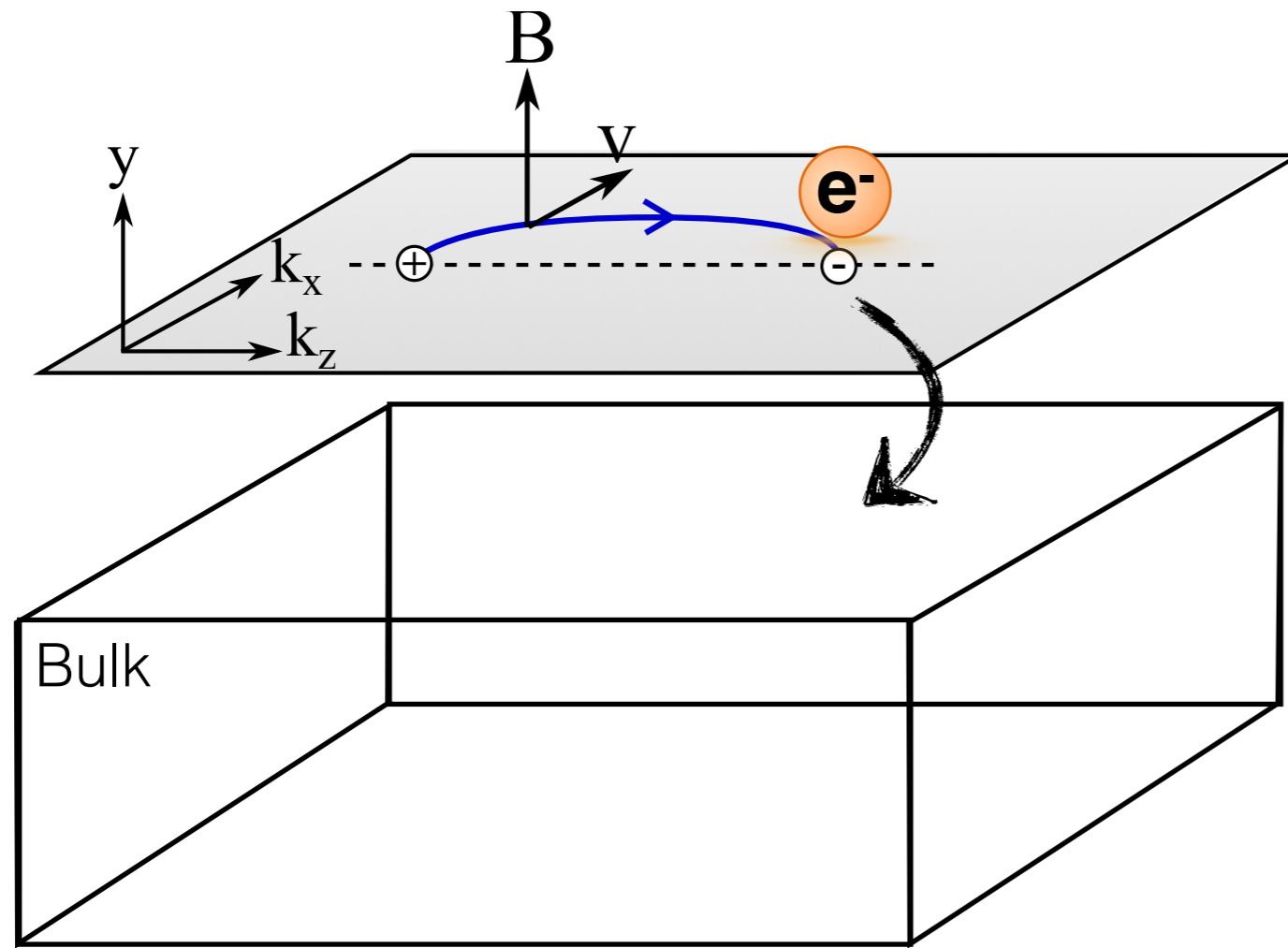
# The chirality conveyor belt



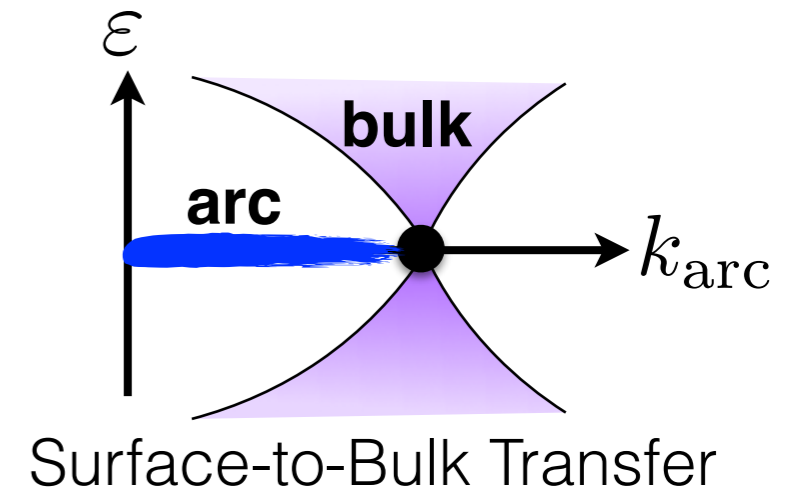
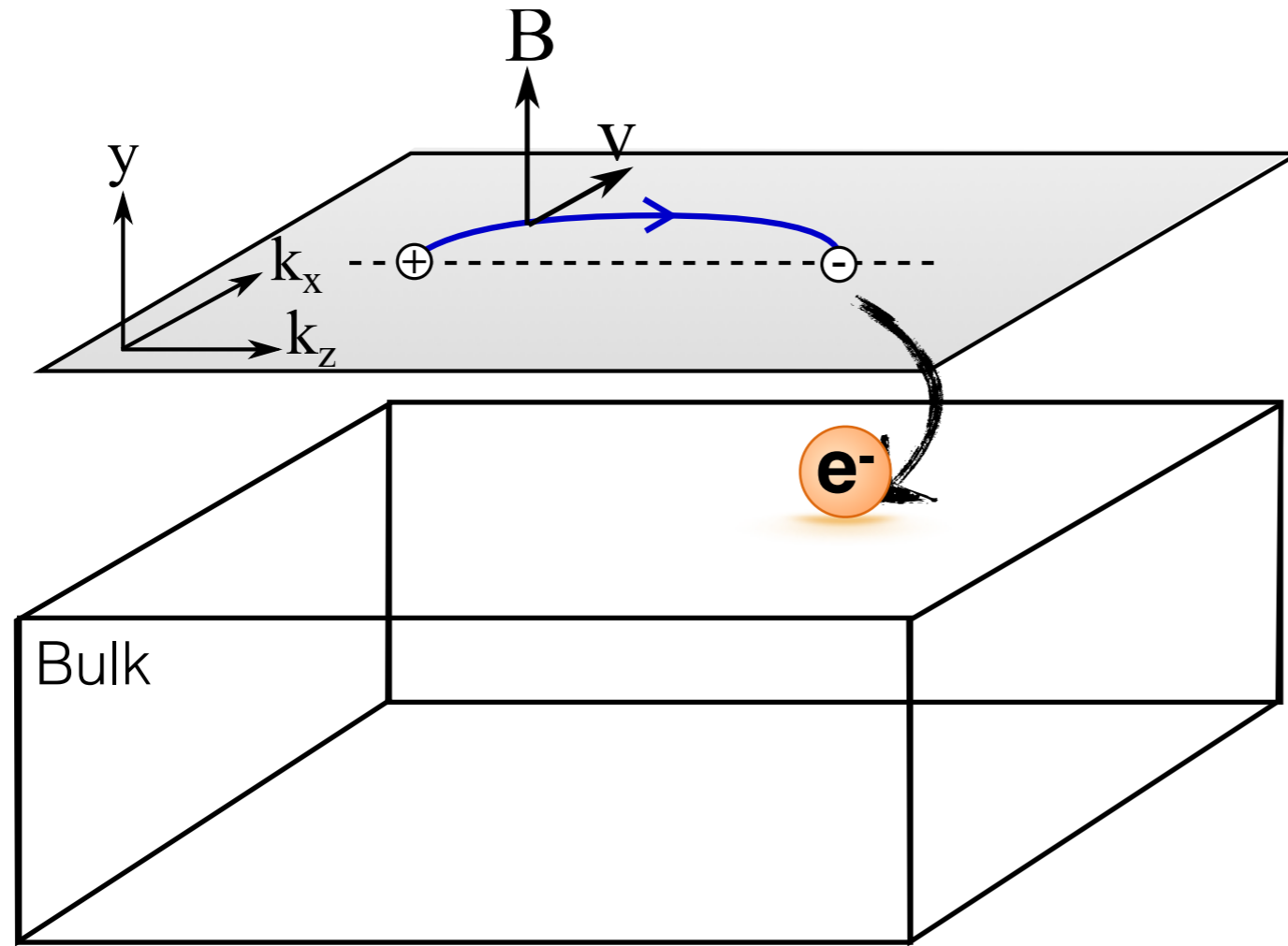
# The chirality conveyor belt



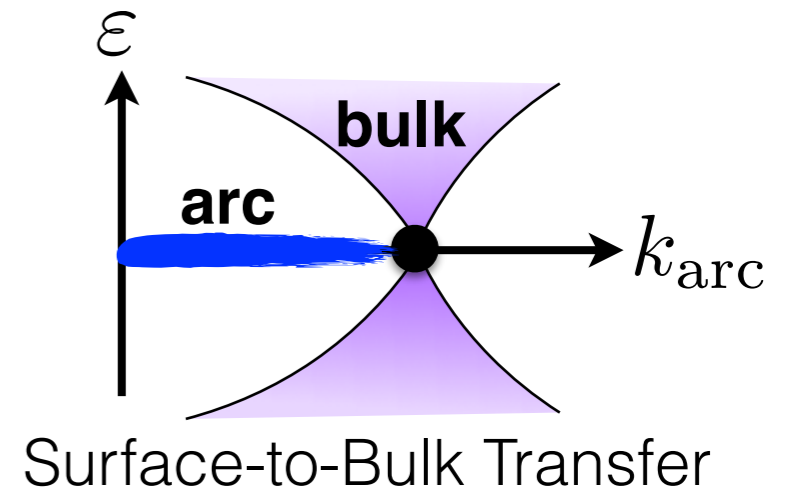
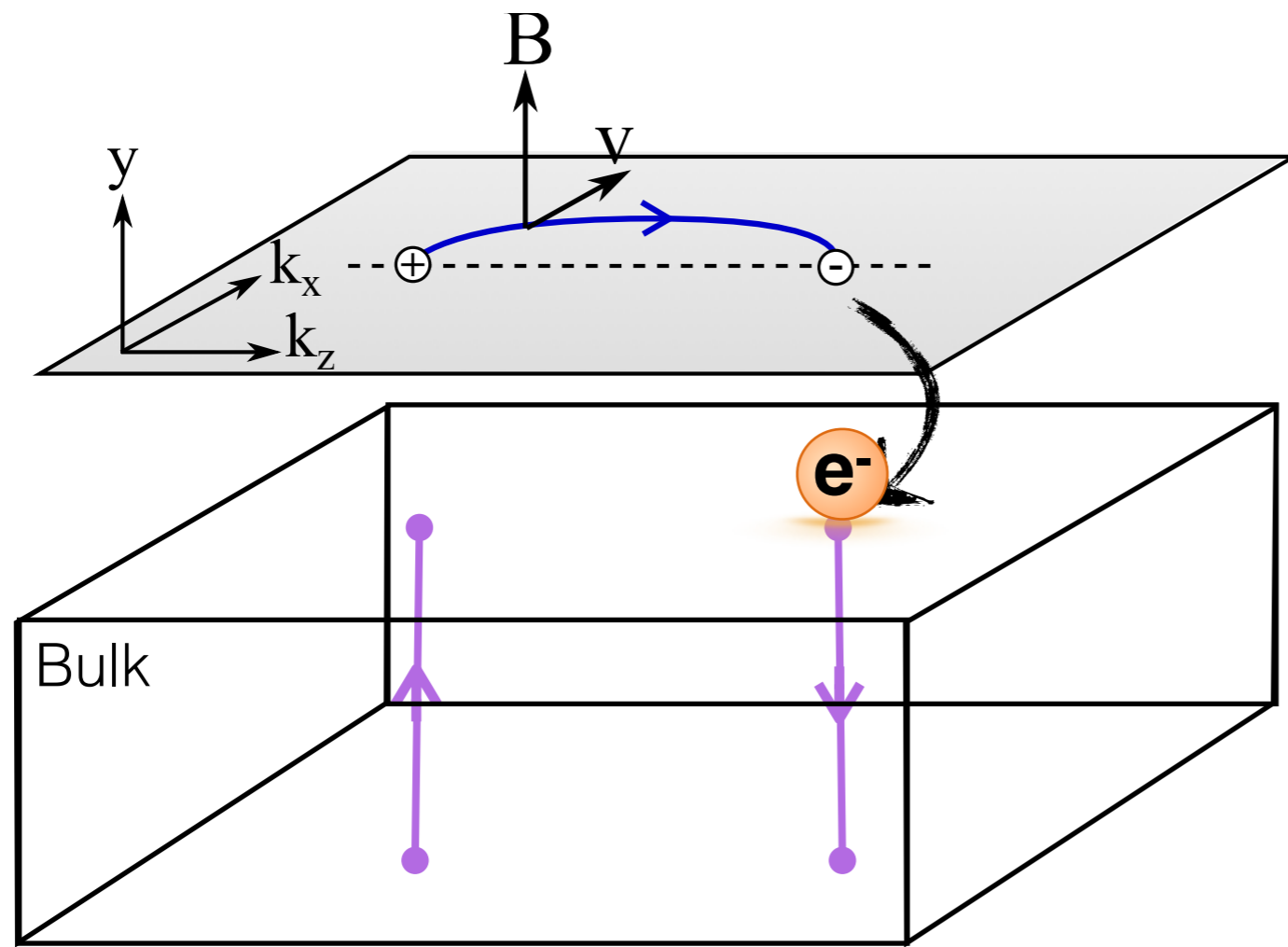
# The chirality conveyor belt



# The chirality conveyor belt

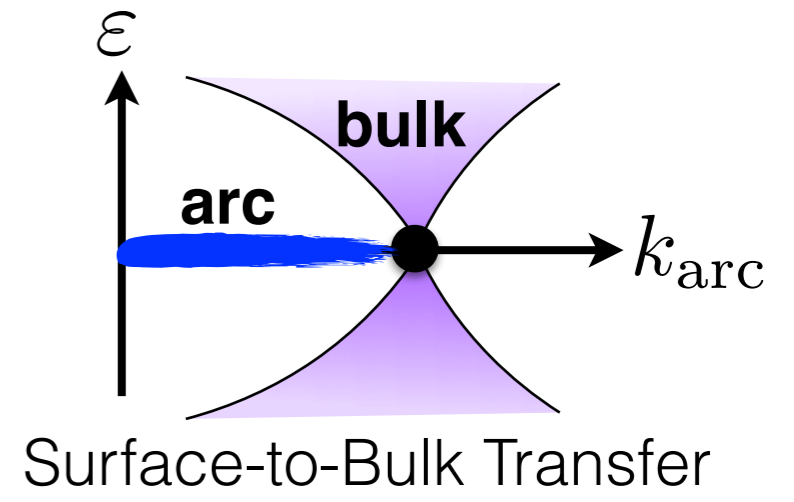
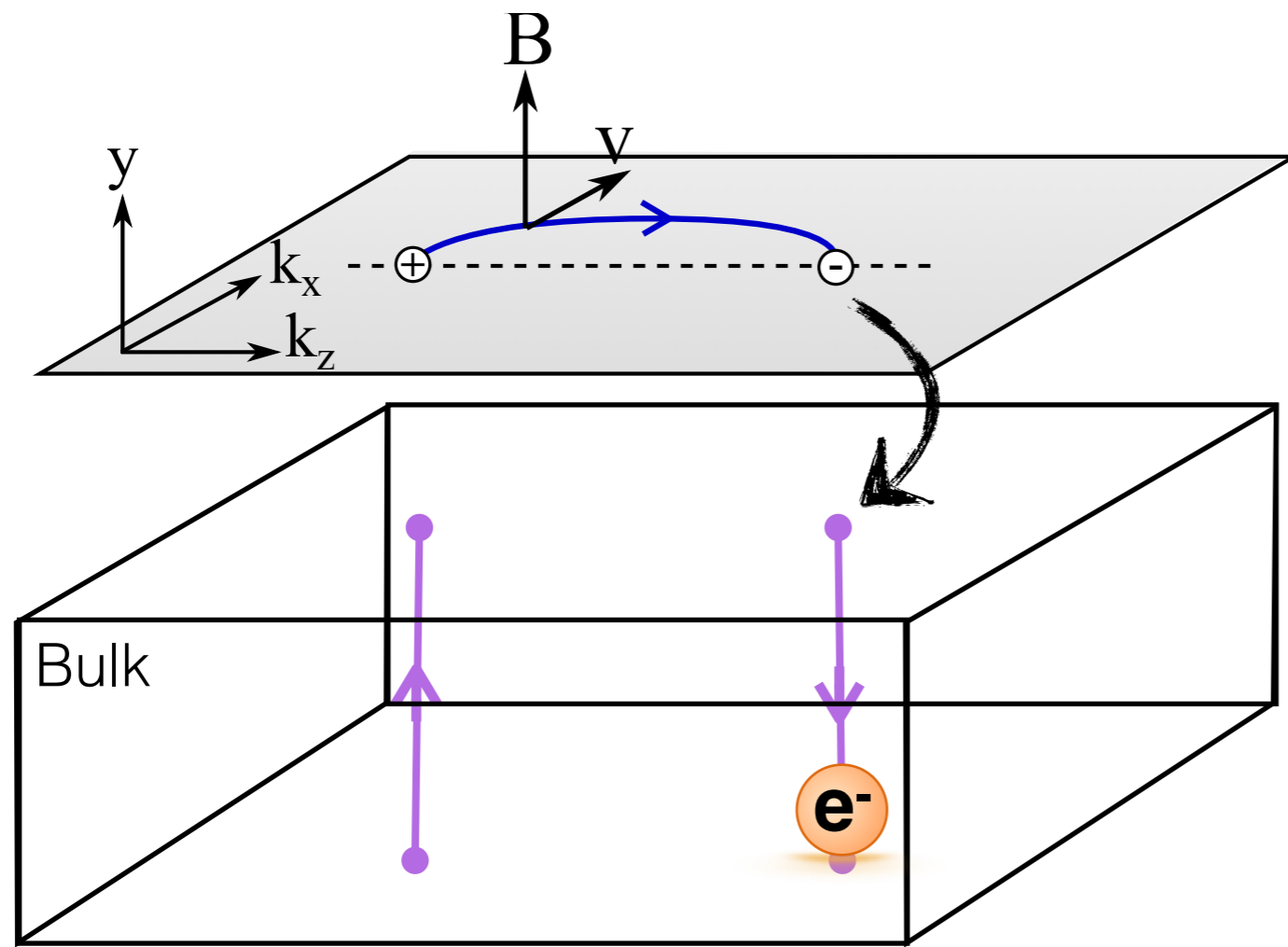


# The chirality conveyor belt

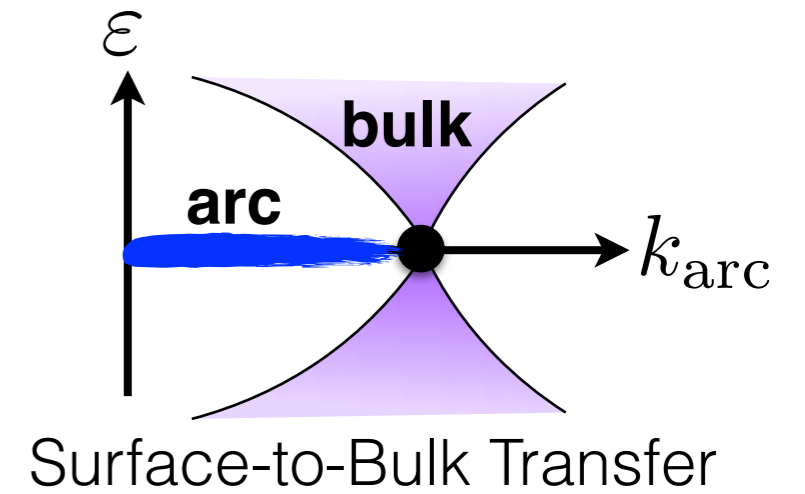
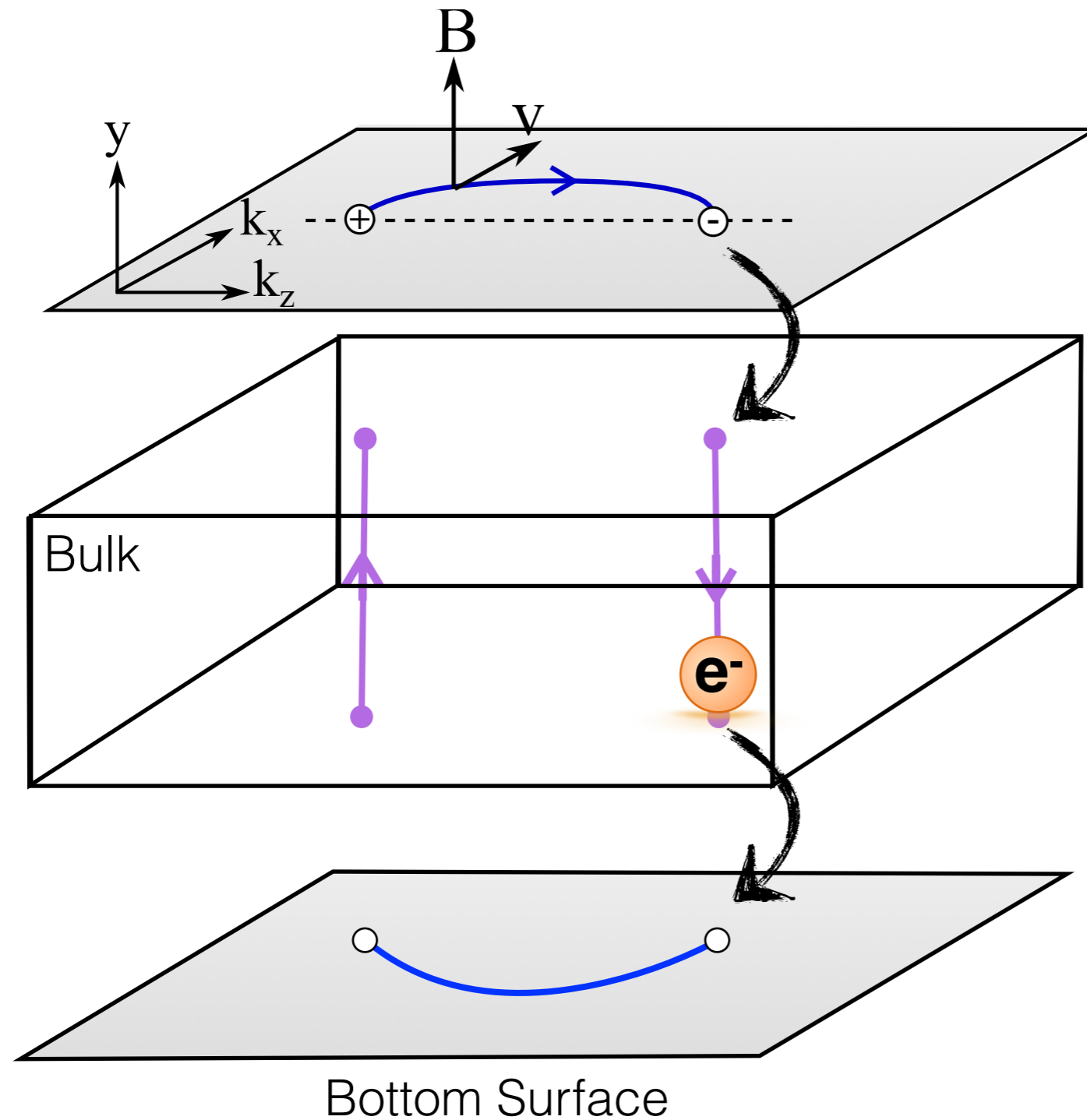




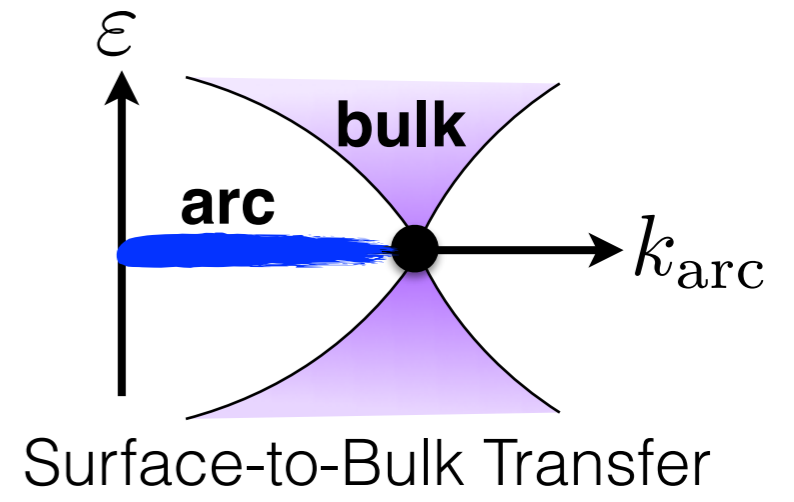
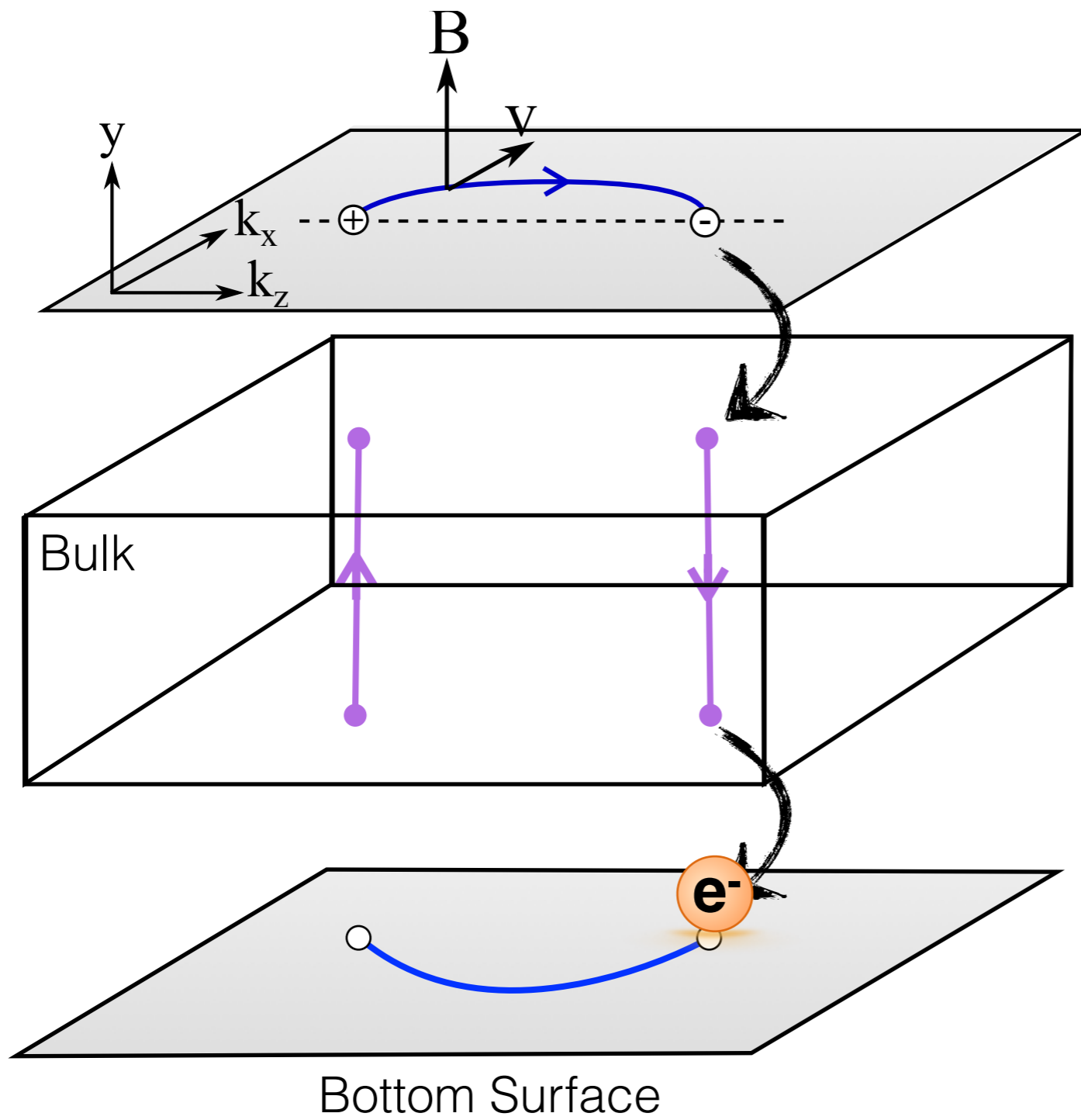
# The chirality conveyor belt



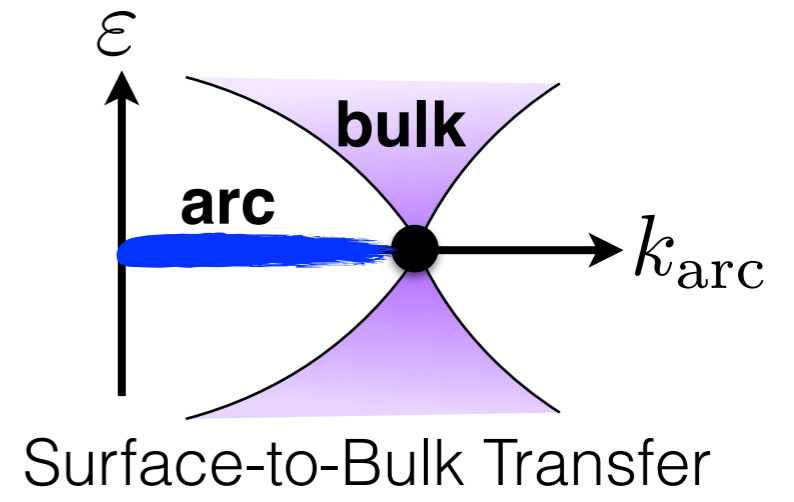
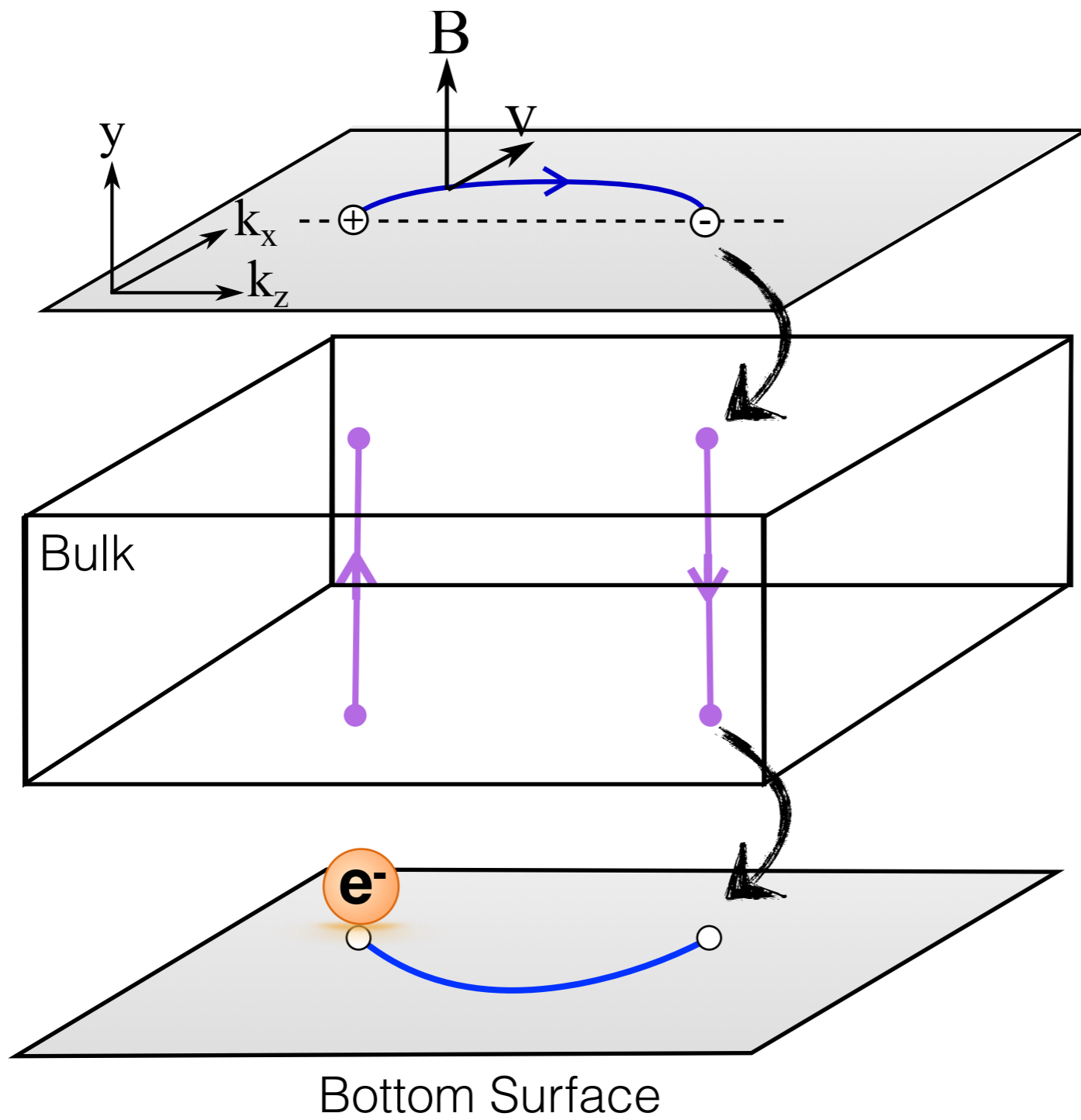
# The chirality conveyor belt



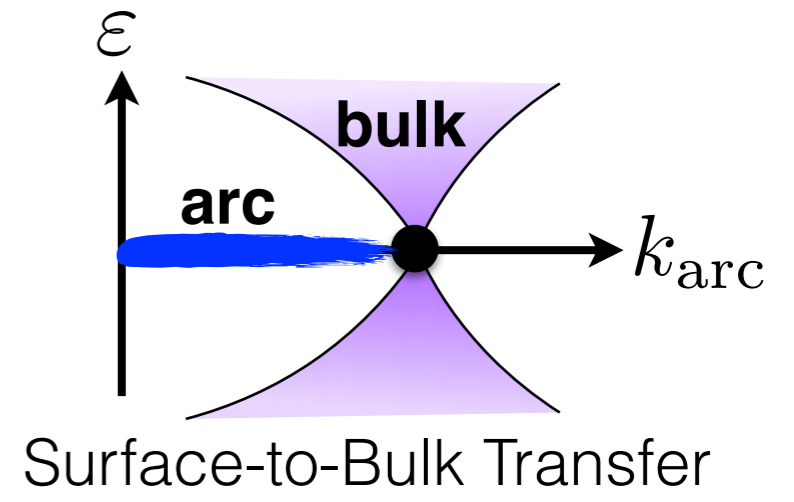
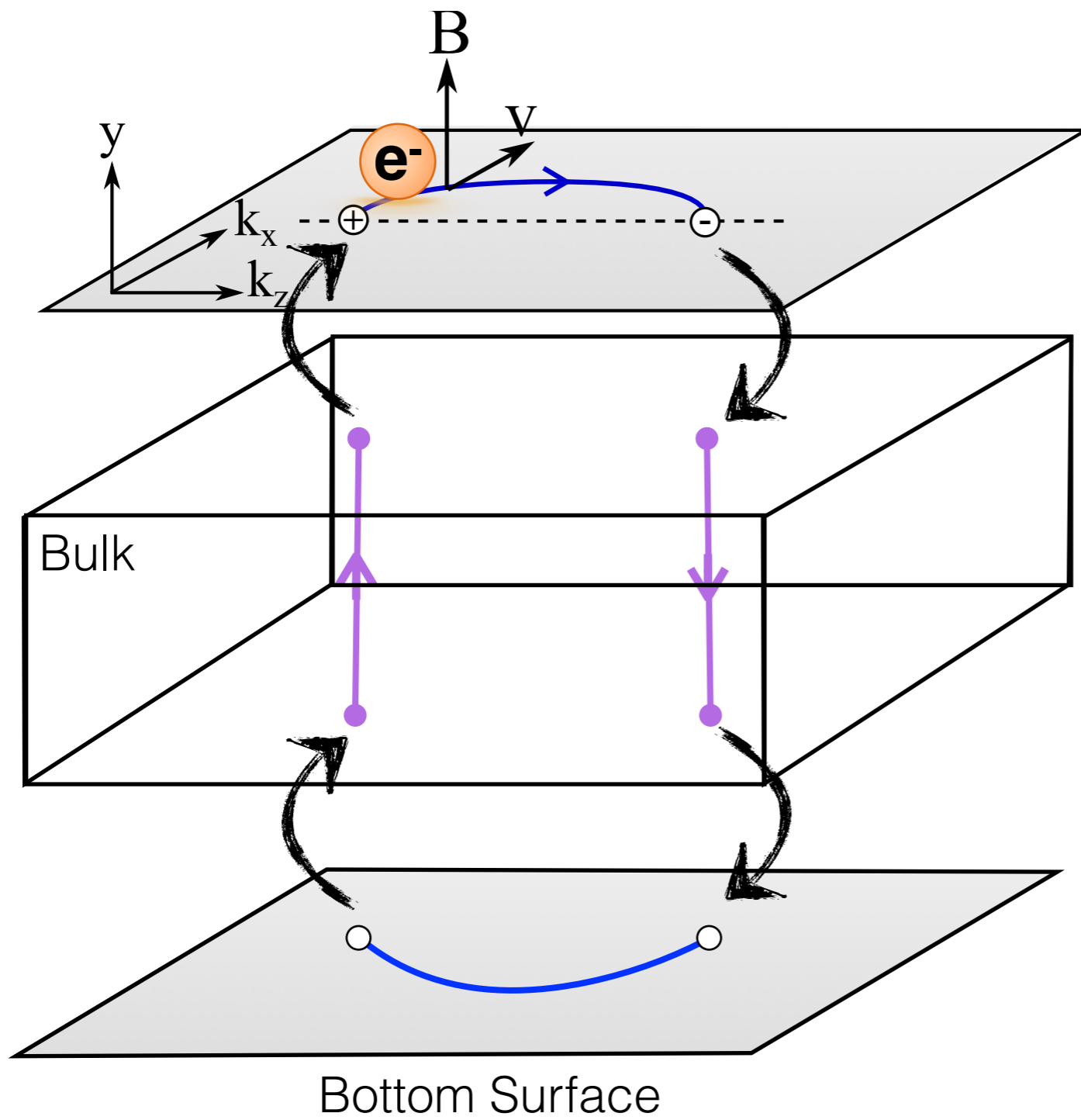
# The chirality conveyor belt



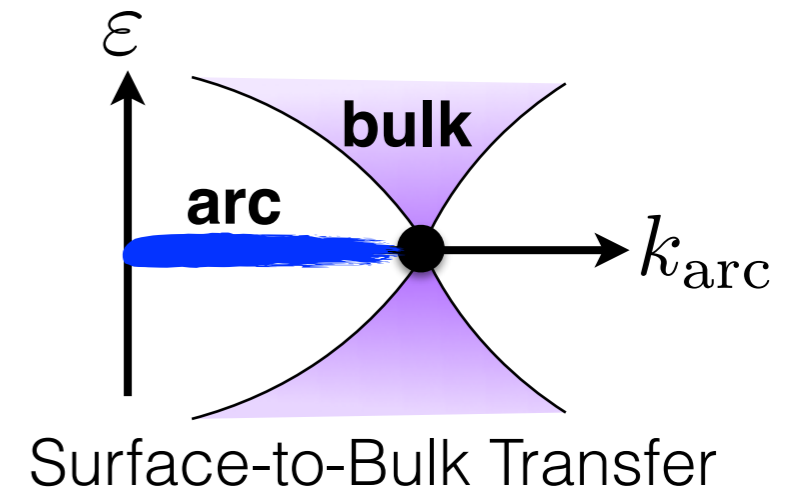
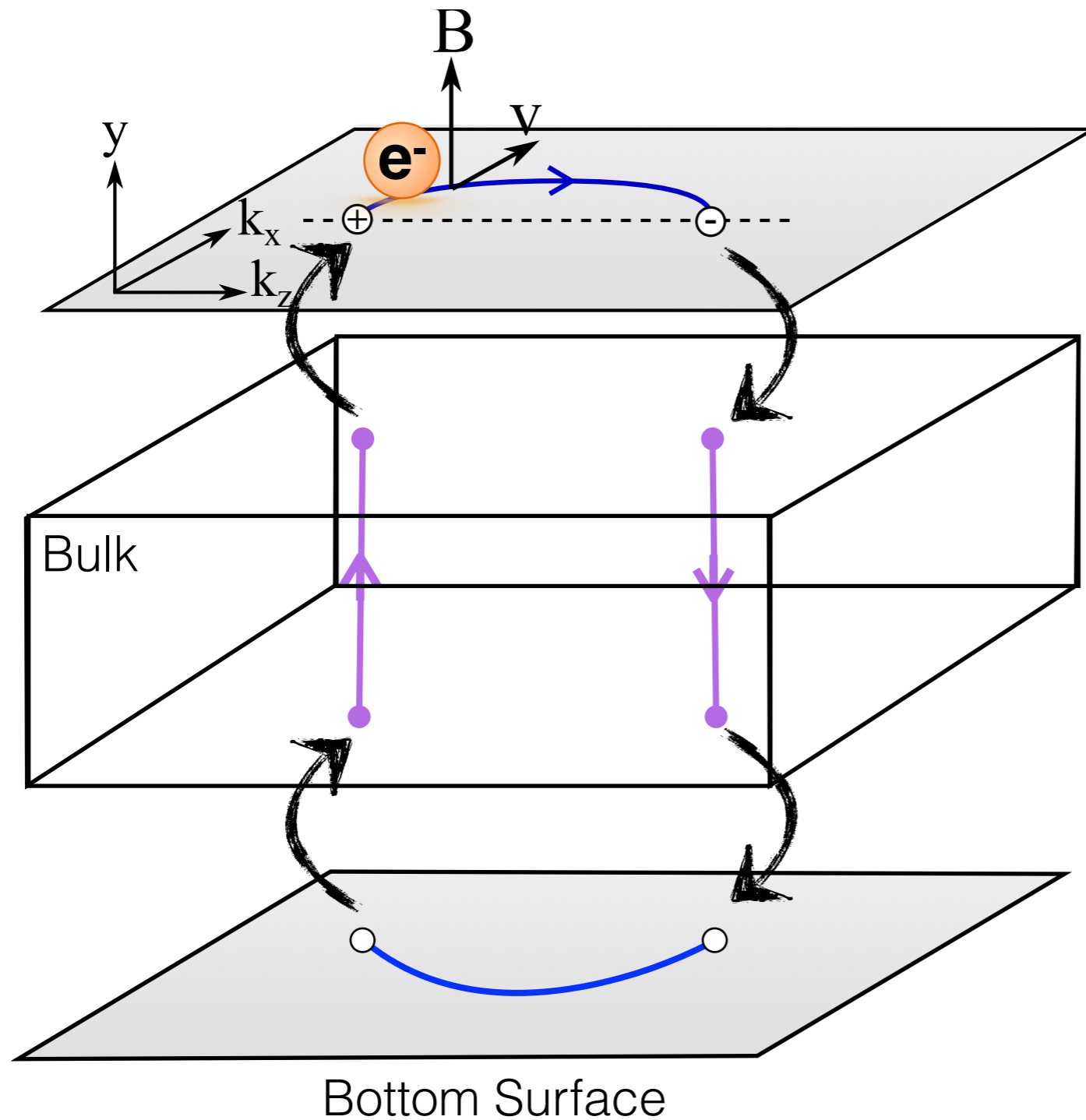
# The chirality conveyor belt



# The chirality conveyor belt



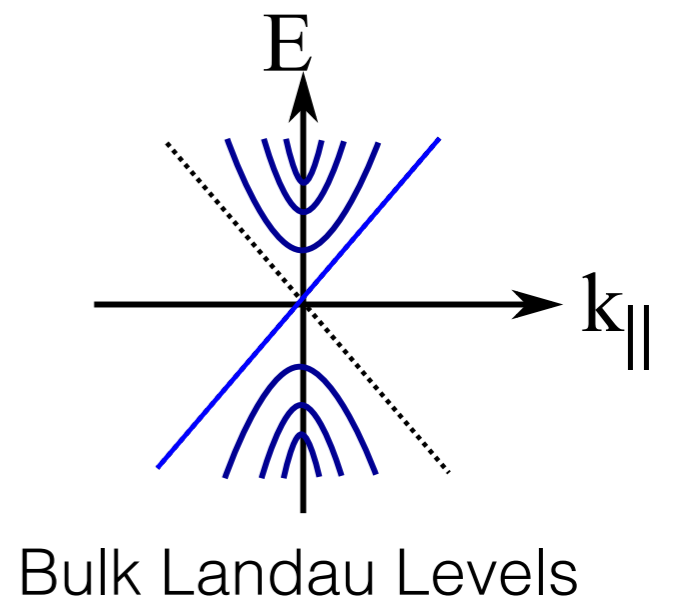
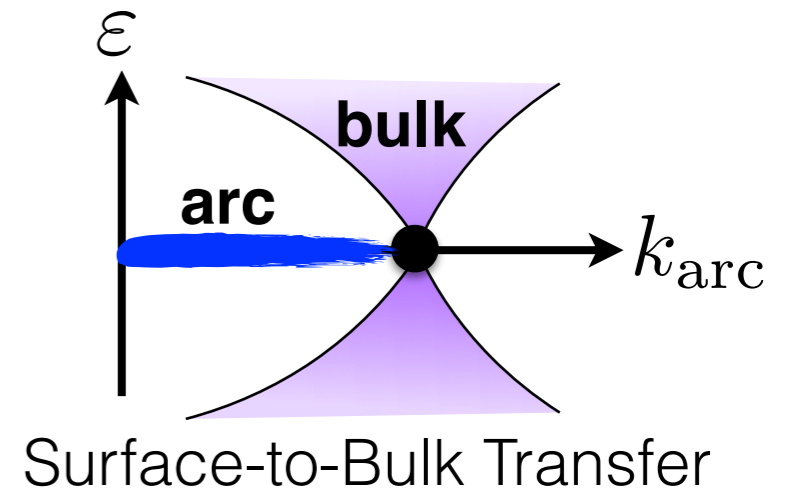
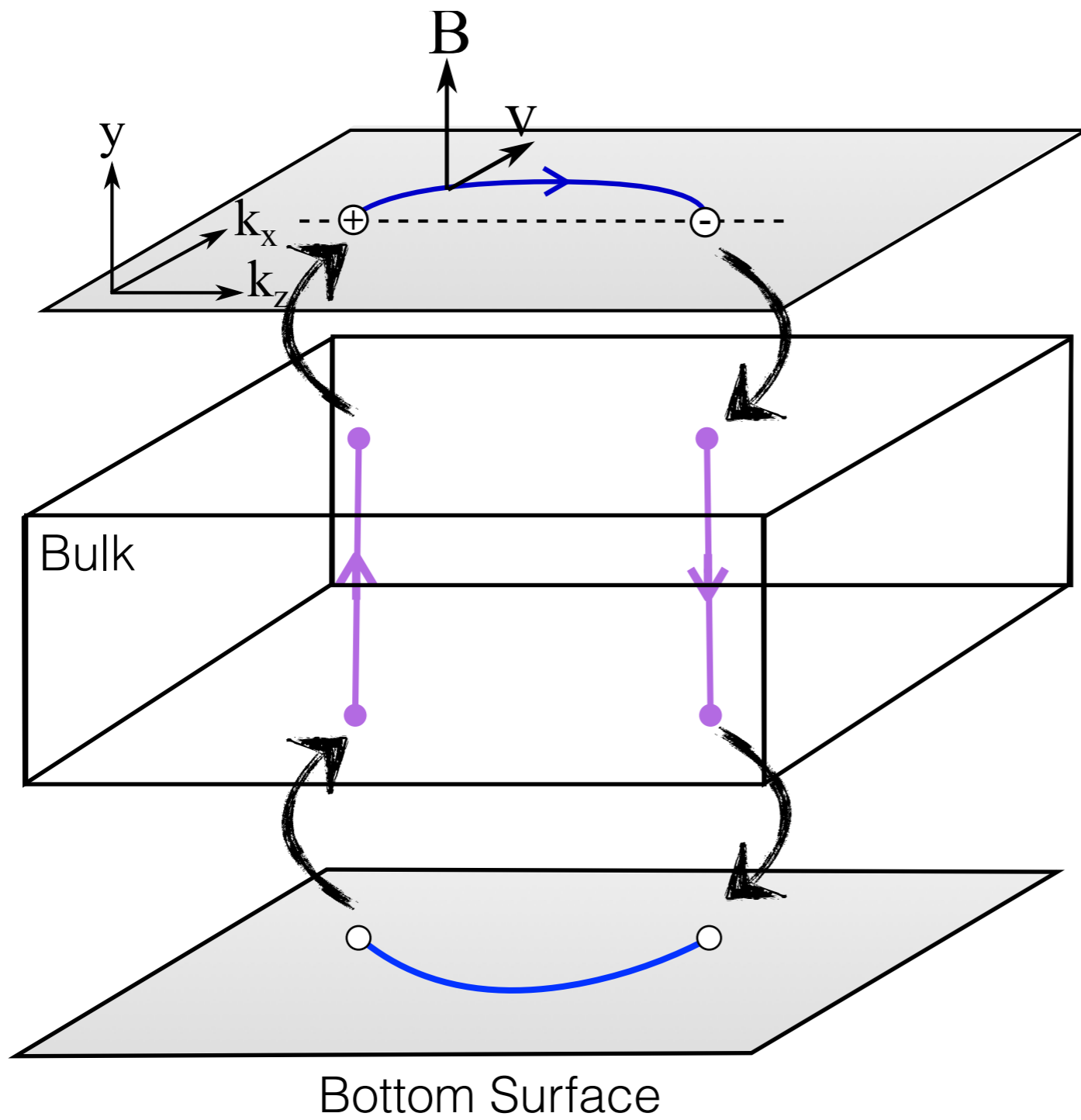
# The chirality conveyor belt



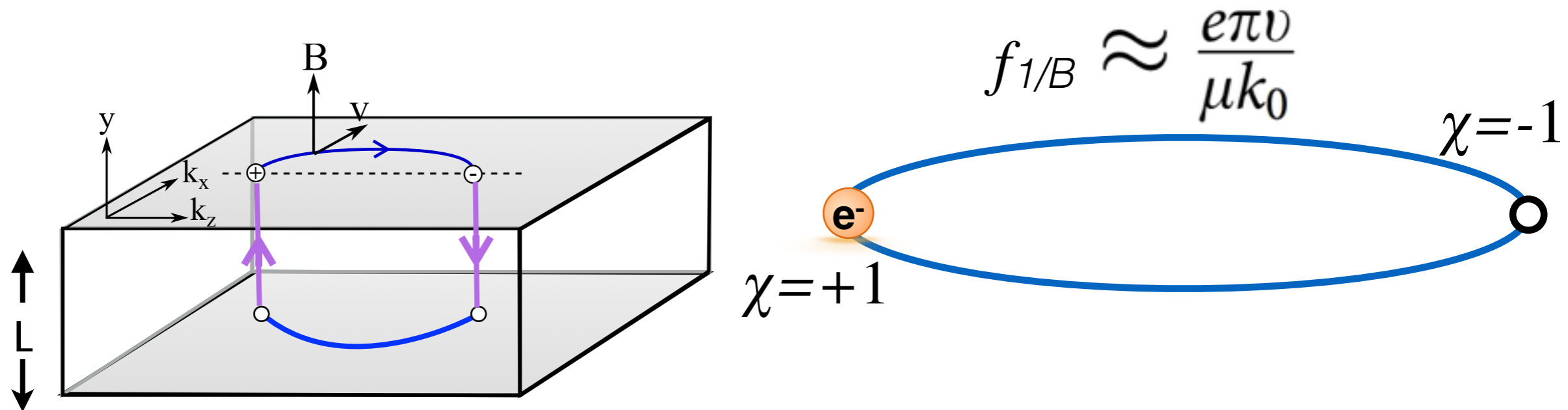
$$t = 2 \left( \frac{k_{\text{arc}}}{evB} + \frac{L}{v} \right)$$

**Arc**      **Bulk**

# Weyl orbits



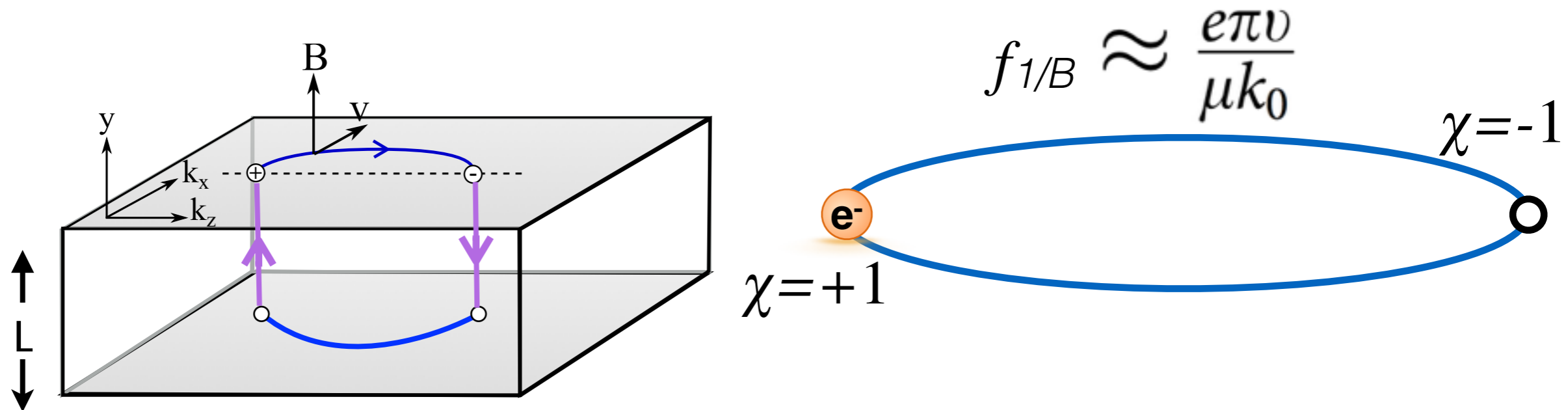
# Some remarks



- The cyclotron “Weyl” orbit involves a real space and  $k$ -space path.
- Real space trajectory encloses no flux (Lorentz force free path).
- From a quantum oscillatory point of view, it looks a lot like a 2D orbit with area  $A_k$ , or equivalently frequency  $f_{1/B}$

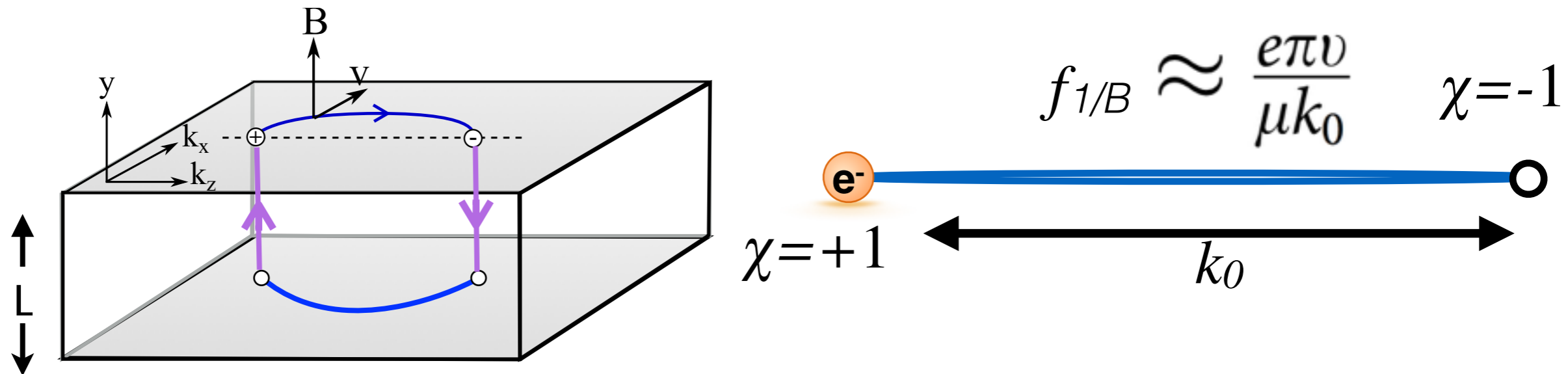


# Some remarks



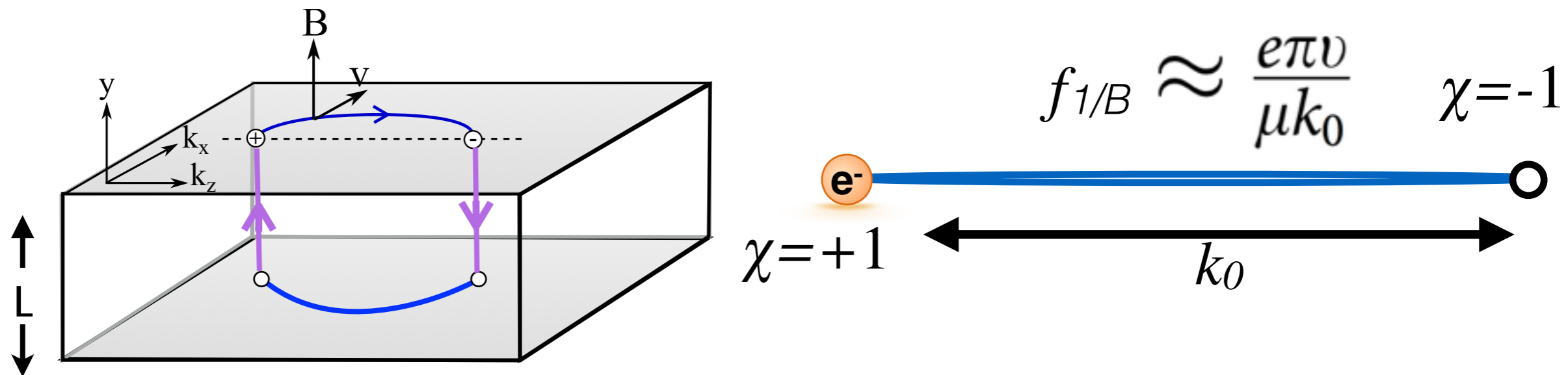
- The cyclotron “Weyl” orbit involves a real space and k-space path.
- Real space trajectory encloses no flux (Lorentz force free path).
- From a quantum oscillatory point of view, it looks a lot like a 2D orbit with area  $A_k$ , or equivalently frequency  $f_{1/B}$

# Some remarks



- The cyclotron "Weyl" orbit involves a real space and  $k$ -space path.
- Real space trajectory encloses no flux (Lorentz force free path).
- From a quantum oscillatory point of view, it looks a lot like a 2D orbit with area  $A_k$ , or equivalently frequency  $f_{1/B}$

# Some remarks

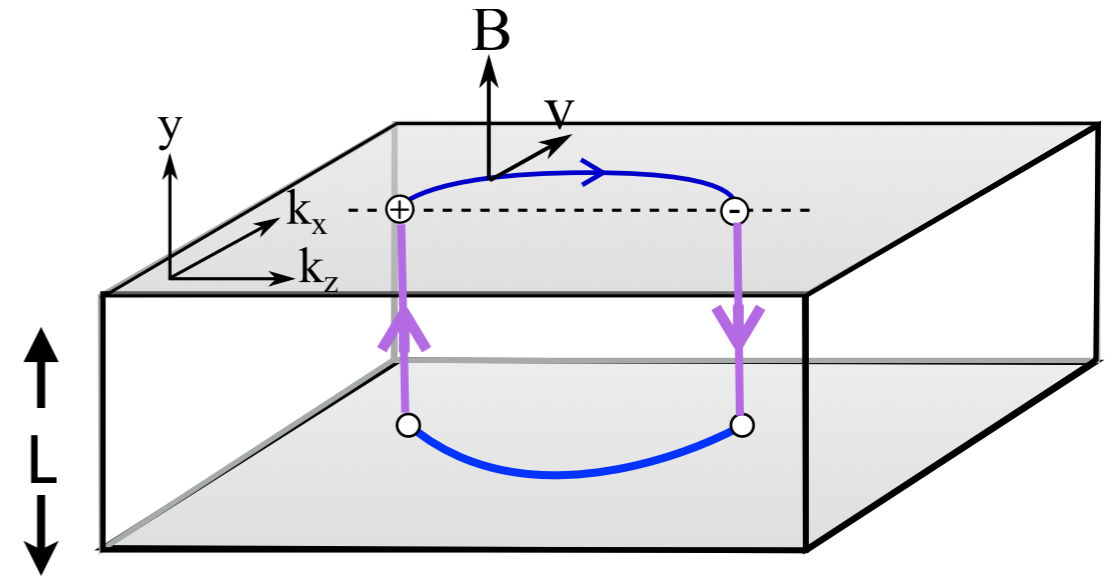


- The cyclotron "Weyl" orbit involves a real space and  $k$ -space path.
- Real space trajectory encloses no flux (Lorentz force free path).
- From a quantum oscillatory point of view, it looks a lot like a 2D orbit with area  $A_k$ , or equivalently frequency  $f_{1/B}$

# Distinguishing features

Quantization of semiclassical orbits

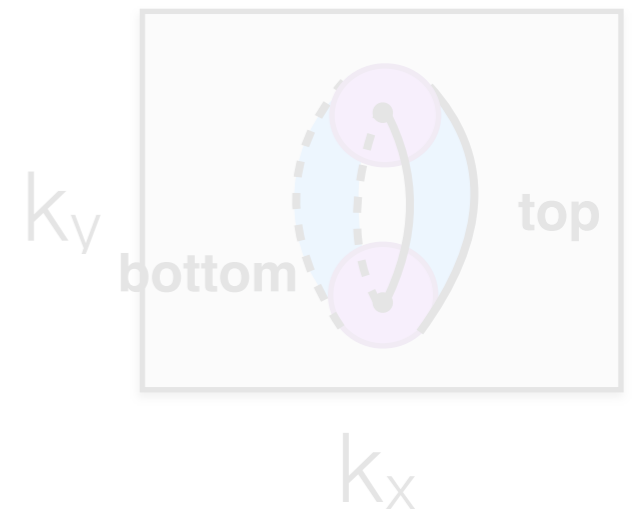
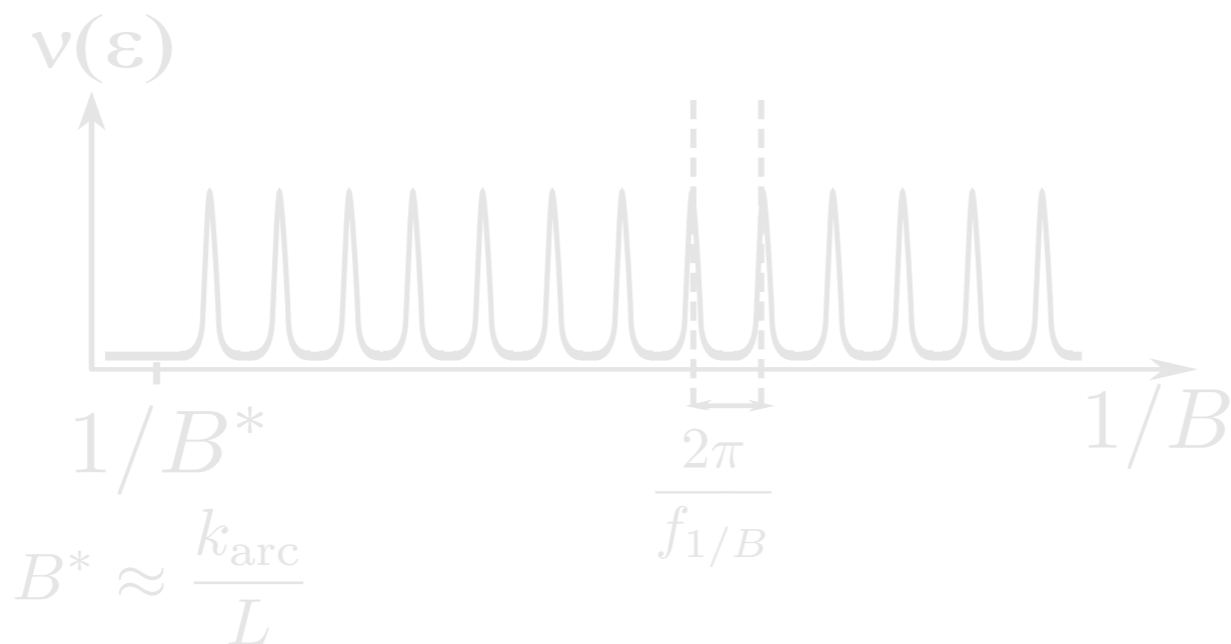
$$\varepsilon_c t_c = (n + \gamma) 2\pi \hbar$$



Quantum oscillations

$$\frac{1}{B_n} = \frac{2\pi n}{f_{1/B}} - \frac{e}{k_{\text{arc}}} L$$

$f_{1/B}$

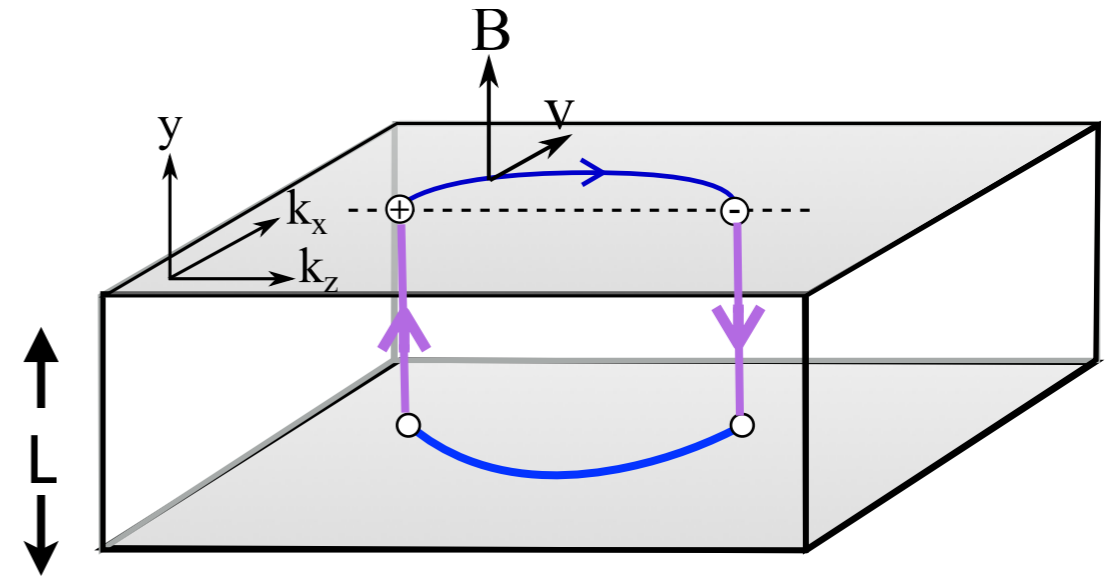


# Distinguishing features

Quantization of semiclassical orbits

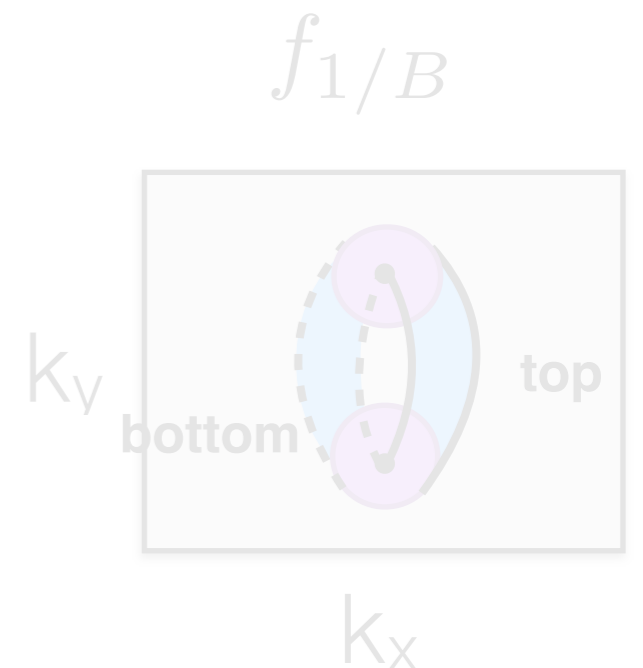
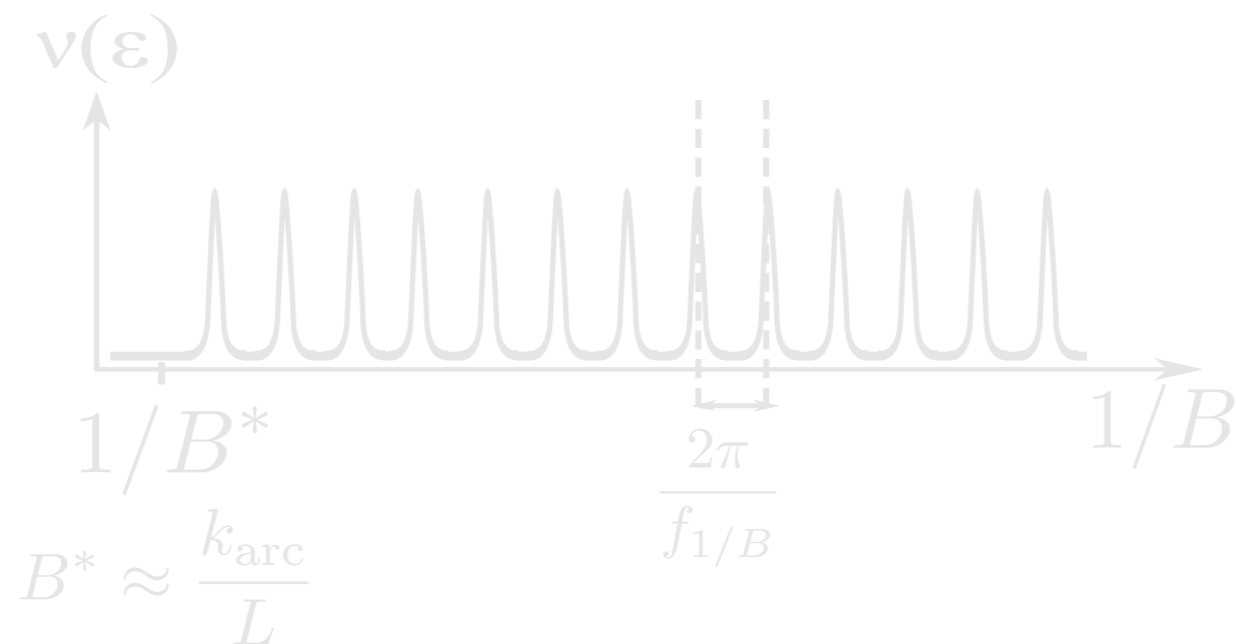
$$\varepsilon_n \approx \frac{2\pi n + \gamma}{t} \approx \frac{2\pi n + \gamma}{2 \left( \frac{k_{\text{arc}}}{evB} + \frac{L}{v} \right)}$$

$\uparrow$   
**Arc**
 $\uparrow$   
**Bulk**



Quantum oscillations

$$\frac{1}{B_n} = \frac{2\pi n}{f_{1/B}} - \frac{e}{k_{\text{arc}}} L$$

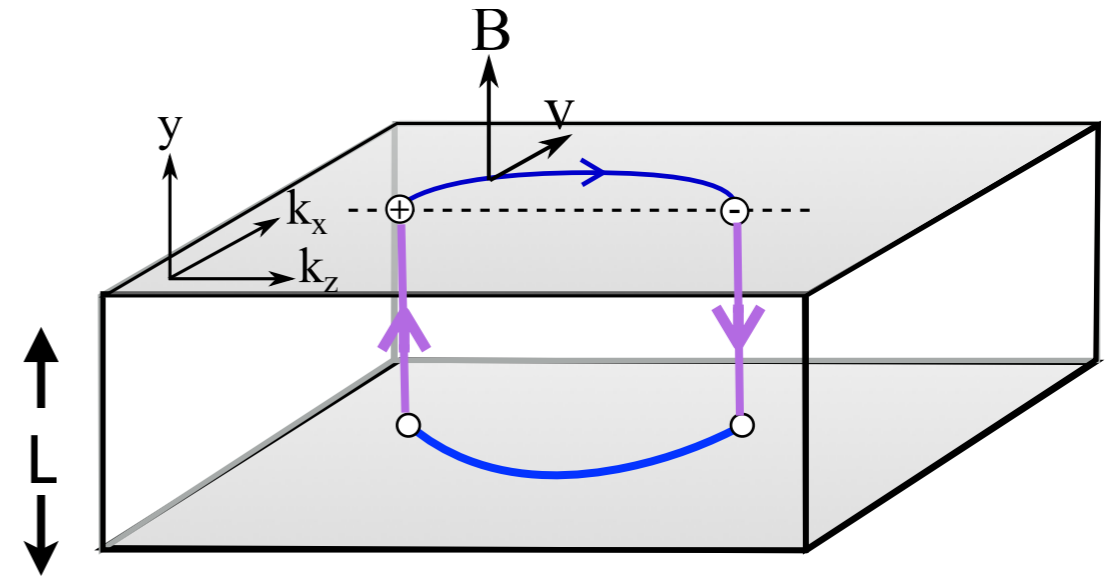


# Distinguishing features

Quantization of semiclassical orbits

$$\varepsilon_n \approx \frac{2\pi n + \gamma}{t} \approx \frac{2\pi n + \gamma}{2 \left( \frac{k_{\text{arc}}}{evB} + \frac{L}{v} \right)}$$

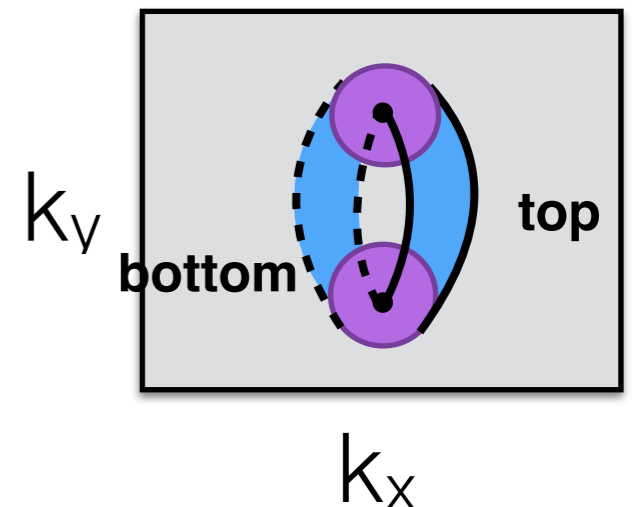
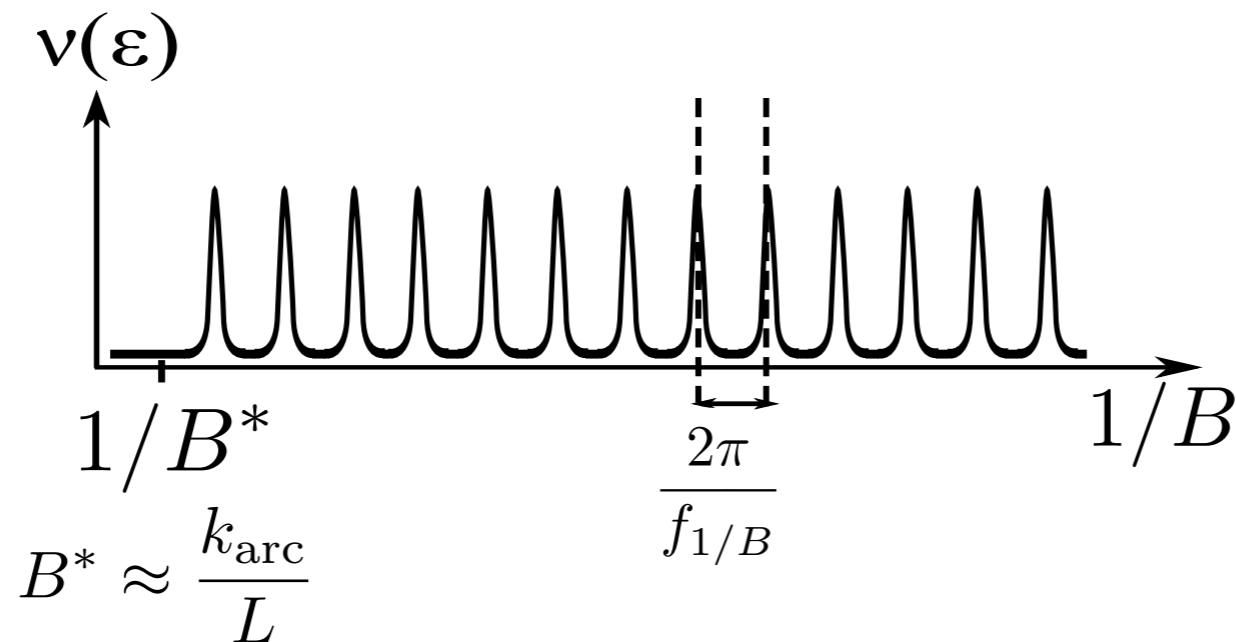
↑
↑  
Arc
Bulk



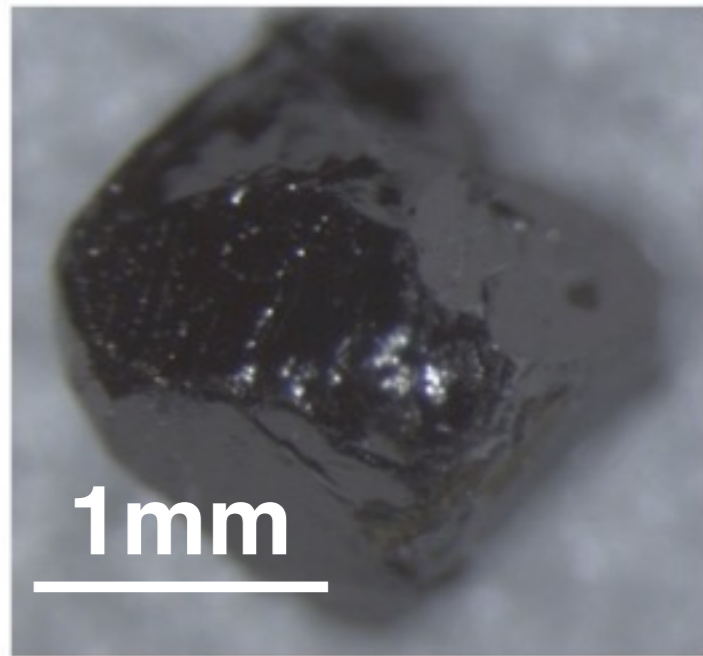
Quantum oscillations

$$\frac{1}{B_n} = \frac{2\pi n}{f_{1/B}} - \frac{e}{k_{\text{arc}}} L$$

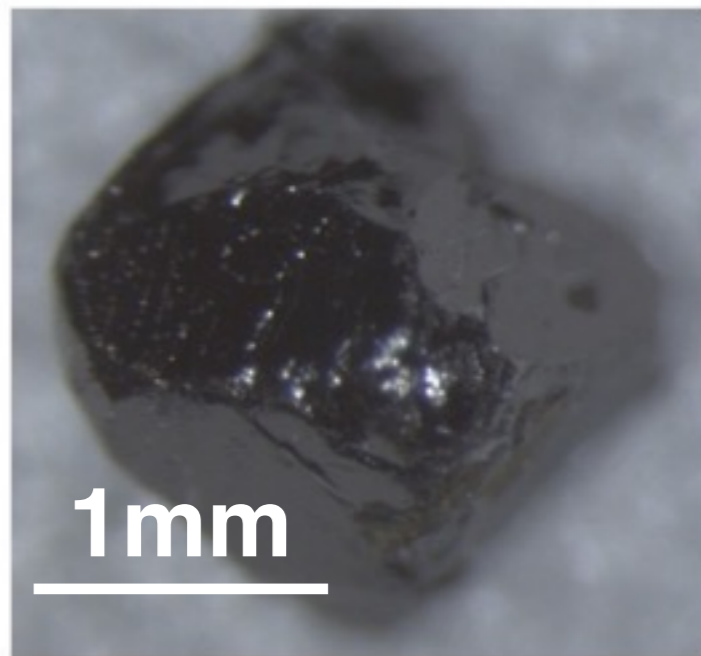
$f_{1/B}$



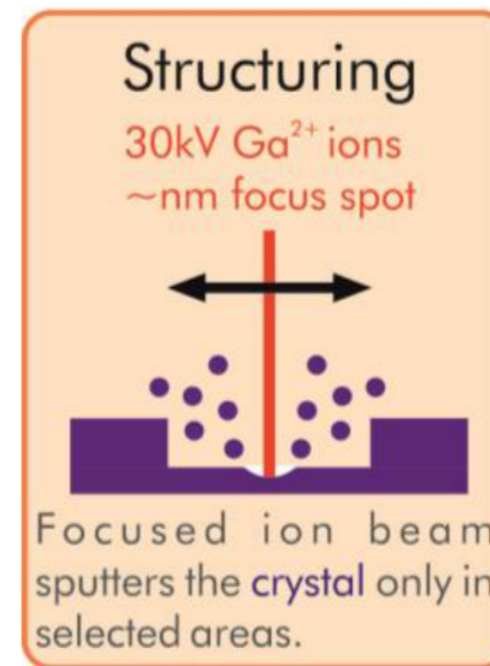
# Focused Ion Beam microstructuring $\text{Cd}_3\text{As}_2$



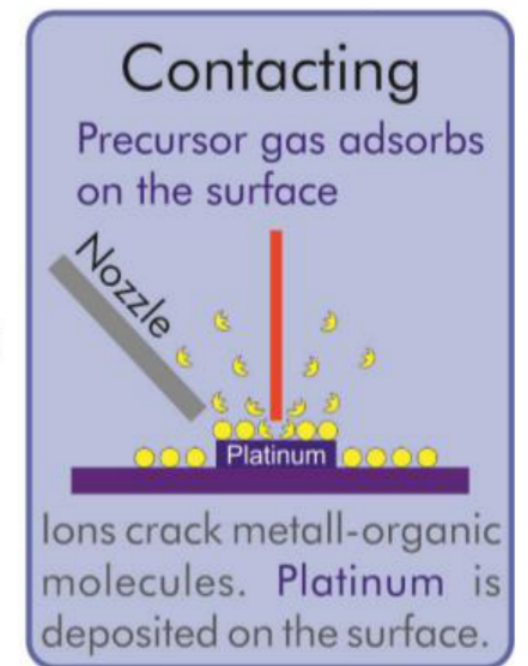
# Focused Ion Beam microstructuring $\text{Cd}_3\text{As}_2$



+

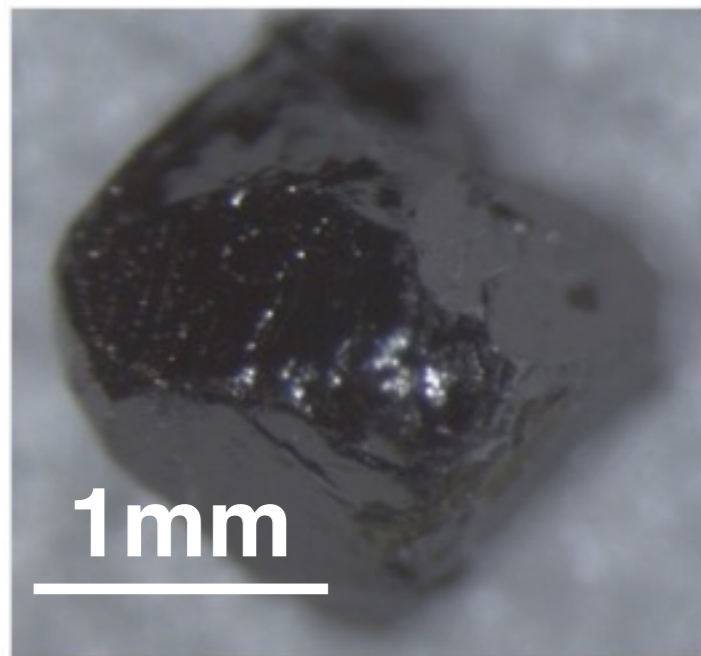


+

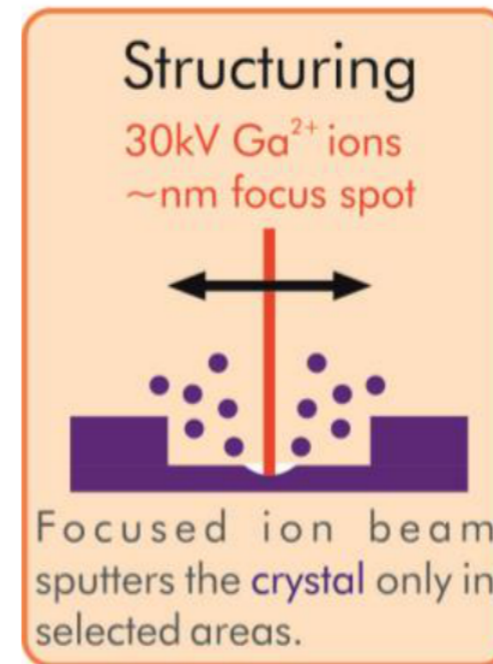




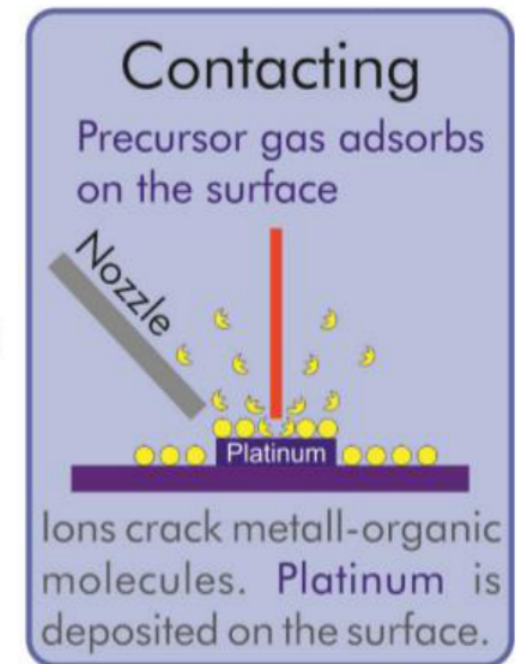
# Focused Ion Beam microstructuring $\text{Cd}_3\text{As}_2$



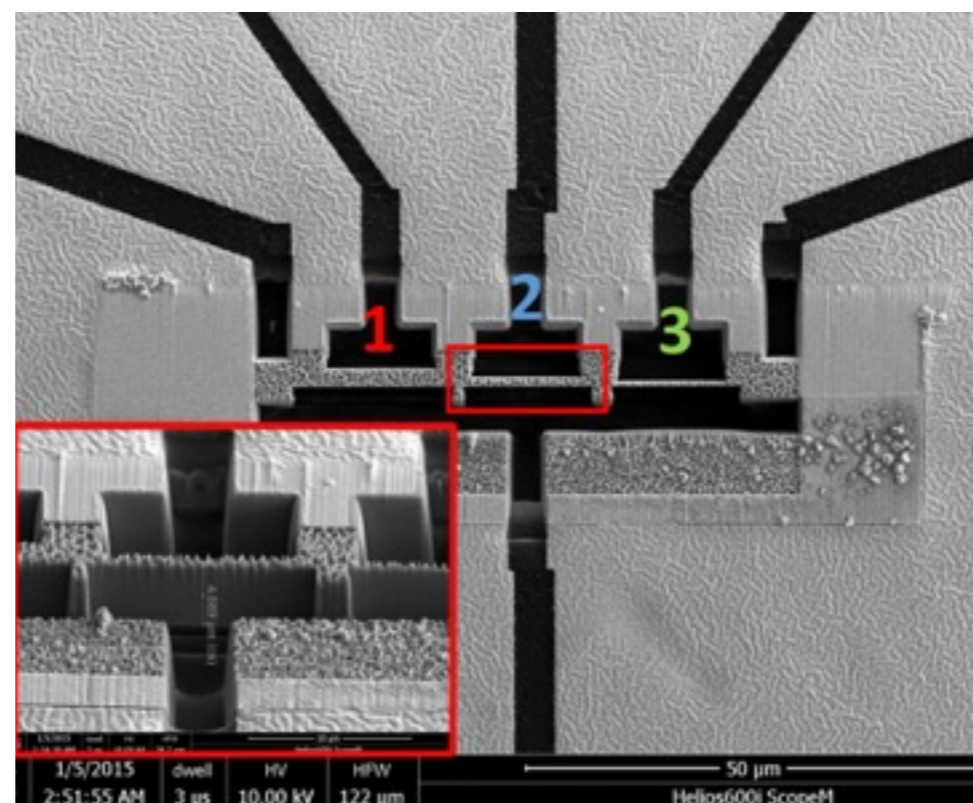
+



+

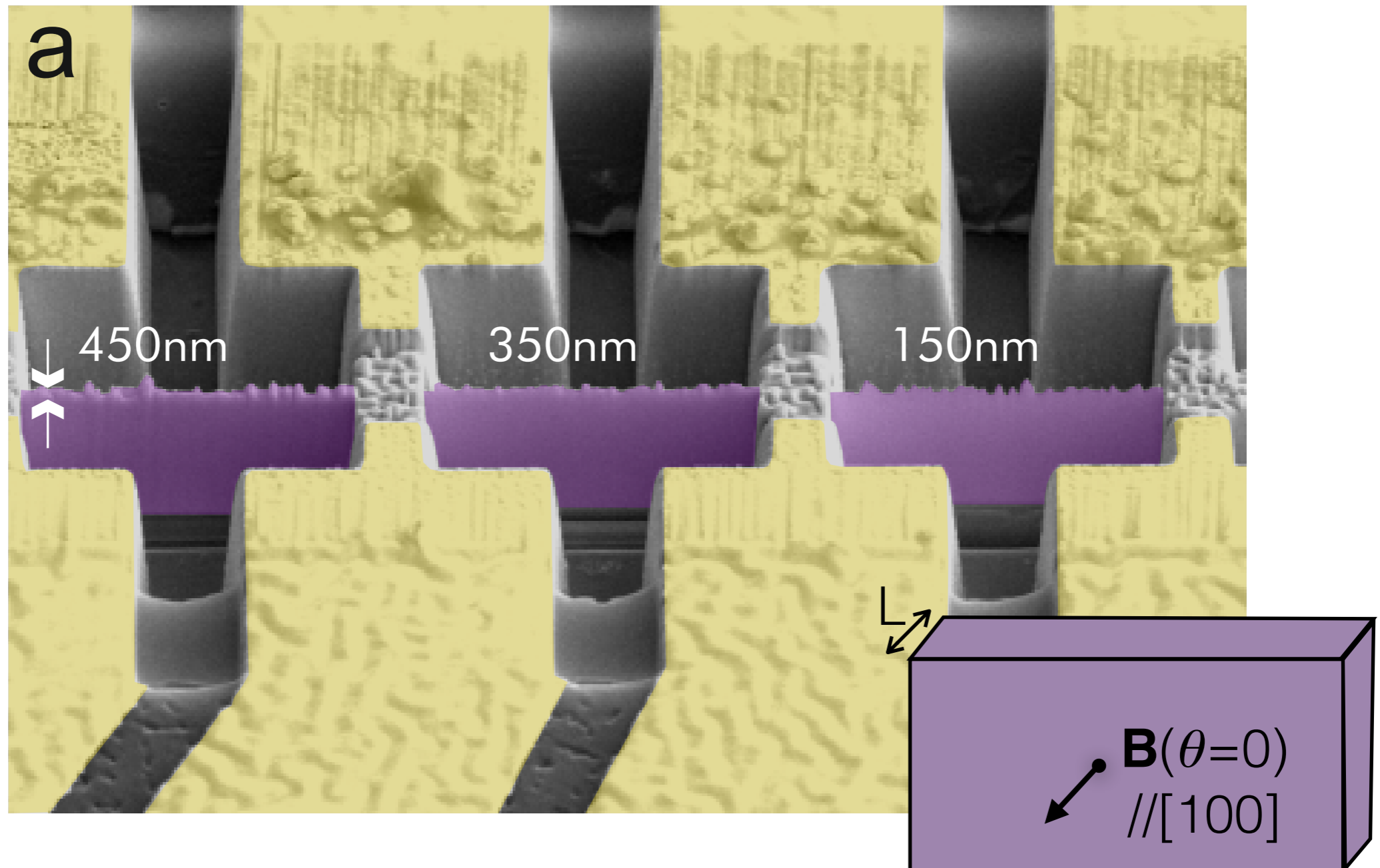


=

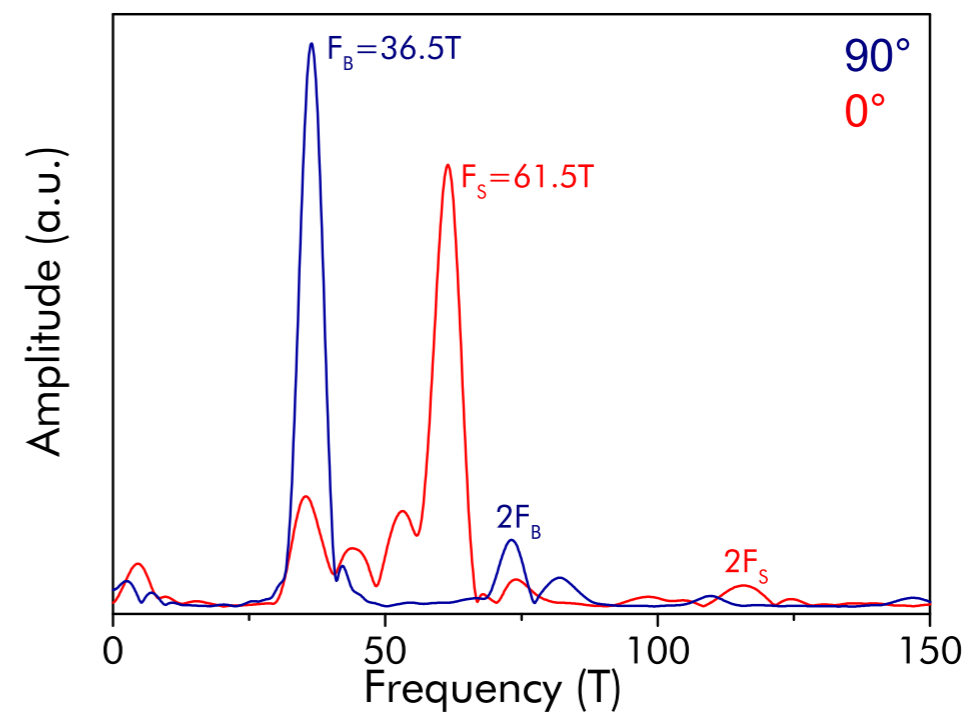
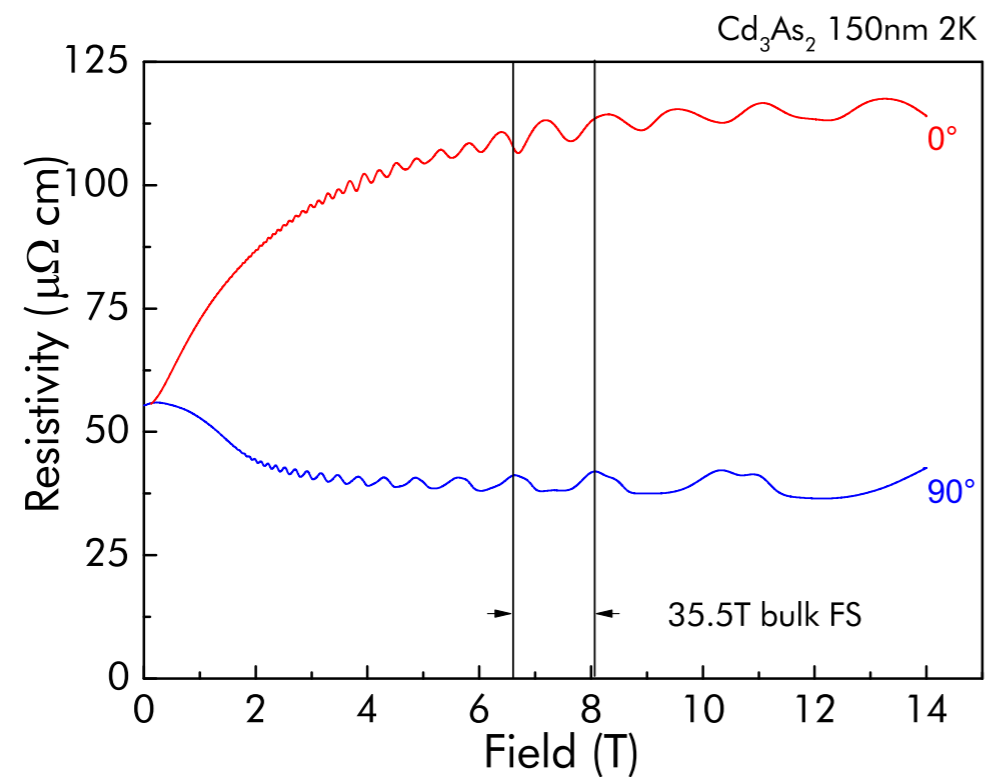


# Thickness-dependent quantum oscillatory study in $\text{Cd}_3\text{As}_2$

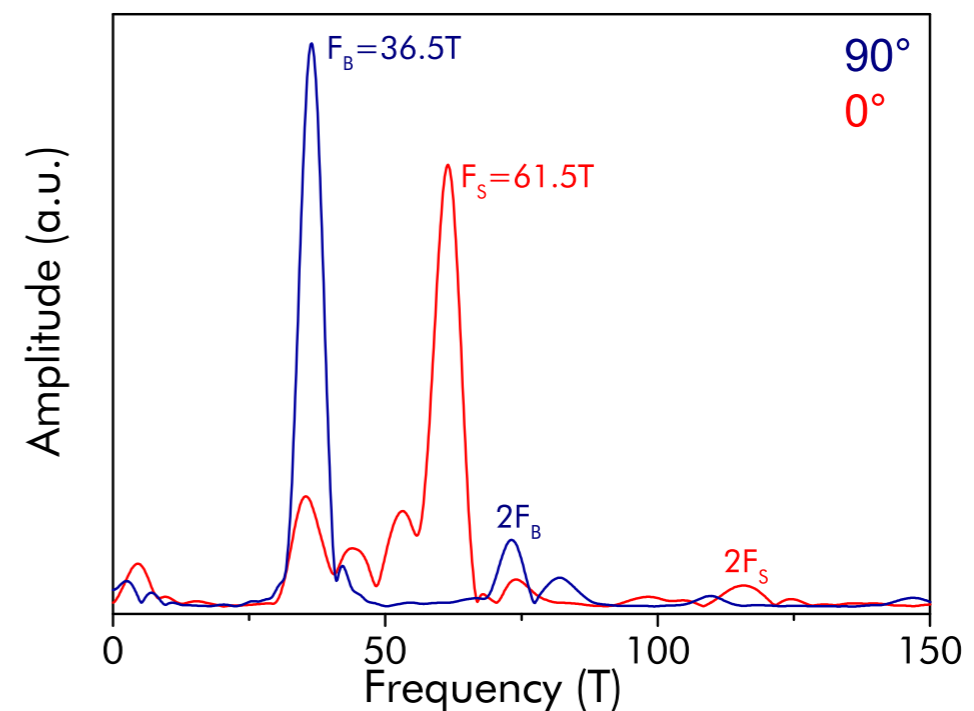
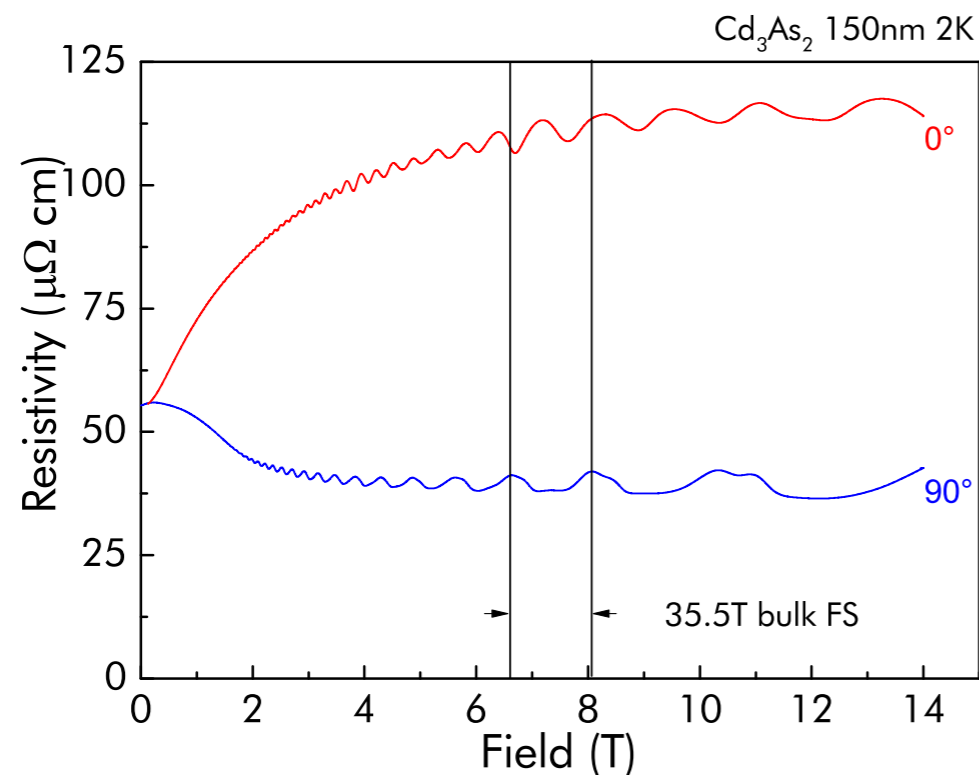
Philip J. W. Moll, JGA et al. arXiv:1505.02817



# New quantum oscillatory frequency at $\sim 60\text{T}$ ( $k_0 \sim 0.08\text{\AA}^{-1}$ )

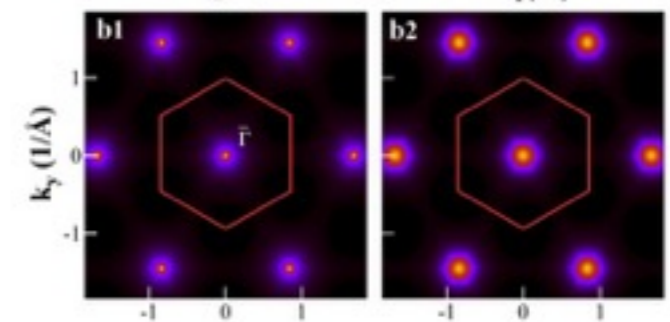


# New quantum oscillatory frequency at $\sim 60\text{T}$ ( $k_0 \sim 0.08\text{\AA}^{-1}$ )

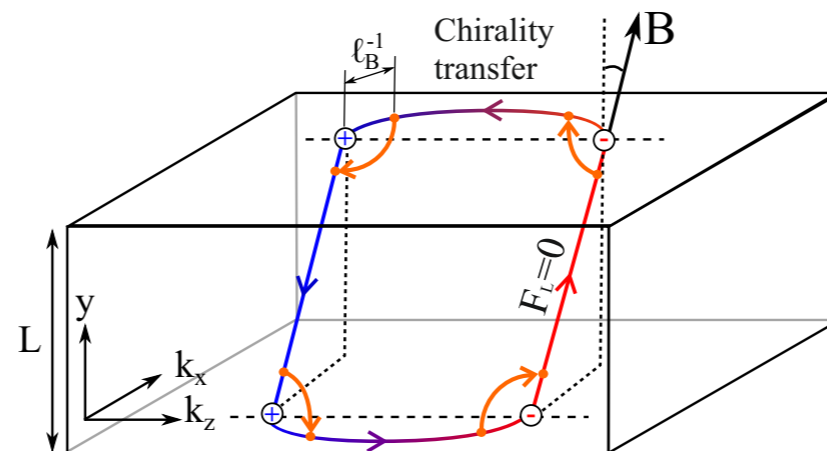
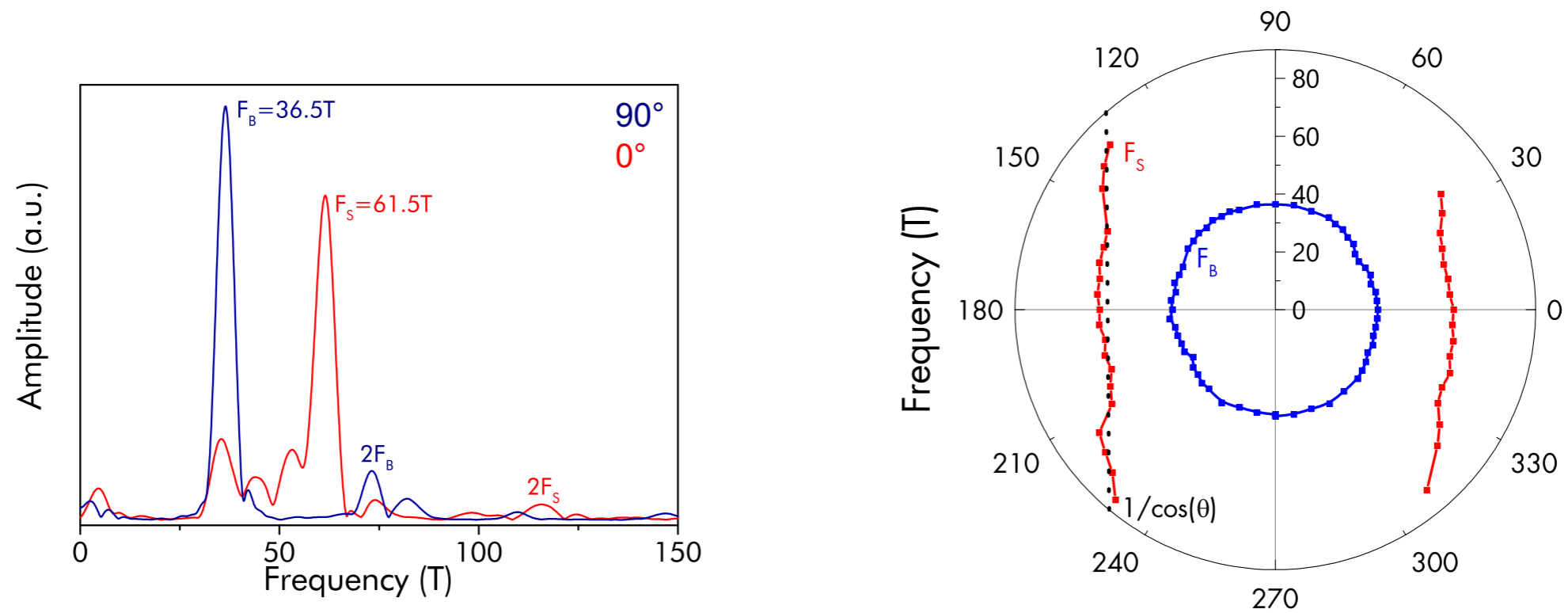


Note this is approximately the  $k_0$  measured by ARPES

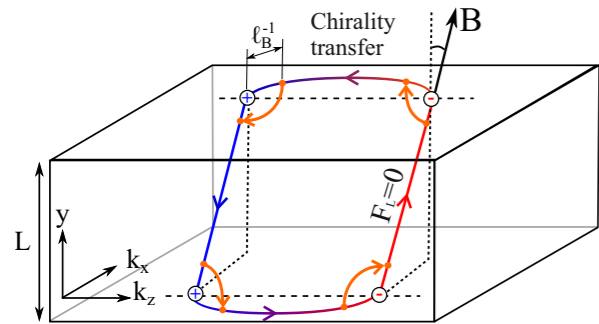
Yi et al. *Sci. Rep.* **4**, 6106 (2014)



# Oscillations are 2D

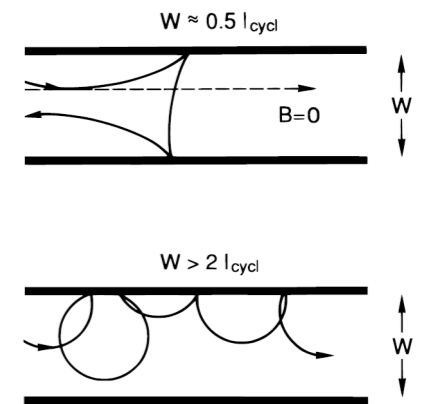


# And grows exponentially with thickness

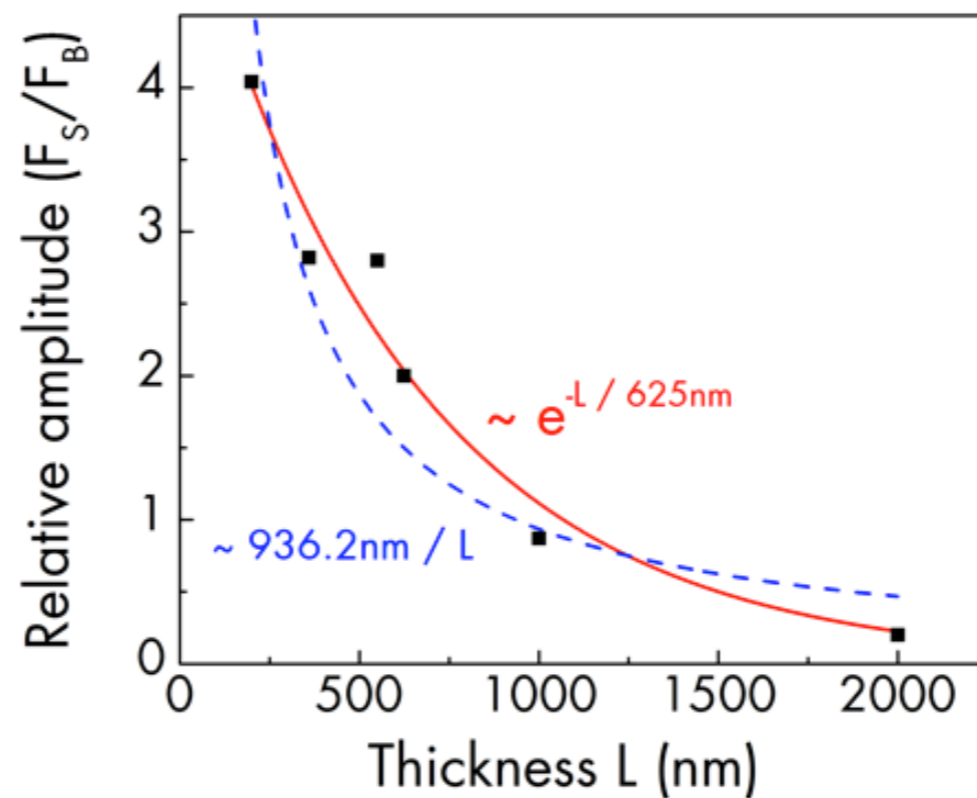
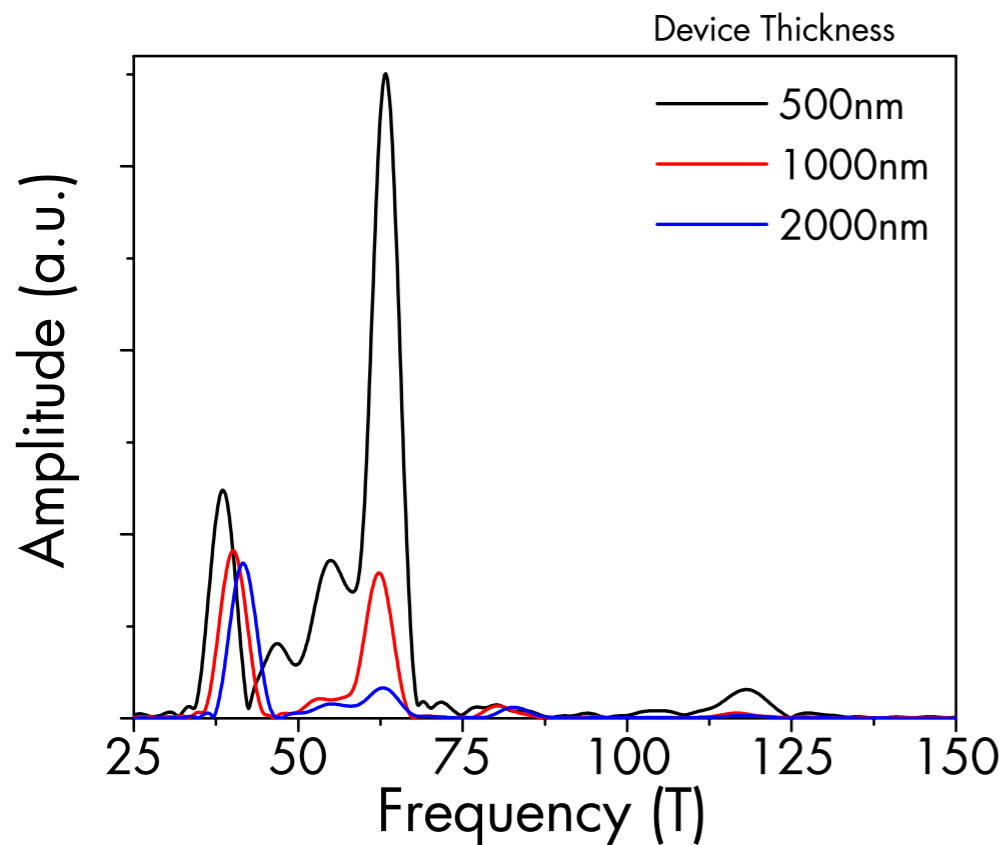


$$A_{\text{SdH}} \sim e^{-1/\omega_c \tau}$$

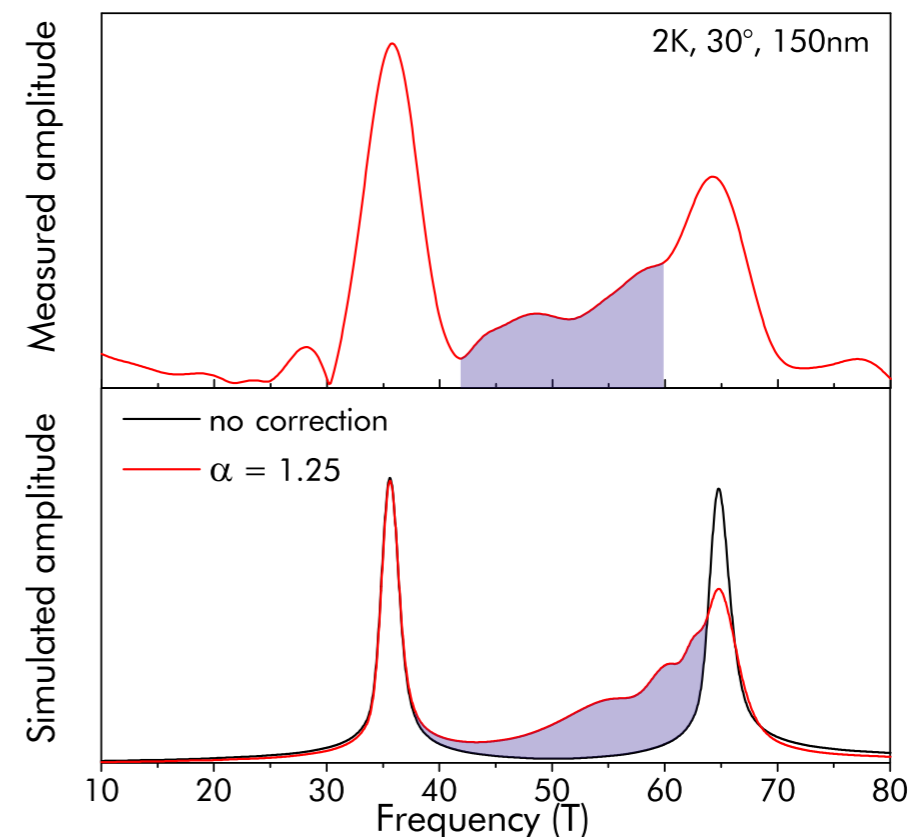
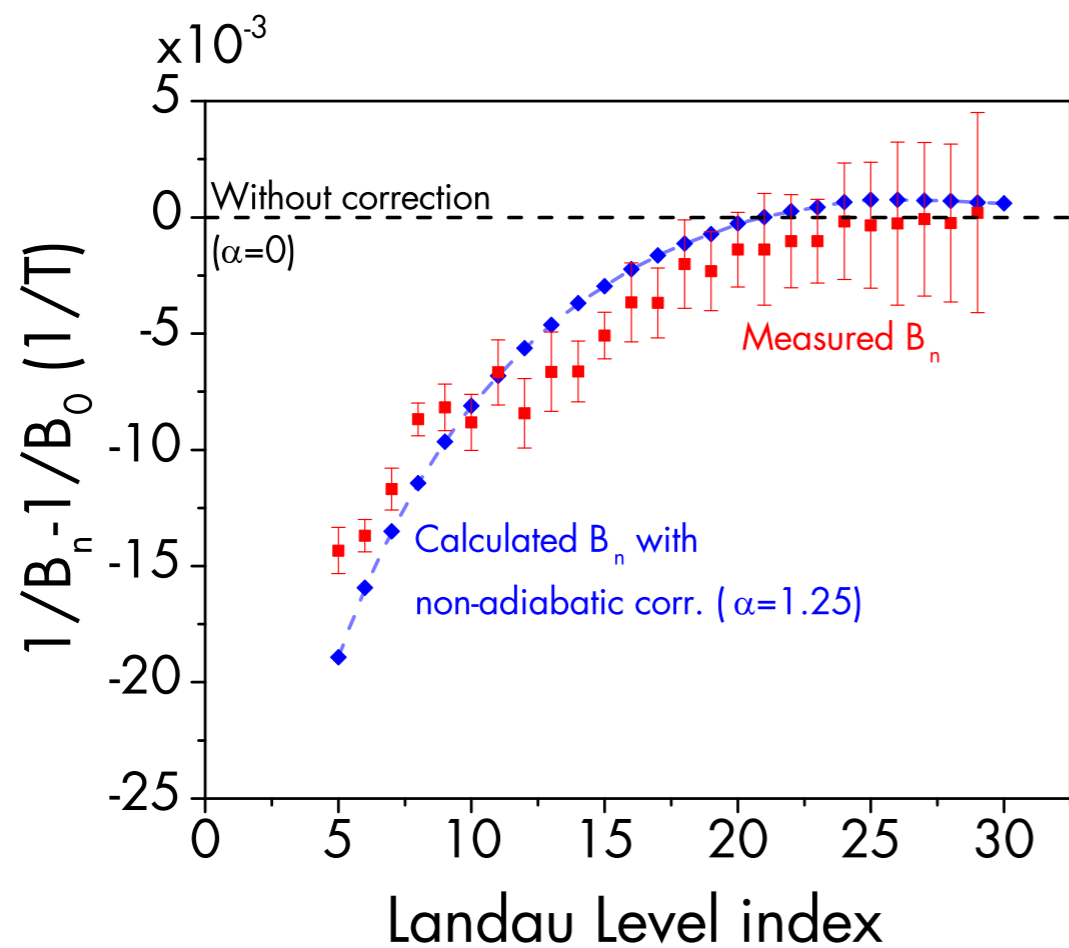
$$\left\langle \frac{1}{\omega_c \tau} \right\rangle \approx \frac{k_0}{e v_s B} \tau_s^{-1} + \frac{L}{v_B} \tau_B^{-1}$$



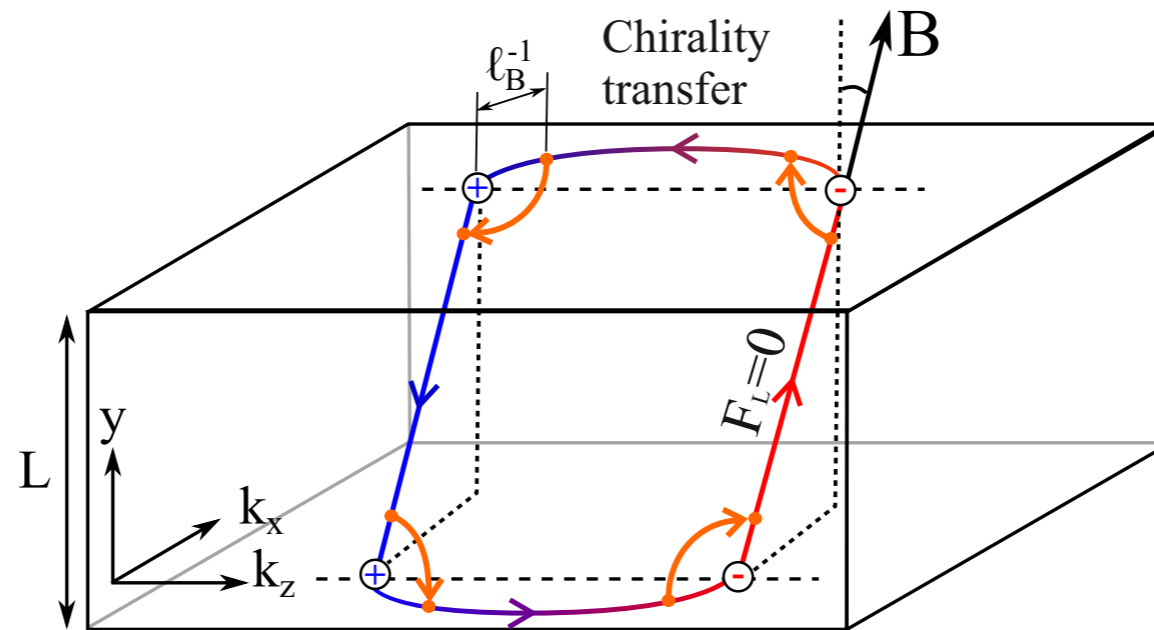
$$l_{\text{MFP}} \approx 1.2 \mu\text{m}$$



# Some other, unexpected details



# Non-adiabatic corrections in Weyl orbits?



$$\delta F_s(B) \approx -4\alpha \frac{\ell_B}{k_{\text{arc}}}$$

*Andrew C. Potter, I. Kimchi, A. Vishwanath, Nature Communications (2014)*

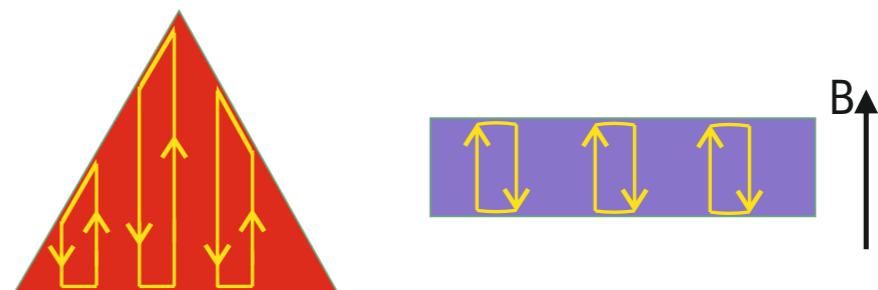
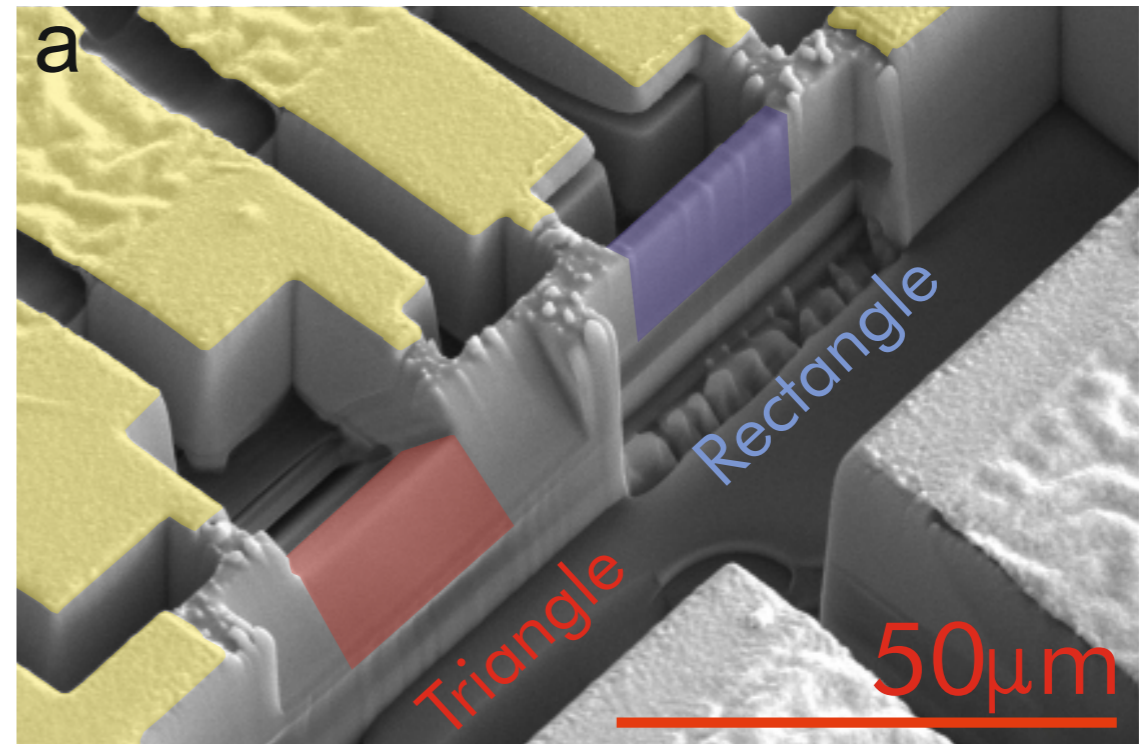
We get  $\alpha \sim 1.2$

*Philip J. W. Moll, JGA et al. arXiv:1505.02817*



# Does the phase of the oscillations depend on thickness?

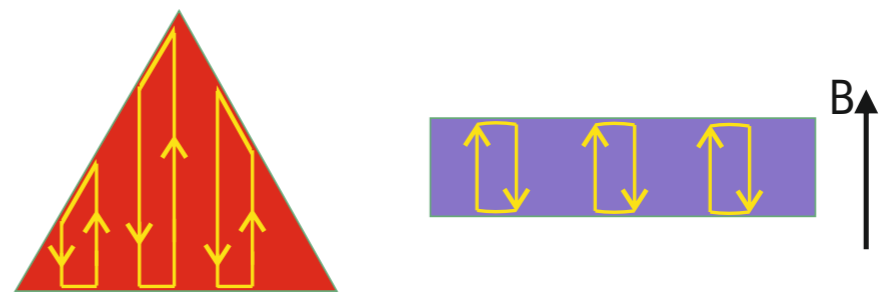
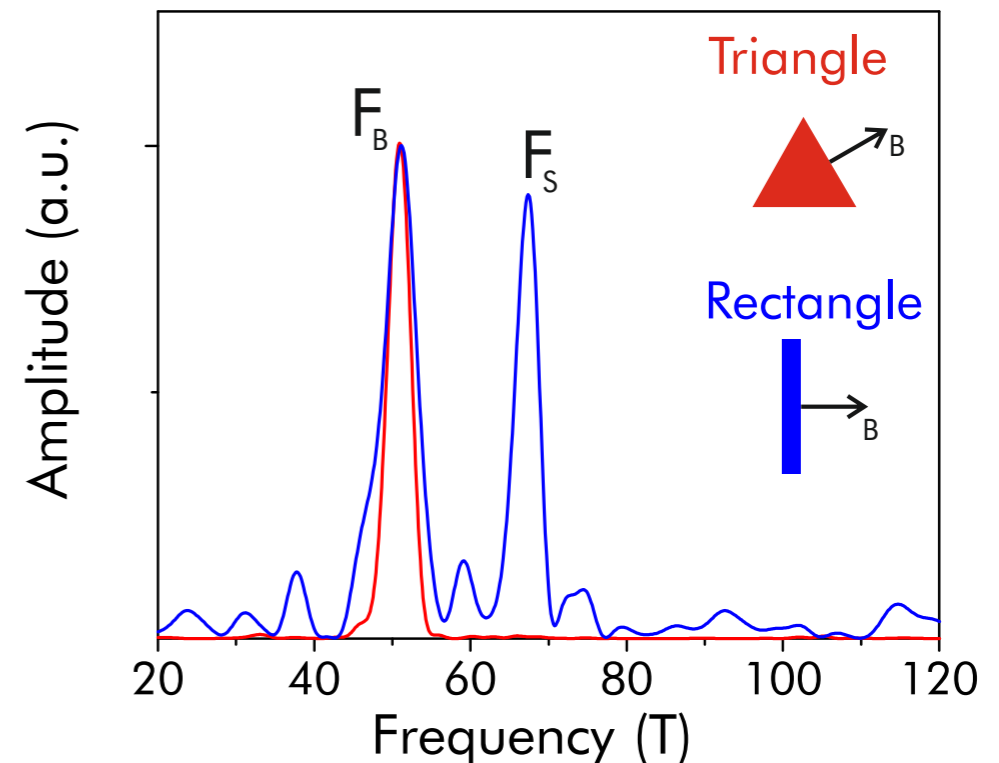
- Detailed thickness dependence prohibitively difficult at the moment (frequency is too high and would require 1nm thickness dependence)
- So we came up with something different - a triangular geometry.
- The orbit is averaging over all length scales, causing the QOs to destructively interfere.



$$\frac{1}{B_n} = \frac{2\pi n}{f_{1/B}} - \frac{e}{k_{\text{arc}}} L$$

# Does the phase of the oscillations depend on thickness?

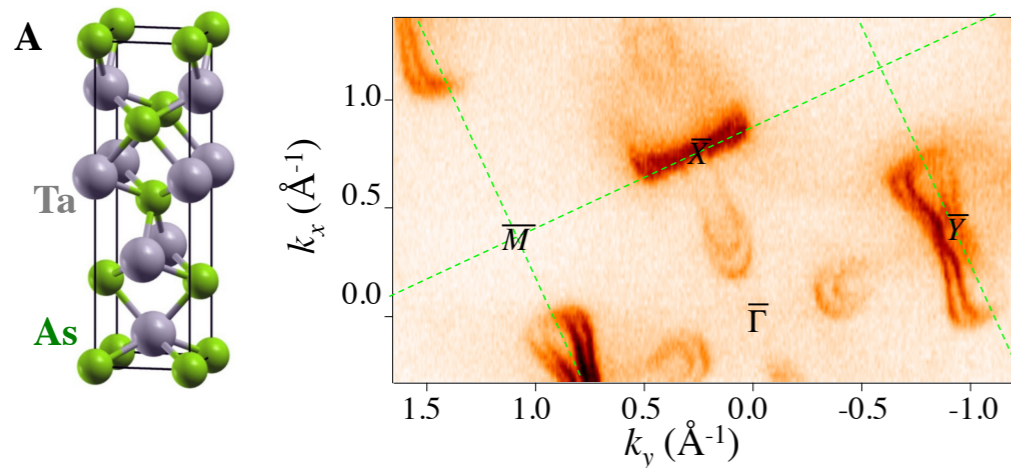
- Detailed thickness dependence prohibitively difficult at the moment (frequency is too high and would require 1nm thickness dependence)
- So we came up with something different - a triangular geometry.
- The orbit is averaging over all length scales, causing the QOs to destructively interfere.



$$\frac{1}{B_n} = \frac{2\pi n}{f_{1/B}} - \frac{e}{k_{\text{arc}}} L$$

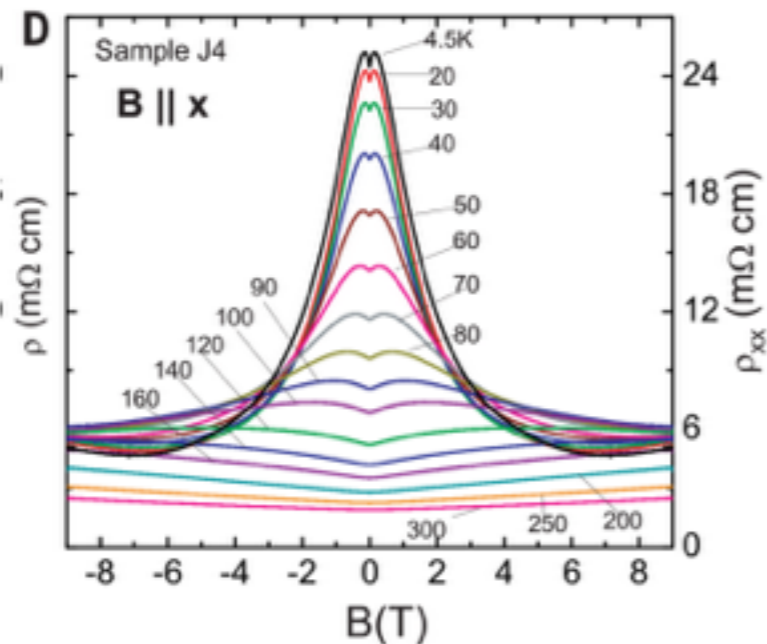
Observation	Trivial	Weyl
2D QOs	Y	Y
Frequency $\sim 56T$	Coincidence	Y
Amplitude exponential with $L$	Close	Y
Onset at $L=2l$	Coincidence	Y
Parallel surface required	N	Y
Field dependent phase.	Unphysical	Y
Saturation field $B^*$	N	N (not yet)

# Take a walk on the Weyl side



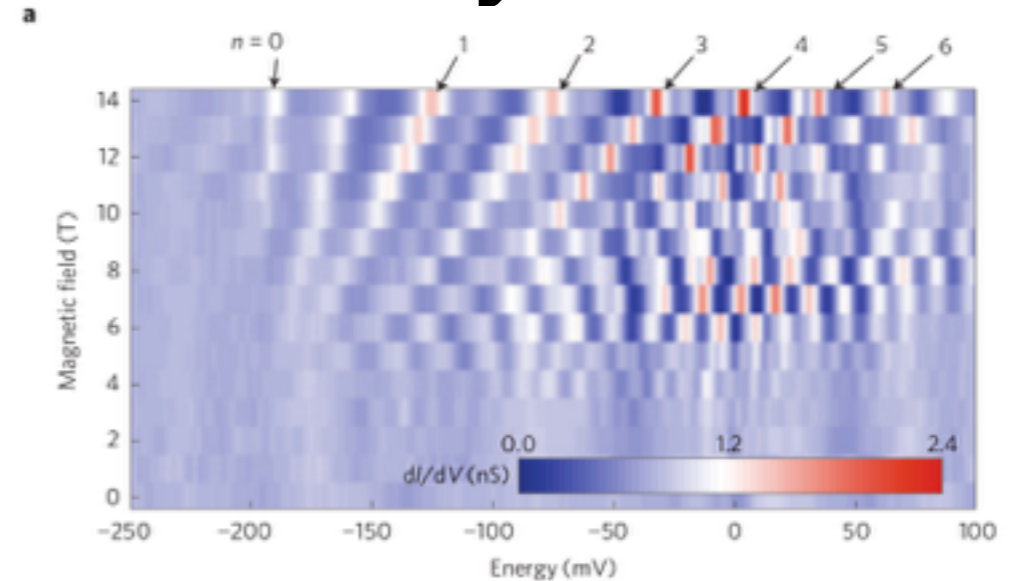
## ARPES on TaAs

(Hasan group, Nat. Comm. '15)



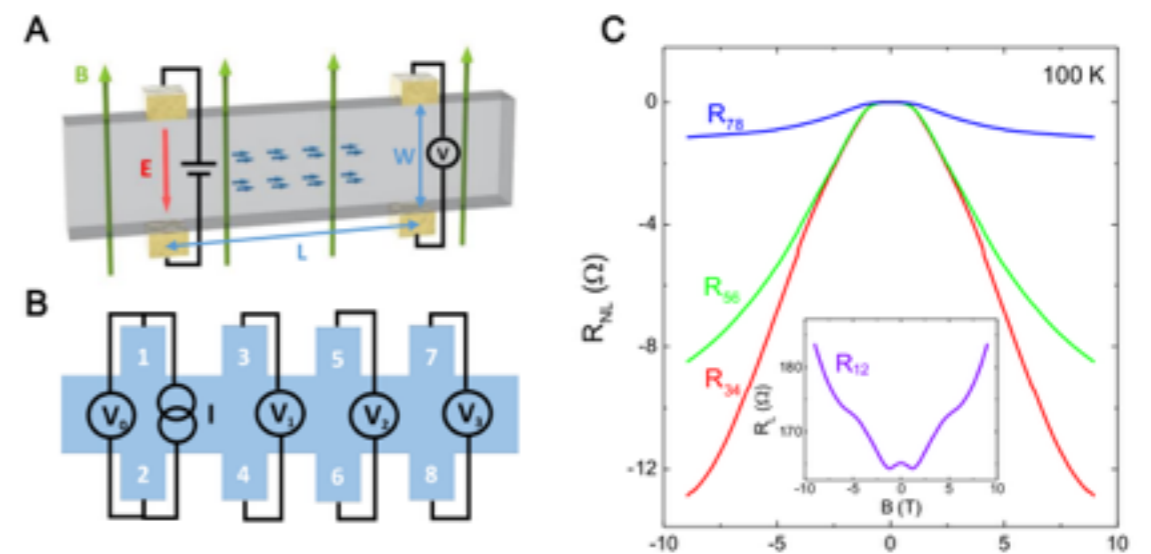
## Negative MR on Na<sub>3</sub>Bi

(Ong group, Science '15)



## STM on Cd<sub>3</sub>As<sub>2</sub>

(Yazdani group, Nat. Mat. '14)

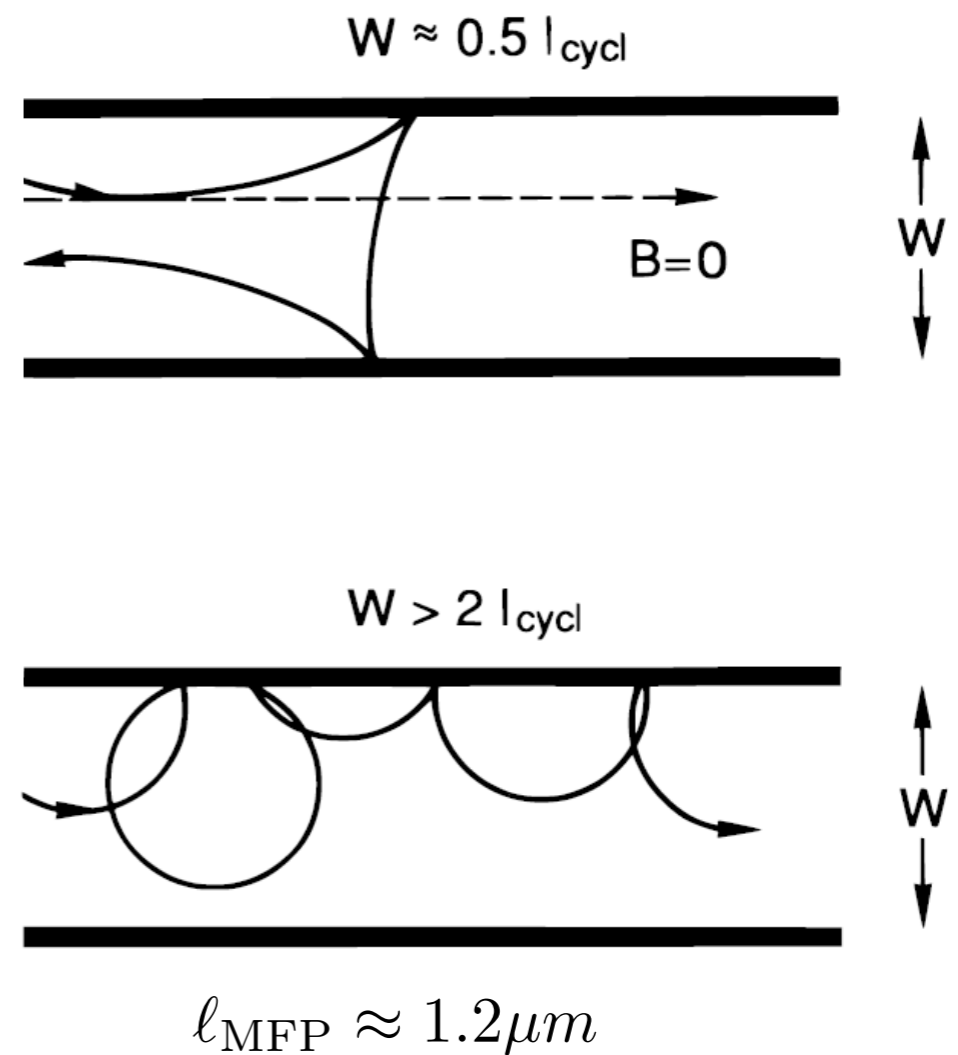
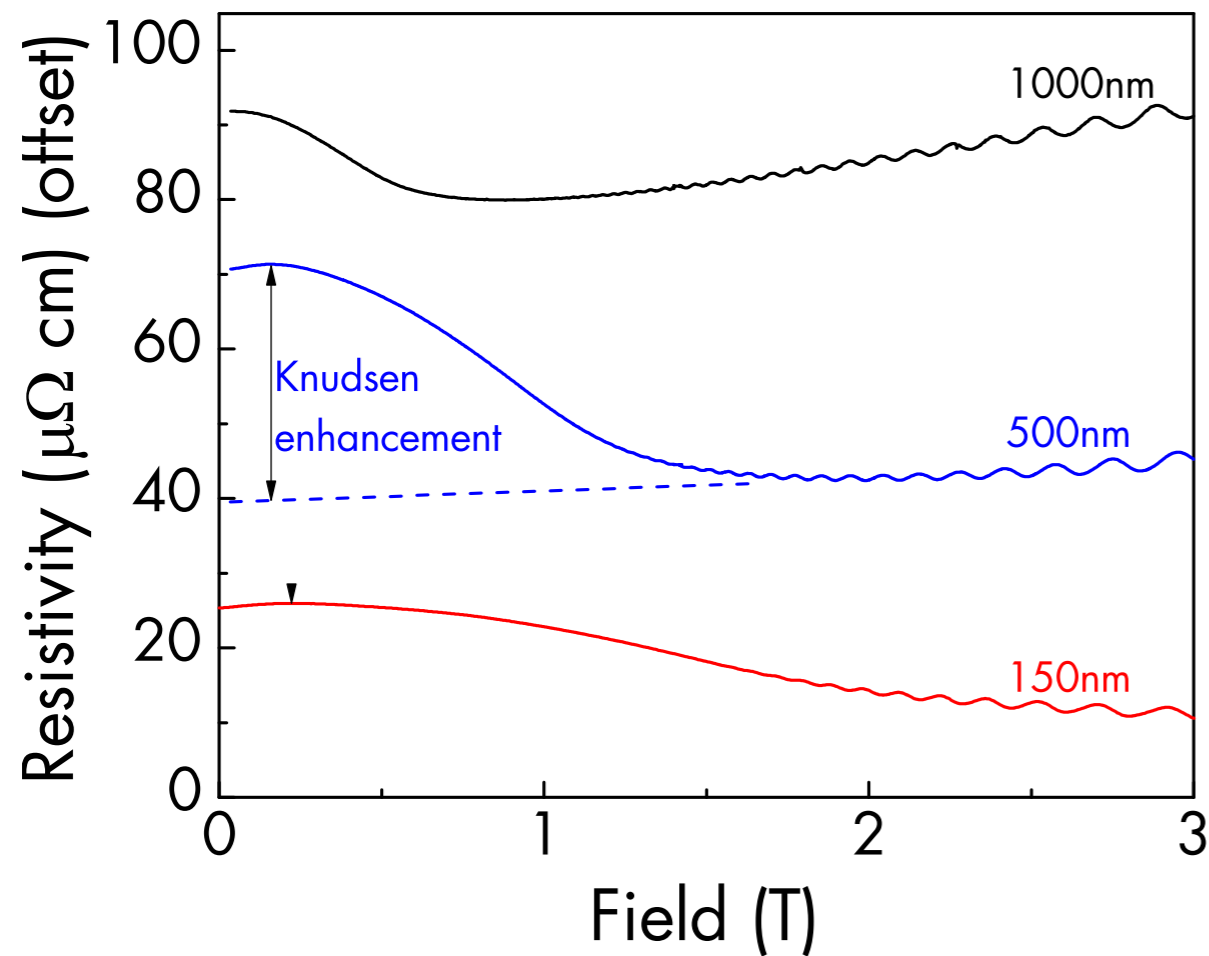


## Non-local transport

(Xiu group, Fudan '15)

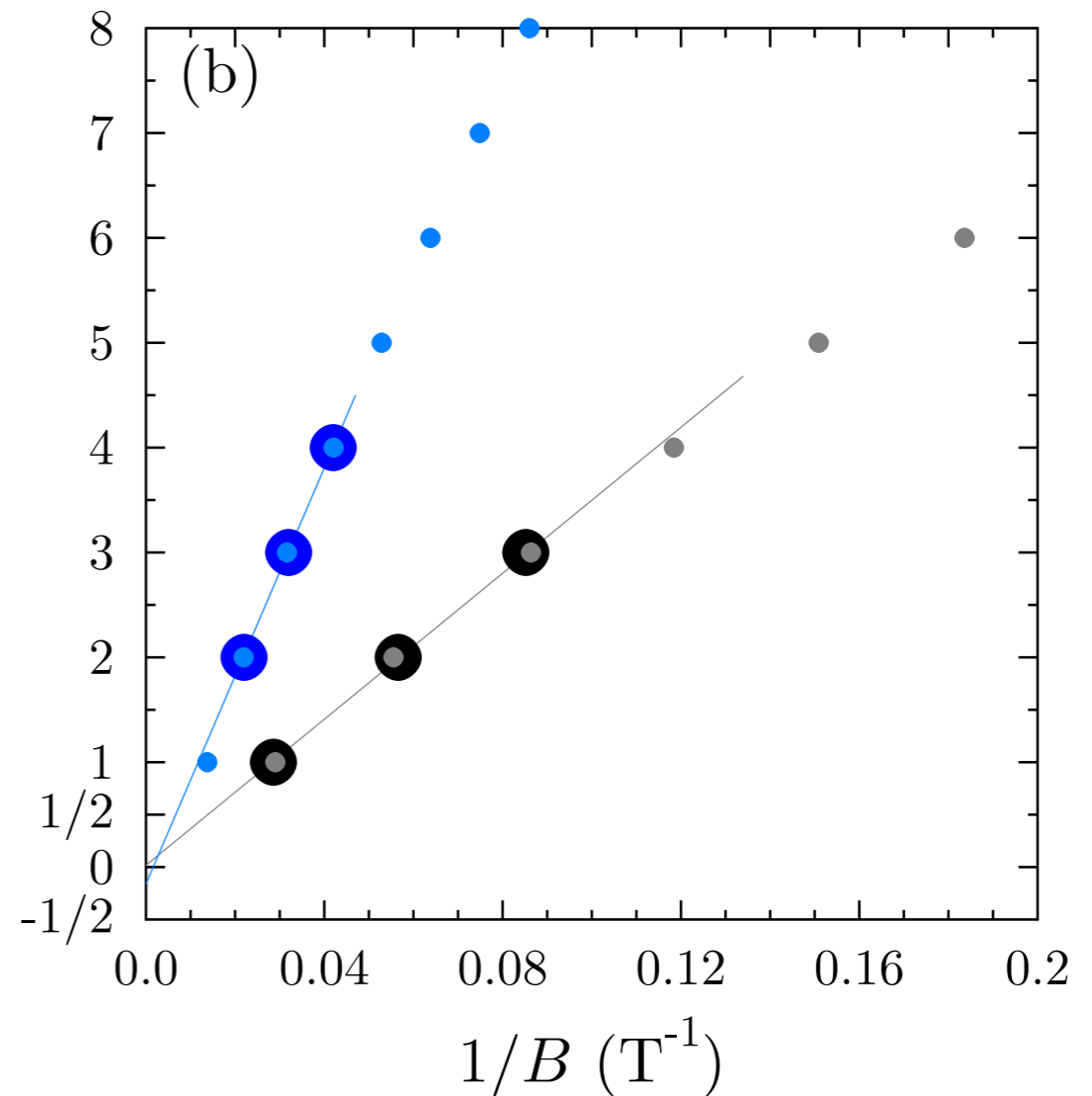
# Amplitude onsets at $L \sim 2l$ (Knudsen effect)

( $B$  Parallel to surface only)



# Mass corrections in TI surface states?

- Seen in Rashba systems (BiTeI) and TIs
- But....
  1. the effect seems to go in the wrong direction
  2. The g-factor required is 300 (10x anything measured in these compounds)



*Analytis et al Nature Physics 2010*

# Transport and Focused Ion Beam microstructuring

# FIB devices



# A new 2D quantum oscillation

# What about trivial surface states?

Exponential dependence on thickness  
Onset at  $L=2\lambda$

# Non-adiabatic corrections

# Triangular vs parallel plate device

